University of Illinois at Urbana-Champaign

ACRC

Air Conditioning and Refrigeration Center   A National Science Foundation/University Cooperative Research Center

An Experimental Analysis of Cycling Losses in Domestic Refrigerator-Freezers

W. H. Coulter and C. W. Bullard

ACRC TR-77   June 1995

Abstract

This report identifies and quantifies the cycling losses in a domestic refrigerator-freezer. During cycling operation the refrigerator was found to operate between 5 and 25% less efficient then the corresponding quasi-steady machine. The cycling refrigerator operates with an evaporator capacity between 3 and 17% less than the quasi-steady refrigerator, while at the same time requiring between 1 and 9% more power to operate.

This refrigerator performance degradation was attributed to several factors, the most important being the refrigerant migration and the thermal mass of the evaporator and compressor. During the off-cycle refrigerant migrates from the condenser to the evaporator as the system pressures equalize. The off-cycle migration increases the temperature of the evaporator and necessitates refrigerant redistribution during the on-cycle, and thereby tends to reduce system performance. The increased power requirements, traced to the compressor, result from slight differences in system pressure and the reduced compressor efficiency due to a cool compressor.

With the cycling losses identified, several possible refrigerator design changes were suggested. It appears that a refrigerator equipped with a reciprocating compressor, solenoid valves to isolate the condenser, and no accumulator should operate in a nearly quasi-steady manner. In addition using the condenser fan to accelerate charge redistribution was investigated. However, since the experimental refrigerator was equipped with an accumulator which held up some charge manipulating the condenser fan showed little payoff.

Table of Contents

List of Figures

List of Tables

Nomenclature

English Symbols

A	area	$[ft^2]$
C	specific heat$[Btu/(lbm\ °R)]$	
C_p	specific heat at constant pressure	$[Btu/(lbm\ °R)]$
COP	coefficient of performance	
D	diameter	[ft]
E	energy	[Btu]
f	air split fraction	
g	acceleration of gravity$[ft/s^2]$	
h	enthalpy or heat transfer coefficient	[Btu/lbm]
k	thermal conductivity$[Btu/(hr\ ft\ °F)]$	
L	length	[ft]
m	mass	[lbm]
n	number	
P	pressure	[psia]
Q	heat transfer	[Btu]
$\dot{Q}$	heat transfer rate	[Btu/hr]
t	time	[hr]
T	temperature	[°F]
$\dot{T}$	rate of temperature change$[°F/hr]$	
u	internal energy$[Btu/lbm]$	
UA	overall conductance$[W/°F]$	
V	volume	$[ft^3]$
W	energy	[Btu]
$\dot{W}$	power	[W]
x	length	[ft]

Greek Symbols

β	thermal expansion coefficient	$[°R^{-1}]$
$?x$	change in variable x	
μ	viscosity	$[lbm/(ft\ s)]$
ρ	density	$[lbm/ft^3]$
τ	time constant	[s]
υ	specific volume	$[ft^3/lbm]$

Subscripts

1	compressor outlet or beginning of off-cycle
2	end of off-cycle
11	compressor inlet
air	air
amb	ambient
alum	aluminum
calc	calculated
cond	condenser

comp	compressor
cyc	cycling
evap	evaporator
exit	exit
f	fresh food compartment
fo	evaporator fan discharge
fan	evaporator fan
fanout	evaporator fan discharge
i	inside
in	inlet or entering the refrigerator
liq line	liquid line
ma	mixed air temperature prior to evaporator inlet
map	compressor map
meas	measured
mig	migration
muf	muffin fan
o	outside
off	off-cycle or compressor shut-off
oil	compressor sump oil
on	on-cycle or compressor start-up
out	outlet or leaving the refrigerator
press	pressure
q-s	quasi-steady
ref	refrigerant
s	constant entropy
sat	saturation
ss	steady state
surf	surface
sys	system
tube	condenser tube
wall	refrigerator cabinet wall
wire	condenser wires
z	freezer compartment
8	free stream conditions

Dimensionless Parameters

Bi	Biot number	$[hL/k]$
Gr	Grashof number $[g\beta\Delta T L^3 / \upsilon^2]$	
Nu	Nusselt number	$[hL/k]$
Ra	Rayleigh number	$[GrPr]$
Pr	Prandtl number $[\mu c / k]$	

Chapter 1: Introduction

Government requirements for more efficient household appliances and the phase-out of chlorofluorocarbons (CFCs) are the two main obstacles facing the refrigerator-freezer industry today. In order to meet these challenges all aspects of the current refrigerator-freezer design are being reexamined in hopes of improving system efficiency. This report looks into one potential area of efficiency improvement, the reduction of "cycling losses".

1.1 Purpose

This analysis builds on the previous work by Rubas and Bullard (1995) and Krause and Bullard (1994) quantifying the factors which reduce the performance of a cycling refrigerator. The concept of a quasi-steady refrigerator, developed by Krause and Bullard, provides the basis for the continued analysis of the Amana test unit used by Rubas and Bullard[†]. These analyses will lead to a better understanding of the mechanisms which reduce the efficiency of a typical domestic refrigerator. Understanding of the causes, it may be possible to implement design changes which reduce or possibly eliminate cycling losses.

This report begins with an analysis of the losses associated with off-cycle migration. The off-cycle refrigerant migration indirectly causes cycling losses by requiring on-cycle refrigerant redistribution. A direct cycling loss is caused by refrigerant migrating and raising the temperature of the evaporator to the point that it begins to reject heat to the surrounding air. The on-cycle is examined next. First, the differences in the heat capacity and system power demand during cycling and quasi-steady operation are quantified. The analysis continues by quantifying differences in coefficient of performance for cycling and quasi-steady refrigerators. Next, the mechanisms causing these cycling losses are examined and explained. Finally, several design strategies are suggested which could help reduce or eliminate cycling losses.

1.2 The Experimental Refrigerator

All the analysis in this report is based upon experimental data. Both the cycling and the steady state data were collected using a 18 cubic foot, top-mount Amana refrigerator, model TC18MBL, charged with 7.0 ounces of R-12 refrigerant. The refrigerator was equipped with a capillary tube/suction line heat exchanger and a reciprocating compressor. The condenser cabinet of the refrigerator has been modified by sealing holes in the bottom and rear of the condenser cabinet. In addition to these modifications a partition was added to condenser grille to reduce recirculation of discharge air with the inlet air. Experiments were conducted at four different ambient temperatures: 60°F, 75°F, 90°F, and 100°F. The thermostat (with its sensor located near the evaporator fan discharge) was set in the middle position and the fresh food damper was removed to ensure repeatability. The average cycling freezer and fresh food compartment temperatures were 1.5°F and 32°F, respectively, slightly lower than "normal" because of the removal of the damper.

[†] Rubas and Bullard (1995) charged the refrigerator with 12.5 ounces of refrigerant R-12 to facilitate comparisons of air- and refrigerant-side energy balances. For this analysis the refrigerator was charged with 7.0 ounces of R-12 to better approximate the performance of actual production refrigerator operation, which often does not permit monitoring of refrigerant-side energy balances during cycling operation.

This report focuses mainly on the 90°F ambient condition with comparisons to other ambient conditions when necessary. The analyses have been conducted using data from all ambient temperatures and the figures are presented in Appendix F.

Chapter 2: Cycling Losses

The purpose of a refrigerator is to preserve food by maintaining the fresh food and freezer compartments within a specified range of temperatures. The refrigerator must be able maintain these conditions even under peak loading conditions such as door opening or ice making. For this reason domestic refrigerators are equipped with an oversized refrigeration system and cycled on and off. This control scheme while effective introduces "cycling losses" which have a net negative effect on the refrigerator's efficiency. In this Chapter these losses will be quantified in order to understand their impact on system performance.

2.1 Choice of Control Volume

Before quantifying and explaining the causes of cycling losses it is necessary to define the control volumes which will be used in the subsequent analyses. Figure 2.1 shows two of the control volumes considered. In control volume "A" the control surface is drawn between the evaporator and the air. This is the appropriate control volume if the evaporator is not considered part of the refrigerator cabinet. A second equally valid control volume is labeled "B" in Figure 2.1. Here the control surface is drawn between the tube and the refrigerant. By selecting this control volume the evaporator is considered part of the refrigerator cabinet.
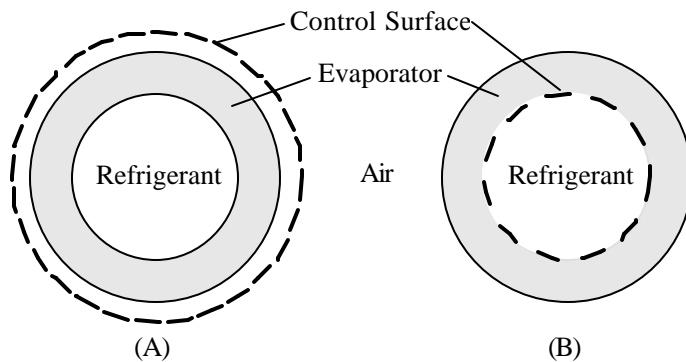
Figure 2.1 Choices of control volumes for cycling analysis

Choosing a control volume does not change the magnitude of the overall cycling losses seen by the refrigerator, but it does change whether a loss is considered an off-cycle or an on-cycle loss. For example during the off-cycle, refrigerant flows from the condenser to the evaporator as the system pressure equalizes. This refrigerant migration causes the temperature of the evaporator to increase. Choosing control volume "A" this off-cycle heating is not considered an off-cycle loss unless heat is transferred across the control surface. However, during the on-cycle the refrigerator must cool the evaporator, now any heat removed from the evaporator is not removed from the air and considered an on-cycle loss. If control volume "B" were chosen the off-cycle heating of the evaporator by the migrating refrigerant would be considered an off-cycle loss and not an on-cycle one, since in this case the off-cycle migration caused heat to be transferred across the control surface.

The above explanation demonstrates the necessity of explicitly defining the control volume and consistently using it throughout the analysis. In this paper the evaporator is not treated as part of the cabinet so control volume "A" is used.

2.2 The Quasi-Steady Machine

To quantify the transient phenomena which degrade system efficiency, the performance of a cycling refrigerator is compared to a quasi-steady machine. This quasi-steady refrigerator is exposed to the same range of heat exchanger air inlet temperatures as seen by the experimental refrigerator during the on-cycle and is assumed to perform in the same manner as the experimental refrigerator does under continuous operation. The evaporator inlet air temperatures of the test unit are maintained at constant values using electric heaters placed in the fresh food and freezer compartments (Staley, et al 1992). A constant condenser inlet temperature is maintained using a test chamber designed to meet AHAM standards (Association of Home Appliance Manufacturers, 1988). Ideally data should be collected over the entire range of operating conditions. However the evaporator air inlet temperature varies only 10°F per cycle, so it is possible to interpolate between the data from five steady state experiments without risk of missing any important steady state phenomena.

2.3 Off-Cycle Losses

When the refrigerator shuts off after the on-cycle, refrigerant migrates through the capillary tube from the condenser to the evaporator until the system pressure equalizes. This migration not only raises the pressure of the evaporator but also increases the temperature of the evaporator itself. This increase in the surface temperature does not affect the food compartments unless the evaporator becomes warm enough to transfer heat to the surrounding air through natural convection. Figure 2.2 compares the temperature of the evaporator surface and surrounding air where the time axis indicates the start of the off-cycle.
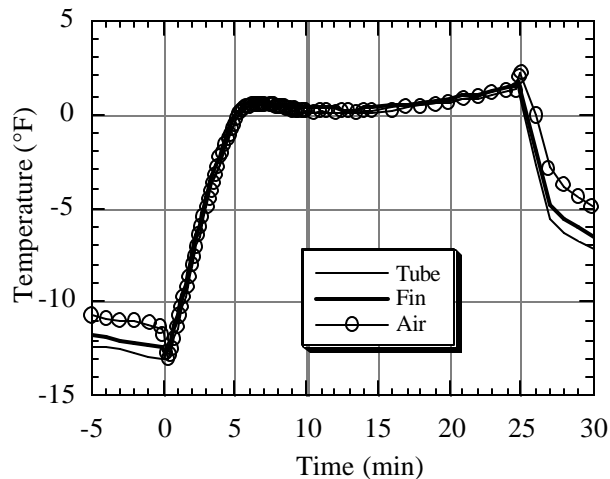
Figure 2.2 Evaporator air, fin, and tube temperatures (T_{amb}=90°F)

There appears to be almost no temperature difference between surface of the evaporator and the air. Therefore heat can not be transferred across the control surface into the cabinet and there are no off-cycle losses. It should be noted that Figure 2.2 represents the evaporator and air temperature profiles in only one location, so it is possible other parts of the evaporator could either be warmer or cooler than the surrounding air. To determine whether a significant amount of heat transfer could occur it was assumed there is a 1°F temperature difference between the entire evaporator and the surrounding air. With this magnitude of a temperature difference and assuming natural convection approximately 3 Btu of heat transfer could occur during a 30 minute off-cycle (Appendix

C). This represents less than 3% of the total heat removed from the cabinet during the shortest on-cycle. Therefore, even if there were a 1°F difference between the evaporator the surrounding air during the off-cycle, the amount of heat transferred to or from the cabinet would be negligible.

2.4 On-Cycle Losses

When the refrigerator turns on after the off-cycle it initially does not operate as efficiently as the quasi-steady machine. This degradation is caused by many things including the redistribution of refrigerant which migrated during the off-cycle as well as the thermal mass of individual components such as the compressor and the heat exchangers. The evaporator capacity is calculated using air side measurements and a volumetric flow rate estimated to be 65 cubic feet per minute (Appendix A). The power required by the compressor and the evaporator fan are measured directly from the test refrigerator using power transducers. To calculate the cycling and quasi-steady power demand and capacity, the data are numerically integrated over the entire on-cycle. Table 2.1 shows the reduction in evaporator capacity and increase in system power requirements due to on-cycle losses. The capacity of the cycling refrigerator is reduced between 3 and 17% when compared to the quasi-steady machine, while the power required to run the cycling refrigerator is between 1 and 9% higher.

Table 2.1 Power penalty and capacity losses

Tamb	Power Demand [W-h/cyc]		Power	Capacity [Btu/cyc]		Capacity
[°F]	Cycling	Quasi-steady	Penalty	Cycling	Quasi-steady	Loss
100	235	233	0.9%	564	579	2.6%
90	116	114	1.8%	286	327	12.5%
75	77	73	5.5%	192	210	6.2%
60	48	44	9.1%	116	140	17.1%

All the information provided in Table 2.1 is based on experimental data and therefore subject to measurement uncertainty. Calculating the magnitude of the evaporator capacity shortfall is subject to considerable uncertainty associated with the reliance on air-side measurements and the small temperature difference across the evaporator, usually less than 10°F. Assuming a ±0.25°F uncertainty in the three air temperature measurements used, the evaporator capacity calculation has an uncertainty of ±25 Btu/hr. The ±0.25°F uncertainty is based on careful and detailed calibration efforts which are described in Appendix B. It includes both the accuracy of the thermocouples as well as any uncertainty in matching the heat exchanger inlet air temperatures. Similarly, estimating the power penalty is subject to the accuracy of the power transducers. According to the manufacturer the transducers used are accurate within ±7.5 Watts for the system power measurement and ±0.5 Watts for the evaporator fan.

2.5 Total Cycling Penalty

The impact of the cycling losses on the cycling refrigerator's efficiency is measured by the system coefficient of performance (COP) which is defined as the ratio of the net heat transferred from the refrigerated space to energy required to perform this work. Equation 2.1 defines the average system (COP) for both the cycling and quasi-steady refrigerators. Equations 2.2-4 define the net evaporator capacity, energy added to the cabinet by the

evaporator fan, and the energy required to operate the refrigerator respectively. Note that both the on- and off-cycle losses in the quasi-steady machine are zero by definition.

$$COP = \frac{Q_{evap} - W_{fan}}{W_{sys}}$$

(2.1)

$$Q_{evap} = \int_0^{t_{on}} \dot{Q}_{evap,on} \cdot \partial t - Q_{loss,off}$$

(2.2)

$$W_{fan} = \int_0^{t_{on}} \dot{W}_{fan} \cdot \partial t$$

(2.3)

$$W_{sys} = \int_0^{t_{on}} \dot{W}_{sys} \cdot \partial t$$

(2.4)

The coefficients of performance for the cycling and quasi-steady refrigerators at several ambient temperatures are compared in Table 2.2. The cycling refrigerator is between 5 and 25% less efficient than the quasi-steady machine. This degradation in cycling efficiency reflects the reduction evaporator capacity and increased system power requirements shown in Table 2.1. Table 2.2 reveals another interesting trend. The refrigerator appears less efficient at lower ambient temperatures. The explanation for this behavior is related to the length of the on-cycle as shown in Figure 2.3. As the ambient temperature is reduced the length of the on-cycle decreases. Since COP is lowest during the first few minutes of the cycle, short cycles have the relatively higher losses seen in Table 2.2. Figure 2.3 shows the instantaneous performance increases with decreasing ambient temperature. The reason for this is simple, as the ambient temperature is lowered the difference between the condensing and evaporating temperatures diminishes, increasing Carnot efficiency. However cycling losses, which are proportionally larger for lower ambients, negate this increase in Carnot efficiency. This causes the cycling refrigerator to operate at an average coefficient of performance which is independent of ambient temperature, as shown in Table 2.2.

Table 2.2 Efficiency comparison of cycling and quasi-steady refrigerators

Tamb	On-Cycle Length	COP		COP
[°F]	[min.]	Cycling	Quasi-steady	Loss [%]
100	61	0.63	0.66	4.5%
90	30	0.65	0.77	15.6%
75	20	0.66	0.77	14.3%
60	12	0.64	0.85	24.7%
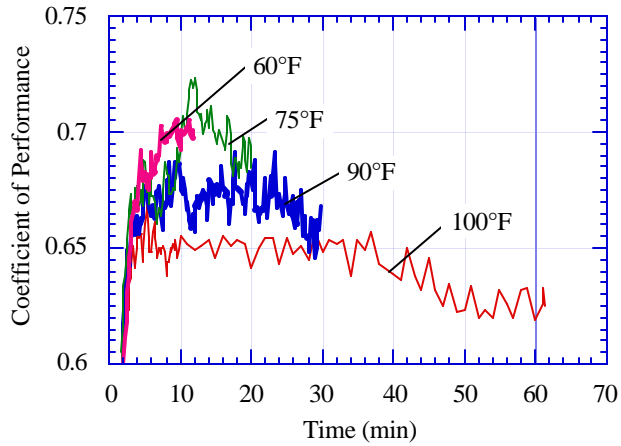
Figure 2.3 Cycling coefficient of performance for 60-100°F ambients

In this Chapter the impact of cycling losses on system performance have been quantified, but no explanation for causes of these losses has been offered. Chapter 3 will take a more detailed look at the on-cycle to identify the causes for the reduced evaporator capacity and increased power demands of the cycling refrigerator.

Chapter 3: On-Cycle Capacity Degradation and Power Penalty

Chapter 2 showed a cycling refrigerator is between 5 and 25% less efficient than a quasi-steady machine. The cycling refrigerator operates less efficiently because the evaporator capacity is lowered while system power requirements are increased. These on-cycle losses can be attributed to issues such as thermal mass of the components (compressor and heat exchangers) as well as the necessity to redistributed refrigerant from the evaporator immediately after start-up. The remainder of this Chapter will explore the reasons for the observed cycling losses in more detail.

3.1 Capacity Degradation Due to the Evaporator Thermal Mass

The capacity of the cycling refrigerator is reduced between 3 and 17% by cycling losses. These losses can be divided into two groups, those associated with the thermal mass of the system components and those associated with the redistribution of the refrigerant after start-up. The thermal mass of all the major components, compressor, condenser, evaporator, and evaporator ductwork were examined in detail but only the evaporator appears to play a significant role in reducing the evaporator capacity (Appendix D). This section will quantify the magnitude of its effect.

The thermal mass of the evaporator can degrade refrigerator efficiency in two ways. First, it lengthens the time required to reach quasi-steady temperatures. Since the heat transfer to the evaporator is proportional to the temperature difference between the air and the surface of the heat exchanger, a warm evaporator removes less heat from the air than a cold one does. Treating the evaporator as a "lumped" body its thermal time constant was calculated to be 8.4 seconds (for more details see Appendix D). This is considerably shorter than the typical cycle length, so it is unlikely the temperature of the evaporator lags sufficiently to effect system performance.

A second way the evaporator thermal mass degrades system performance is by reducing the effective evaporator capacity. Since the control volume has been selected such that the evaporator tubing is not considered part of the cabinet, any capacity used to cool the evaporator must be considered an on-cycle loss. If the evaporator is massive, cooling it could represent a significant portion of the evaporator's total capacity.

Equation 3.1 represents the total energy removed from the evaporator metal. Knowing the weight of the evaporator (3.5 lbm), the specific heat of aluminum (0.22 Btu/lbm °R), and the temperature of the evaporator at the beginning and end of the on-cycle it is possible to calculate how much heat is removed from the evaporator metal (see Appendix D). Table 3.1 shows that between 11 and 14 Btu/cyc of heat are removed during the on-cycle. This is significant portion of the total on-cycle losses. However, there are still between 4 and 30 Btu/cyc of on-cycle losses which can not be attributed to the evaporator thermal mass. These "other" losses are likely associated with the redistribution refrigerant after compressor start-up, the next several sections explore in more detail why refrigerant maldistribution causes the refrigerator to operate less efficiently.

$$Q = mc(T_{on} - T_{off})$$

<div style="text-align:right">(3.1)</div>

Table 3.1 Breakdown of on-cycle capacity degradation

Tamb	Capacity Loss [Btu/cyc]		
[°F]	Total	Thermal Mass	Other
100	15	11	4
90	42	12	30
75	18	14	4
60	24	14	10

3.2 A New Control Volume

Until now the goal was to understand the impact of all cycling losses on the refrigerator's ability to efficiently cool the cabinet. With this in mind a control volume was drawn around the evaporator. The goal of the following sections is to understand the impact of refrigerant redistribution on system performance, therefore a new control volume must be selected. Now all cooling done by the refrigerator should be considered, since from the perspective of the refrigerant loop it does not matter whether it is cooling the air or the evaporator mass. The new control volume used in following analyses is shown in Figure 3.1.

Control Surface

T_{air}

T_{ref}

T_{wall}
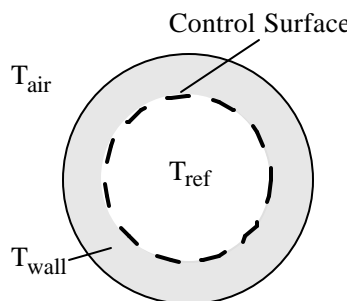
Figure 3.1 Control volume for refrigerant redistribution and power penalty analysis

Once again the goal of the following sections is to compare the performance of a cycling refrigerator to a quasi-steady one. To accurately compare the cycling refrigerator with the quasi-steady machine it is necessary match the heat exchanger wall temperatures instead of the heat exchanger air inlet temperatures as in the previous Chapter. However, matching wall temperatures is difficult to do experimentally, so once again the heat exchanger inlet air temperatures were matched instead. This is a reasonable approximation since both the evaporator and condenser respond quickly to temperature changes (time constants less than 10 seconds) and the heat exchanger inlet air temperatures change by no more than 0.4°F per minute.

3.3 System Coefficient of Performance

With the new control volume defined, it is possible to investigate factors other than the evaporator thermal mass which reduce the evaporator capacity as well as the reasons behind the increased system power requirement. The coefficient of performance, as defined by Equation 3.2, combines the effects of a reduced evaporator capacity and increased system power requirement. Using the experimental data collected, the performance of the cycling refrigerator can be compared to a quasi-steady one. Figures 3.2a-d show this comparison for the test unit operating at several different ambient temperatures. Initially the cycling refrigerator is less efficient the quasi-steady one, but within ten minutes both operate with the same efficiency. Since Figures 3.2a-d show similar trends, the following

sections will analyze the causes for the reduced cycling efficiency using data collected under 90°F ambient temperature conditions. Results for the other ambient temperatures are presented in Appendix F for comparison.

$$\text{COP} = \frac{\dot{Q}_{evap} - \dot{W}_{fan}}{\dot{W}_{sys}}$$

(3.2)
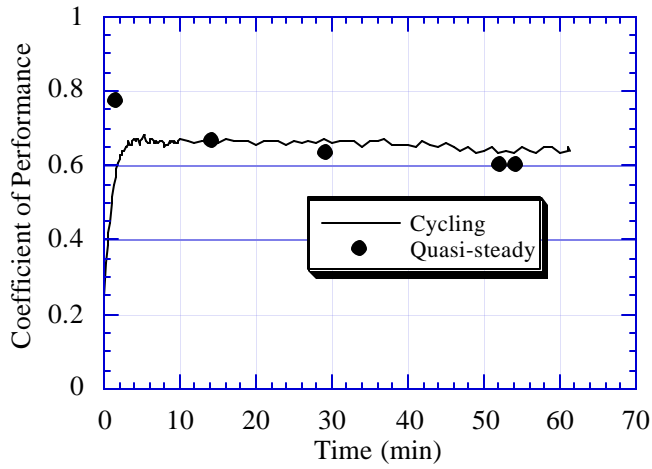
Figure 3.2a Coefficient of performance ($T_{amb}=100°F$)
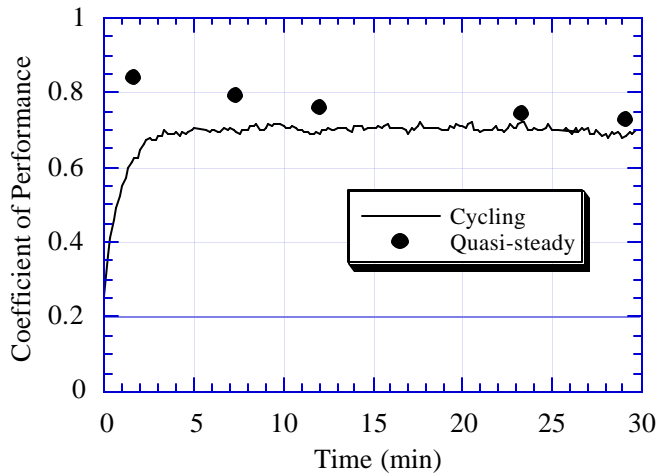
Figure 3.2b Coefficient of performance ($T_{amb}=90°F$)

10
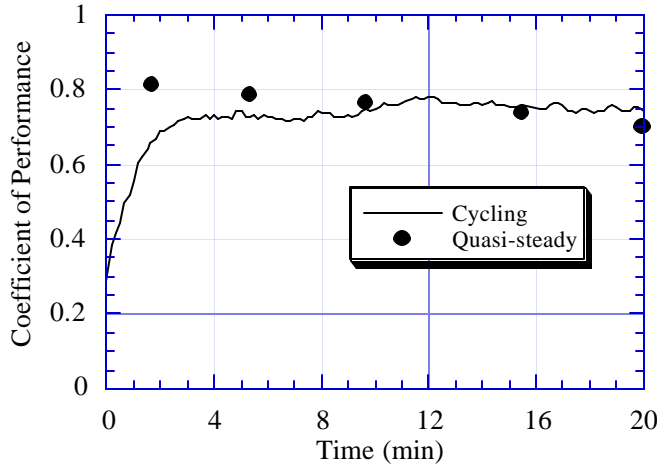
Figure 3.2c Coefficient of performance (T_{amb}=75°F)
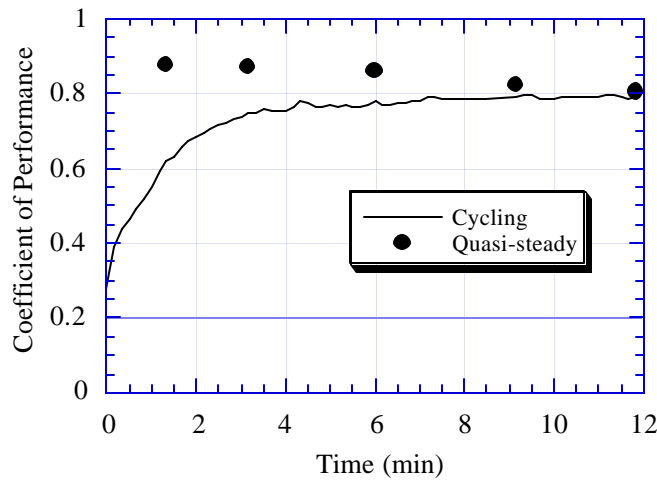
Figure 3.2d Coefficient of performance (T_{amb}=60°F)

3.3 Capacity Degradation Due to Refrigerant Redistribution

This section examines how the evaporator capacity of a cycling and quasi-steady refrigerator compare over the course of a typical on-cycle. Equation 3.3 defines evaporator capacity for the control volume shown in Figure 3.1. The third term in Equation 3.3 represents the heat removed from the metal. To accurately estimate the total heat removed by the refrigerant during cycling it is important to include this term. However, it is unnecessary when calculating the capacity at steady state since the temperature of the evaporator remains constant during continuous operation.

$$\dot{Q}_{cyc} = \dot{V} \cdot \rho_{air}(h(T_{ma}) - h(T_{fanout})) + \dot{W}_{fan} + (mC \cdot \dot{T})_{evap}$$

(3.3)

The inlet air temperature is calculated using Equation 3.4, where T_f and T_z are temperatures of air returning from the fresh food and freezer compartments measured just before they mix upstream of the evaporator (see Figure

11

3.3). The fraction of air returning from the freezer and the volumetric flow rate were estimated from 32 steady state data points (see Appendix A for details) and is assumed constant because the evaporator geometry remains fixed. The value of these two parameters are 0.89 and 65 cfm respectively. The evaporator exit air temperature is measured at the point where it discharges into the freezer (see Figure 3.3).

$$\frac{h(T_{ma})}{\upsilon(T_{ma})} = (1-f) \cdot \frac{h(T_f)}{\upsilon(T_f)} + f \cdot \frac{h(T_z)}{\upsilon(T_z)}$$

(3.4)
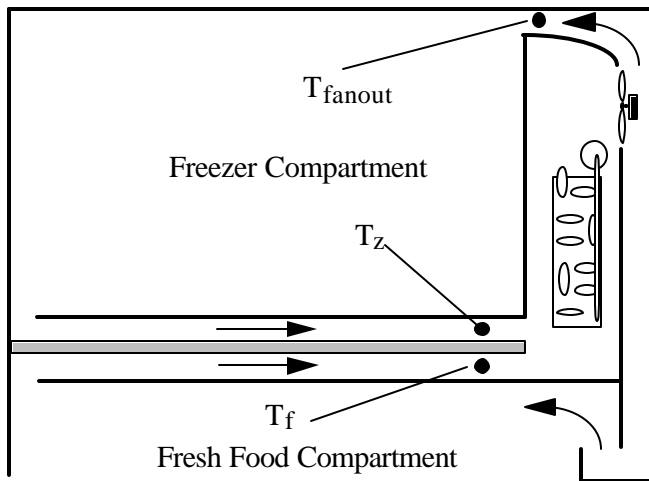
Figure 3.3 Schematic of the evaporator ductwork

With cycling and steady state evaporator capacities thus defined Figure 3.4 compares the evaporator capacity of a cycling refrigerator to one operating under quasi-steady conditions. The refrigerator's capacity shortfall is initially quite large, but diminishes later in the cycle. Once again it should be noted that due to the temperature measurement uncertainties the evaporator capacity is only accurate within ±25 Btu/hr.
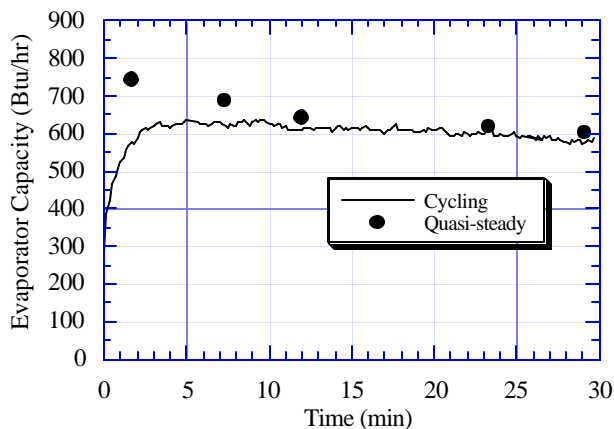
Figure 3.4 Evaporator capacity (T_{amb}=90°F)

During the first ten minutes of the on-cycle the cycling refrigerator operates with a reduced capacity. This reduction in capacity is linked indirectly to the refrigerant migration which occurred during the off-cycle. When the

compressor starts up, most of the refrigerant is located within the evaporator and must redistributed before the refrigerator can begin to operate at quasi-steady efficiency. The initial four to five minutes of the on-cycle mark the highest levels of capacity degradation. It is during this time that the majority of the charge redistribution takes place. When the refrigerator is operating under steady conditions the mass flow through the capillary tube and the compressor are identical; this is not the case immediately after start-up. By the end of the off-cycle condenser is totally filled with superheated vapor, therefore initially the capillary tube has superheated inlet. This superheated inlet severely reduces the mass flow rate of refrigerant flowing through the capillary tube, therefore initially more refrigerant is flowing into the condenser from the compressor than is being removed by the capillary tube. This works to fill the condenser until the compressor and capillary tube mass flow rates balance. As can be seen in Figure 3.5 this process seems to take about five minutes, since the condensing pressure appears to reach quasi-steady levels indicating it is full of refrigerant. This process, in addition to working to fill the condenser, has the disadvantage of reducing the evaporator capacity. Since the capillary tube and compressor mass flow rates are not matched, the net flow rate through the evaporator is reduced which in turn limits the evaporator capacity. Until quasi-steady flow is established in the evaporator, it is likely that the walls of the evaporator are not fully wetted, increasing the refrigerant-side resistance to heat transfer. This would also tend to reduce the evaporator capacity.
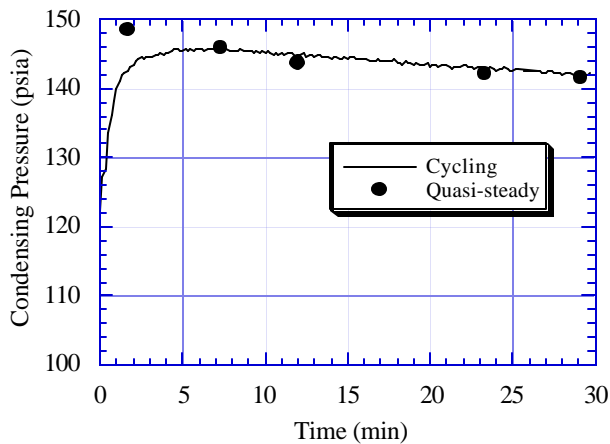
Figure 3.5 Condensing pressure (T_{amb}=90°F)

During the initial five minutes, the capacity degradation occurs as the refrigerator struggles to redistribute the excess charge from the evaporator, however the cycling refrigerator still appears to have a slightly lower capacity for next five minutes especially while operating under 90°F and 100°F ambient conditions. There are several variables which contribute to this degradation. One of these in the level of superheat seen in the evaporator. Figure 3.6 compares the superheat seen in the cycling refrigerator to the quasi-steady machine. During the five minutes in question the cycling refrigerator has between 3 to 5 degrees more superheat than the quasi-steady machine, indicating that the evaporator is starved. This extra superheat increases the fraction of the evaporator which is filled by superheated vapor; since the heat transfer resistance is much higher in the superheated region than in two-phase region, increasing the superheated region reduces effective heat transfer area of the evaporator (Admiraal and Bullard, 1995). An increase in superheat of 3 to 5 degrees represents a reduction of useful (two-phase) evaporator

area by 4 to 6%. This is almost totally accounts for the 4 to 8% reduction in evaporator capacity seen when this superheat is present.
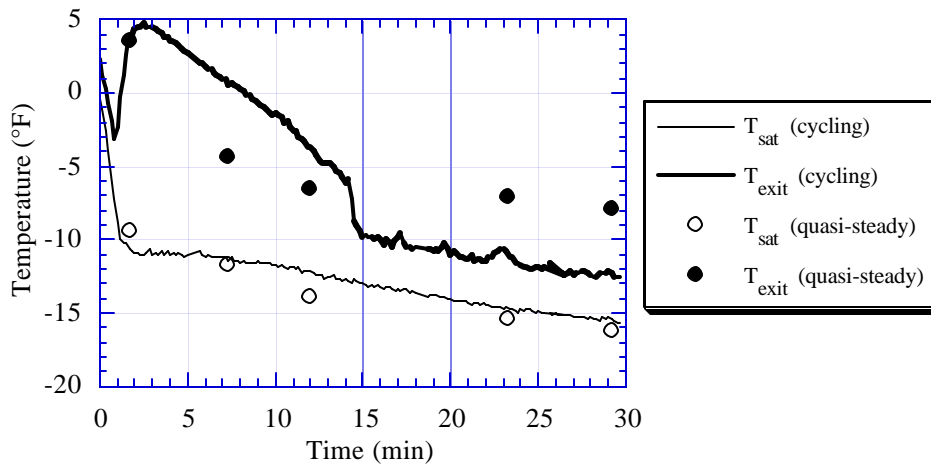
Figure 3.6 Evaporator exit and saturation temperatures (T_{amb}=90°F)

While the starved evaporator explains why the evaporator capacity is lower than the quasi-steady machine even after most of the redistribution has taken place, it does not explain why it's starved. A starved evaporator indicates that some refrigerant which belongs in the evaporator is held up somewhere else. In this particular refrigerator, charge appears to be trapped in the accumulator. Located immediately downstream of the evaporator the accumulator protects the compressor from liquid slugs following start-up. It is possible some of these liquid slugs remain in the accumulator, starving the evaporator of needed refrigerant. To test this theory two surface thermocouples were added to the accumulator, one located at the inlet and a second at the exit. If no refrigerant is present in the accumulator both thermocouples will read the same temperature. However, when liquid is trapped the accumulator acts like an evaporative cooler, reducing the temperature of the superheated refrigerant as it passes over the pool of liquid. Figure 3.7 shows the a plot of the accumulator inlet, exit, and saturation temperatures. As can be seen the temperature profiles are consistent with refrigerant being trapped in the accumulator. In addition this figure indicates refrigerant may remain in the evaporator for as long as 15 minutes, about the same period of time the evaporator appears starved. Calculations indicate as much as 0.5 ounces of refrigerant could held here, more than enough to cause the level of excess superheat seen in Figure 3.6.
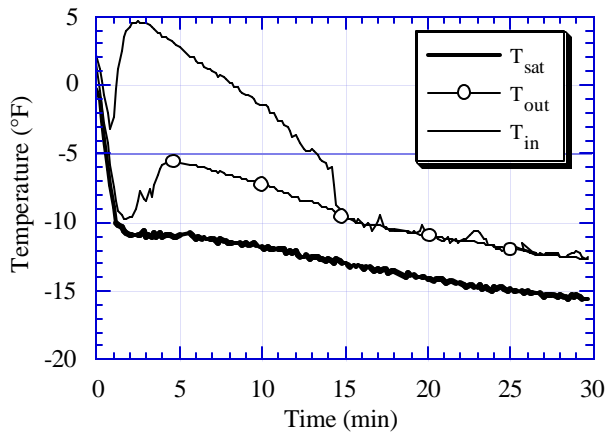
Figure 3.7 Refrigerant trapped in the accumulator after start-up (T_{amb}=90°F)

3.4 Power Penalty

The previous sections have explained and quantified the on-cycle losses reducing the evaporator capacity of the cycling refrigerator. However, not all the on-cycle losses have been explained. As shown in Chapter 2 the cycling refrigerator requires more power than quasi-steady machine. This section explores the reasons why the cycling refrigerator has an increased power requirement.

Figure 3.8 illustrates how the required system power for the cycling refrigerator compares to the quasi-steady machine. The system power includes the power required by compressor and both heat exchanger fans. From this figure it is clear the cycling refrigerator requires more power than the quasi-steady refrigerator. It also demonstrates that the power penalty is initially large, nearly 20 watts, but decreases slowly. By the end of the thirty minute on-cycle, both the cycling and quasi-steady machines have about the same power consumption. Since the power requirements of the heat exchanger fans do not change during steady state and cycling operation the difference seen in Figure 3.8 are caused only by the compressor power requirements.
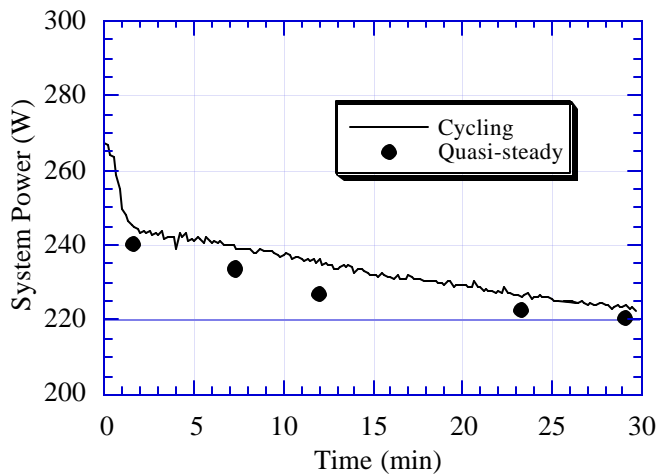
Figure 3.8 System power (T_{amb}=90°F)

15

While redistributing the refrigerant the evaporating and condensing pressures of a cycling refrigerator differ from the quasi-steady machine. The power requirements of a compressor are strongly dependent on the evaporating and condensing pressures, therefore changes in these pressures will effect the power consumption. To estimate the impact of refrigerant redistribution the power penalty due to pressure differences is calculated using the measured pressures, the compressor map, and Equation 3.5. Since the map is a function of pressure (saturation temperature) only, differences the power penalty due to other variables is not included in this comparison.

$$\Delta \dot{W}_{press} = \dot{W}_{map} \left(P_{evap}, P_{cond} \right)_{cyc} - \dot{W}_{map} \left(P_{evap}, P_{cond} \right)_{ss}$$

(3.5)

Figure 3.9 compares the total measured power penalty to the power penalty due solely to differences in the system pressures. If pressure were the only factor influencing compressor performance the power penalty integergrated over the entire cycle would have been approximately 0.5 W-hr. Since the total power penalty is approximately 2 W-hr other factors must be influencing compressor performance. The third bar represents this "other" power penalty, which is initially quite large but slowly decreases over time. One explanation for this additional power penalty is that the compressor is less efficient at lower temperatures (Krause and Bullard, 1994). To test this theory, the ratio of cycling to quasi-steady compressor isentropic efficiencies were calculated using equation 3.6.
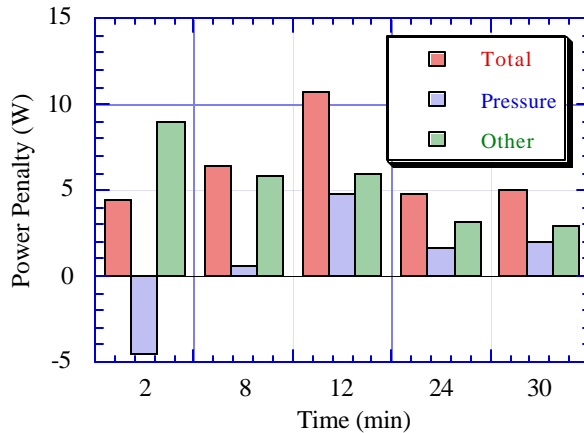
Figure 3.9 Breakdown of power penalty

$$\frac{\eta_{cyc}}{\eta_{q-s}} = \frac{\left(\dfrac{(h_{1,s} - h_{11})}{\dot{W}_{comp}} \right)_{cyc}}{\left(\dfrac{(h_{1,s} - h_{11})}{\dot{W}_{comp}} \right)_{q-s}}$$

(3.6)

Figure 3.10 shows the compressor isentropic efficiency ratio varies during the on-cycle. Initially the cycling compressor has a lower efficiency than the quasi-steady machine, then the ratio slowly increases throughout the on-cycle. The increase in the efficiency ratio parallels to the decrease in the "other" power penalty shown in Figure 3.9. The reasons for the decrease in isentropic efficiency can be seen in Figure 3.11. This figure compares the difference

between quasi-steady and cycling compressor suction and discharge temperatures. Initially both the compressor suction and discharge gases are cooler in the cycling refrigerator. The suction gas quickly reaches quasi-steady temperatures as the suction line heat exchanger begins to operate effectively. Unlike the suction temperature, the cycling compressor's discharge temperature remains cooler through the on-cycle. This lower temperature reduces the discharge enthalpy and therefore the cycling compressor's isentropic efficiency. The discharge temperature is lower because the compressor motor, block, and shell are cooler in the cycling refrigerator. Additionally the cooler compressor means the oil in the compressor sump is more viscous. This increased viscosity could mean the compressor is unable to distribute sufficiently oil to the piston/cylinder, causing mechanical losses which reduce compressor efficiency.
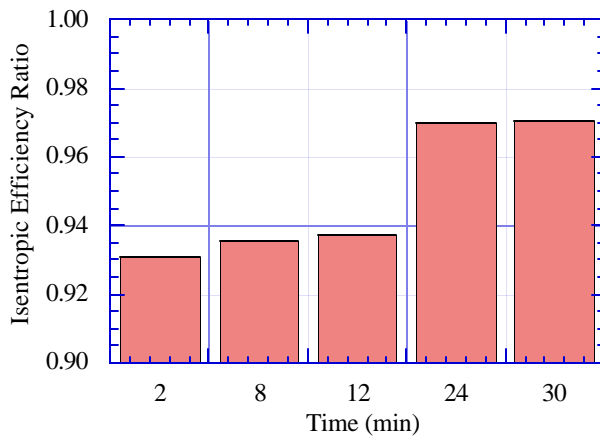
Figure 3.10 Isentropic efficiency ratio (T_{amb}=90°F)
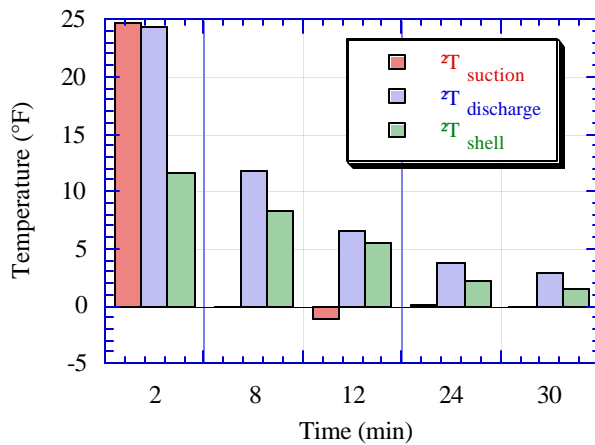
Figure 3.11 Differences in suction and discharge temperatures (T_{amb}=90°F)

17

Chapter 4: Eliminating Cycling Losses

The previous Chapters have shown that most of the cycling losses are associated with the migration of refrigerant from the condenser to the evaporator during the off-cycle. This migration reduces the refrigerator's efficiency in two ways. First the migration warms the aluminum evaporator, which then must be cooled during the on-cycle reducing the amount of heat removed from the air. Second, it necessitates refrigerant redistribution during the initial five to ten minutes of on-cycle which also reduces the refrigerator efficiency. Changes in refrigerator design which reduce or eliminate the impact of these losses could increase the refrigerator's efficiency to the level achieved in quasi-steady operation. This Chapter explores several possible design changes which could help achieve this goal.

4.1 Solenoid Valve

Since off-cycle refrigerant migration appears to be the root cause of most cycling losses seen in the experimental refrigerator any design change which would eliminate this should improve the refrigerator's efficiency. One possible solution is to install a solenoid valve after the condenser as shown in Figure 4.1.
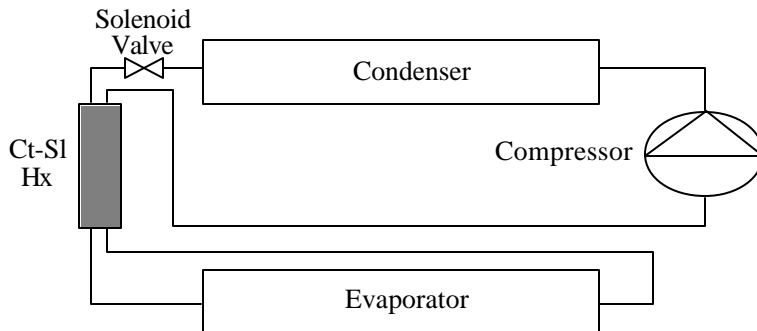
Figure 4.1 Schematic of refrigeration loop equipped with solenoid valve

Controlling this valve so it is open when the compressor is running and closed when it is not, would effectively isolate the evaporator from the condenser during the off cycle, preventing any refrigerant migration. Wang and Wu (1989) installed a solenoid valve on a room air conditioner and found a 4% reduction in power required by the compressor. Janssen et al. (1992) conducted similar work using a breadboard-style freezer and found an increase in system performance of 6%. Finally, Okazaki (1992), cited in Radermacher (1994), claimed a refrigerator equipped with a rotary compressor and a solenoid valve uses 22% less energy than a similar refrigerator without a valve. While this sounds like the ideal solution there are several drawbacks which must be considered. First, refrigerant migration allows the system pressure to equalize reducing the required starting torque of the compressor motor (Stoecker and Jones, 1986). Installing solenoid valve would increase the required starting torque and therefore the cost of the compressor motor. Second, adding valves increases the number of moving parts in the refrigerator. As the number of moving parts increases so do the chances of failure reducing system reliability. Since refrigerator reliability and first cost are extremely important these drawbacks must be weighed against the potential savings.

4.2 Compressor Type (Reciprocating vs. Rotary)

The reduction of the noise is one goal shared by all refrigerator manufacturers. For this reason compressor design (reciprocating vs. rotary) has been a subject of recent debate. Rotary compressors are typically quieter than

reciprocating compressors since the gas flow is continuous and no suction valve is required (ASHRAE, 1992). Therefore from a noise reduction standpoint the rotary compressor is the clear choice. However, a recent study by Krause and Bullard (1994) pointed out a significant cost associated with rotary compressors used in domestic refrigerators.

This study found during cycling the oil sump of a rotary compressor trapped almost an ounce of refrigerant immediately after start-up. This starved the evaporator reducing its effective heat transfer area and therefore its efficiency. According to Grebner and Crawford (1992) the amount of refrigerant dissolved in oil is proportional to pressure and inversely proportional to temperature. During cycling the compressor shell is cooler than during continuous operation (Appendix D). This cool shell means the oil in the sump is also cooler allowing more refrigerant to dissolve into the oil. This problem is exaggerated since the oil sump is located on the high-side (discharge) of the compressor where the pressure is high. Switching to a reciprocating compressor with a low-side (suction) sump would solve this problem and reduce cycling losses.

In our test unit equipped with a reciprocating compressor less than one tenth of a ounce of extra refrigerant dissolves in the oil sump during cycling (see Appendix D). This suggests a system equipped with a reciprocating compressor should approach quasi-steady operation quicker than the same system equipped with a rotary compressor. Therefore a reciprocating compressor should be chosen if the goal is to simply reduce cycling losses. Since these compressors are generally noisier than rotary compressors, the benefit of a more efficient refrigerator must be weighed against the cost of a noisier one.

4.3 Accumulator

Refrigerators are sometimes equipped with accumulators to protect the compressor from slugs of refrigerant, especially during start up after an off-cycle. As pointed out in the previous Chapter refrigerant can be trapped in the accumulator for ten minutes. This lack of refrigerant can starve the evaporator reducing system efficiency. One solution to this problem is to remove the accumulator. While this eliminates any possibility of charge being trapped, it leaves the compressor unprotected. If the accumulator were placed closer to the compressor instead of the evaporator, the heat from the compressor would quickly evaporate any trapped liquid trapped thus speeding up refrigerant redistribution. However, net energy savings would be positive only if refrigerating effect forgone is less than the cycling loss due to charge maldistribution. In the test refrigerator these effects are similar in magnitude.

4.4 Heat Exchanger Fans

Speeding up refrigerant redistribution should make the refrigerator operate more quasi-steady and therefore reduce cycling losses. One possible method of doing this is by controlling the heat exchanger fans. In theory controlling the speed of the heat exchanger fans it should be possible to fill or empty the evaporator depending upon the needs of the system.

Changing the speed of the heat exchanger fan changes the air side heat transfer coefficient, quantified by Cavallaro and Bullard, 1995. Since heat transfer through the refrigerator heat exchangers is dominated by air side resistance, changes in the air side heat transfer coefficient significantly affect performance. To meet the new heat transfer requirements imposed by air-side changes the refrigerant side properties, especially temperature or pressure,

must change. Assuming this argument is correct, the heat exchanger fans can be used indirectly manipulate refrigerant side properties making it possible to alter the distribution of charge within the refrigerator.

Since the interaction between the heat exchanger fans and the rest of the refrigerator is complex it is difficult to know exactly how to control these fan in order to properly distribute the charge. Therefore a detailed analysis was necessary to fully understand the consequences heat exchanger fan speed. This analysis was performed using the refrigerator simulation program RFSIM (Goodson and Bullard, 1994).
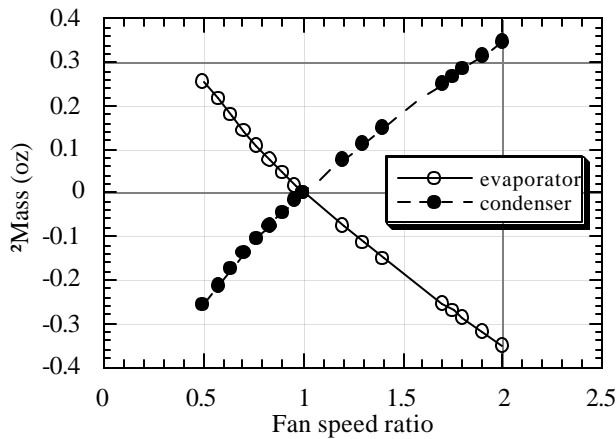
Figure 4.2 Effect of condenser fan speed on charge distribution

Using RFSIM it's possible to determine the effect of increasing or reducing the condenser and evaporator fan speed on charge distribution and other important system parameters. Figure 4.2 shows how the condenser fan speed affects the distribution of charge in the refrigerator. Reducing the condenser fan speed shifts charge from the condenser to the evaporator. Conversely, increasing the condenser fan speed moves charge from the evaporator to the condenser. During the initial portions of the on-cycle the evaporator is starved, therefore decreasing the condenser fan speed may help refill the evaporator and improve performance. A similar study was conducted on the evaporator fan. Once again fan speed changed the distribution of charge within the refrigerator. However, changing the speed of the evaporator fan had one drawback not seen when manipulating the condenser fan. A 50% reduction in the evaporator fan speed reduced the system COP by 14% (too large to be affected by the reduction in fan power requirement), because of the reduction in air side heat transfer coefficient or temporary "loss of UA." The same reduction in condenser fan speed 50% only reduced COP by 8%. For this reason the condenser fan should be used to redistribute charge, since the desired results can be achieved with less effect on COP.

As described in Chapter 3 the evaporator is starved immediately after start up (T_{amb}=90°F), therefore slowing the condenser fan during the initial portion of the on-cycle should fill the evaporator and reduce the cycling losses. To test this theory an experiment was run on the Amana test unit. During the first five minutes of the on-cycle the condenser fan was slowed to 1320 RPM then increased to the nominal speed (1680 RPM) for the remainder of the cycle.
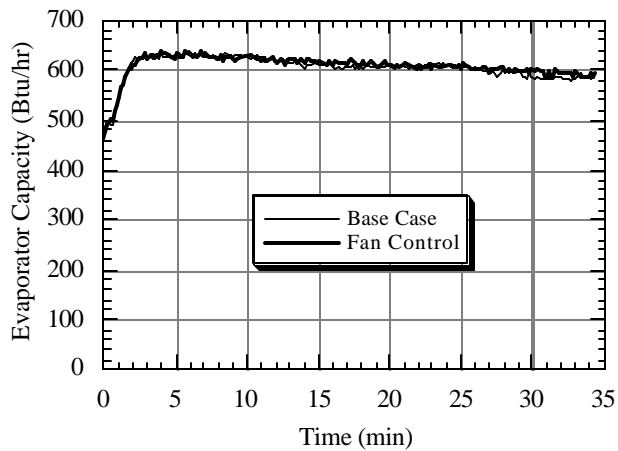
Figure 4.3 Effect of condenser fan control on evaporator capacity

Figure 4.3 indicates that controlling the condenser fan speed during the initial portions of the on-cycle had a negligible affect on evaporator capacity. This is not totally unexpected. While changing the condenser fan tends to refill the evaporator it does not address the fundamental reason the evaporator is starved, the accumulator. The accumulator holds charge during the first ten minutes of the cycle and until this charge is removed the system will not reach quasi-steady performance. For this reason manipulating the heat exchanger fans had little effect on cycling performance of this accumulator-equipped refrigerator. Therefore if the reason for charge maldistribution is something which fan speed does not affect (e.g. the accumulator or temperature of the oil sump) changing the speed of the condenser fan does nothing to reduce these cycling losses. However, in system with a reciprocating compressor and no accumulator, where maldistribution is caused by a poorly matched capillary tube/compressor combination, controlling the heat exchanger fans may help reduce cycling losses under off-design conditions.

Chapter 5: Conclusions and Recommendations

This report identified and quantified the cycling losses in a domestic refrigerator-freezer. During cycling operation the refrigerator was found to operate between 5 and 25% less efficient than the corresponding quasi-steady machine. The cycling refrigerator operates with an evaporator capacity between 3 and 17% less than the quasi-steady refrigerator, while at the same time requiring between 1 and 9% more power to operate.

This refrigerator performance degradation was attributed to several factors, the most important being the refrigerant migration and the thermal mass of the evaporator and compressor. During the off-cycle refrigerant migrates from the condenser to the evaporator as the system pressures equalize. The off-cycle migration increases the temperature of the evaporator and necessitates refrigerant redistribution during the on-cycle, and thereby tends to reduce system performance. The increased power requirements, traced to the compressor, result from slight differences in system pressure and the reduced compressor efficiency due to a cool compressor.

With the cycling losses identified, several possible refrigerator design changes were suggested. It appears that a refrigerator equipped with a reciprocating compressor, solenoid valves to isolate the condenser, and no accumulator should operate in a nearly quasi-steady manner. In addition using the condenser fan to accelerate charge redistribution was investigated. However, since the experimental refrigerator was equipped with an accumulator which held up some charge manipulating the condenser fan showed little payoff.

Some other design changes, which may reduce cycling losses but were not considered in this report are charge minimization and improved capacity control. Many of the losses seen in the experimental refrigerator were due to refrigerant migration or redistribution. If the amount of refrigerant in the system were reduced, these losses could in theory be minimized. Second, since most losses occur during the initial portion of the cycle, increasing the length of the on-cycle reduces the proportional impact of these losses. If the refrigerator could be designed to operate with a variable capacity it may be possible to reduce the cycling frequency without increasing the required power. However, since both of these approaches require major design changes, studies should initially be conducted using simulation models to gain a understanding of the impact these design changes have on other system parameters before designing experiments.

References

Admiraal, D.M., and C.W. Bullard, "Heat Transfer in Refrigerator Condensers and Evaporators," University of Illinois at Urbana-Champaign, ACRC TR-48, 1993.

Admiraal, D.M., and C.W. Bullard, "Heat Transfer in Refrigerator Condensers and Evaporators," ASHRAE Transactions, Vol. 101, Part 1, 1995.

AHAM, "Household refrigerators/household freezers," ANSI/AHAM STANDARD HRF-1-1988, Chicago, IL, pp. 1-94, 1988.

ASHRAE, ASHRAE Handbook HVAC Systems and Equipment, 1992.

Beckwith, T.G. and R.D. Marangoni, Mechanical Measurements, Addison-Wesley Publishing Company, Menlo Park CA, 1990.

Cavallaro, A.R. and C.W. Bullard, "Effects of Varying Fan Speed on a Refrigerator/Freezer System," University of Illinois at Urbana-Champaign, ACRC TR-63, 1994.

Cavallaro, A.R., "Air side forced, natural, and mixed convection," ME-323 project, 1992.

Grebner, J.J. and R.R. Crawford, "Measurement of Pressure-Temperature-Concentration Relations for Mixtures of R-12/Mineral Oil and R-134a Synthetic Oil," ASHRAE Transactions, Vol. 99, Part 1, pp. 387-396, 1993.

Goodson, M.P., and C.W. Bullard, "Refrigerator/Freezer system modeling," University of Illinois at Urbana-Champaign, ACRC TR-61, 1994.

Hamm, E.K., "Design, Construction, and Evaluation of a Domestic Household Refrigerator, Environmental Test Chamber," University of Illinois at Urbana-Champaign, ACRC TR-13, 1994.

Incropera, F.P. and D.P. DeWitt, Fundamentals of heat and mass transfer, John Wiley & Sons, Inc., New York, NY, 1985.

Kline, S.J. and F.A. McClintock, "Describing Uncertainties in Single-Sample Experiments," Mechanical Engineering, January 1953.

Krause, P.E., personal communication, University of Illinois at Urbana-Champaign, 1994.

Krause, P.E. and C.W. Bullard, "Cycling and Quasi-Steady Behavior of a Refrigerator," University of Illinois at Urbana-Champaign, ACRC TR-58, 1994.

Peixoto, R. and C.W. Bullard, "A Design Model for Capillary Tube-Suction Line Heat Exchangers," University of Illinois at Urbana-Champaign, ACRC TR-53, 1994.

Porter, K.J. and C.W. Bullard, "Modeling and Sensitivity Analysis of a Refrigerator/Freezer System," University of Illinois at Urbana-Champaign, ACRC TR-31, 1992.

Reyes-Gavilan, J., T. Flak, and T. Tritcak (Witco Corporation), "Lubricants for Refrigeration Compressor Applications," unpublished paper presented at the International CFC and Halon Alternatives Conference, Washington DC, 1993.

Reeves, R.N., C.W. Bullard, and R.R. Crawford, "Modeling and Experimental Parameter Estimation of a Refrigerator/Freezer System," University of Illinois at Urbana-Champaign, ACRC TR-9, 1992.

Rubas, P.J. and C.W. Bullard, "Assessment of Factors Contributing to Refrigerator Cycling Losses," University of Illinois at Urbana-Champaign, ACRC TR-45, 1993.

Rubas, P.J., and C.W. Bullard, "Factors Contributing to Refrigerator Cycling Losses," International Journal of Refrigeration, Vol. 18, pp. 168-176, 1995.

Staley, D.M., C.W. Bullard, and R.R. Crawford, "Steady-State Performance of a Domestic Refrigerator/Freezer Using R12 and R134a," University of Illinois at Urbana-Champaign, ACRC TR-22, 1992.

Stoecker, W.F., and J.W. Jones, Refrigeration and Air Conditioning, Second edition, McGraw-Hill, New York, 1986.

Van Wylen, G.J. and R.E. Sonntag, Fundamentals of Classical Thermodynamics, John Wiley and Sons, New York, NY, 1986.

Wang, J. and Y. Wu, "Start-up and shut-down operation in a reciprocating compressor refrigeration system with capillary tubes," International Journal of Refrigeration, Vol. 13, pp. 187-190, 1989.

White, F.M., Heat and Mass Transfer, Addison-Wesley, Menlo Park, CA, 1988.

Woodall, R.J., personal communication, University of Illinois at Urbana-Champaign, 1995.

Appendix A: Parameter Estimation and Validation

In order to perform the experimental data reduction values for physical parameters such as evaporator fan volumetric flow rate, air split fraction, and refrigerator cabinet heat transfer conductance are necessary. Values for these parameters have been estimated by previous researchers working with this refrigerator. However, since their work the refrigerator has undergone many modifications which may have caused changes in these parameters. This Appendix presents the results of a study conducted to determine whether or not the evaporator fan volumetric flow rate, air split fraction, and cabinet heat transfer conductance had changed significantly since they were last estimated.

A.1 Refrigerator Cabinet Heat Transfer Conductance

The refrigerator cabinet heat transfer conductance allows the heat transfer through the cabinet walls to be calculated using equation A.1.

$$Q_{wall} = UA_{frig}\left(T_{frig} - T_{amb}\right) + UA_{frez}\left(T_{frez} - T_{amb}\right)$$

(A.1)

Values for UA_{frig} and UA_{frez} were estimated by Rubas and Bullard (1993) using the reverse heat leak test. Their work concluded the values of UA_{frig} and UA_{frez} were 0.898 and 0.530 [W/°F] respectively.

Over time the physical properties of the cabinet insulation can change causing changes in the heat transfer conductance. For this reason it is necessary to verify whether the heat transfer conductance had changed since last estimated by Rubas. The make this determination a single reverse heat leak test was run. To perform the reverse heat leak test the environmental chamber was set to 50°F and the fresh food and freezer compartments were set to 85°F. To eliminate any temperature gradients and replicate the test conditions used by Rubas, the evaporator fan and a small 14 cfm muffin fan were run.
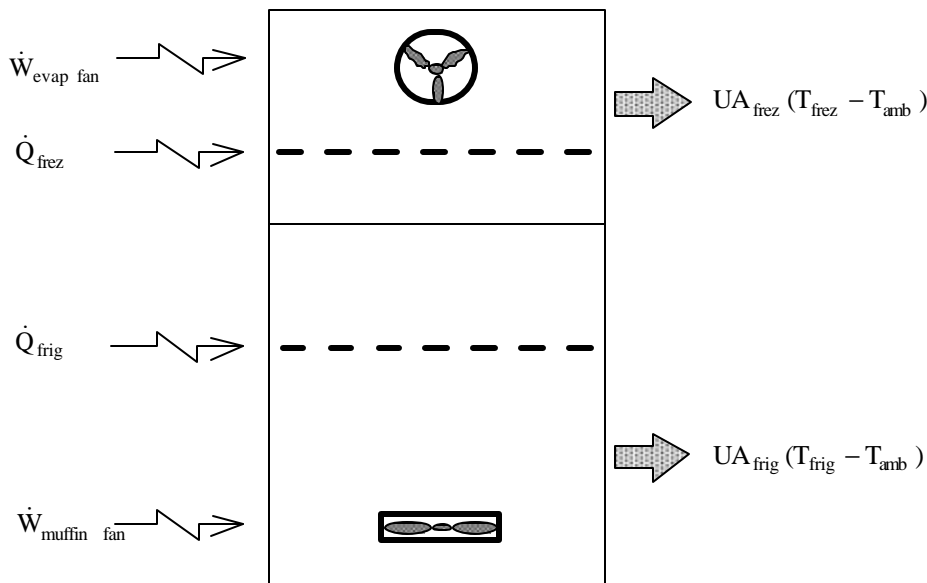
Figure A.1 Control volume around refrigerator cabinet

By using the control volume shown in figure A.1 an energy balance is performed on the refrigerator. Equation A.2 defines the heat follow into control volume, while equation A.3 represents the heat flow out of the control volume.

$$\dot{Q}_{in} = \dot{Q}_{frez} + \dot{Q}_{frig} + \dot{W}_{evap.fan} + \dot{W}_{muf.fan}$$

(A.2)

$$\dot{Q}_{out} = UA_{frig}\left(T_{frig} - T_{amb}\right) + UA_{frez}\left(T_{frez} - T_{amb}\right)$$

(A.3)

The heat flow into the control volume is made up of power to the two fans and the heaters. Heat transfer out of the control volume is only the heat transfer through the refrigerator walls. Any internal heat transfer (through the mullion) is ignored since both the fresh food and freezer compartments are set to identical temperatures. By comparing the measured heat flow into the refrigerator and the calculated heat flow out of the refrigerator the accuracy of the cabinet heat transfer conductance can be tested. Using data from the reverse heat leak test 42.7 watts entered the control volume while 44.5 watts leak through the walls. This is a difference of 1.8 watts between the calculated and measured heat flow. The original estimations made by Rubas proved to be no more accurate than 2.0 watts. Therefore, the heat transfer conductance has not changed appreciably.

A.2 Evaporator Volumetric Flow Rate and Air Split Fraction

The evaporator volumetric flow rate and the air split fraction are two parameters needed to make the air side evaporator load calculations used extensively in the cycling analysis presented earlier. For this reason accurate values for both parameters are an essential part of the cycling analysis.

The air flow through the Amana evaporator is broken into two streams. One stream circulates air through the freezer compartment while the second circulates air through the fresh food compartment. In order to make air side evaporator load calculations both the total volumetric flow rate and the fraction of air circulating through each compartment must be estimated. Previous work by Reeves and Bullard (1992) and Admiraal and Bullard (1993) have shown the volumetric flow rate is between 65 and 70 cfm and the air split fraction is about 0.85. However, since this work was completed the Amana refrigerator has undergone extensive modifications especially around the evaporator. For this reason two new data sets were gathered and parameters estimated.
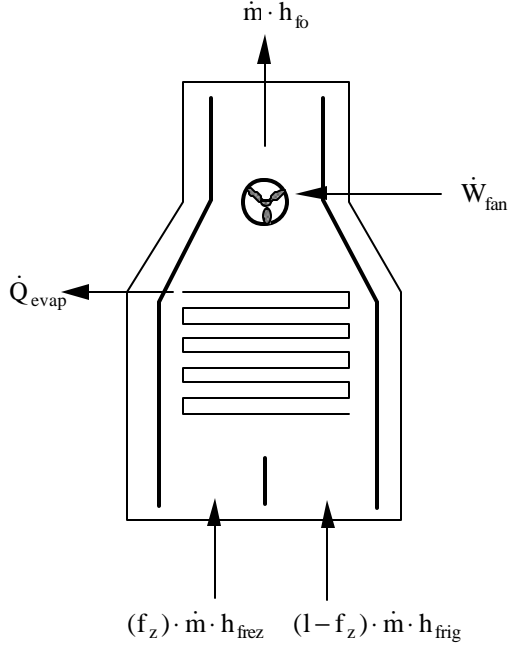
Figure A.2 Air split fraction control volume

Figure A.2 shows the control volume used to estimate the air split fraction and volumetric flow rate. Equations A.4-5 describe the air side. Equation A.6 represents the heat removed from the air. Instead of using a refrigerant side energy balance the sum of all heat transfer and power entering the refrigerator cabinet is used. Finally, to simultaneously estimate both air split fraction and volumetric flow rate, calculated from $\dot{m}$, the objective function shown in equation A.7 is minimized. Results are given in Table A.1.

$$\frac{h(T_{ma})}{\rho(T_{ma})} = (1-f) \cdot \frac{h(T_f)}{\rho(T_f)} + f \cdot \frac{h(T_z)}{\rho(T_z)}$$
(A.4)

$$\dot{Q}_{evap} = \dot{m}(h(T_{ma}) - h(T_{fo})) + \dot{W}_{fan}$$
(A.5)

$$\dot{Q}_{evap} = \dot{Q}_{frez} + \dot{Q}_{frig} + UA_{frig}(\Delta T_{frig}) + UA_{frez}(\Delta T_{frez}) + \dot{W}_{fan}$$
(A.6)

$$F_{obj} = \left| \frac{\sum_{i=1}^{n}(T_{fo\,meas} - T_{fo\,calc})}{n} \right| + 2 \cdot \sqrt{\frac{\sum_{i=1}^{n}((T_{fo\,meas} - T_{fo\,calc}) - bias)^2}{n-1}}$$
(A.7)

Table A.1 Air split fraction and volumetric flow rate

	Spring 94	Spring 95
Air split fraction	0.860	0.885
Volumetric flow rate	63 cfm	64 cfm
Precision interval (F_{obj})	0.4°F	0.2°F

For the Spring 94 data set the values of air split fraction and volumetric flow rate which minimized equation A.7 where 0.860 and 63 cfm. The split fraction and volumetric flow rate found for this data set were slightly different than the values previously estimated by Admiraal in 1993. Some of the differences can probably be attributed to changes in the evaporator geometry which may have occurred while adding instrumentation. A more likely answer is shown in figure A.3. This figure shows how the objective function varies with both air split fraction and volumetric flow rate. The minimum division is chosen to be 0.5°F because it is possible that the thermocouples used to measure the temperature difference have that much uncertainty (Rubas and Bullard, 1993). Due to our calibration procedures, and observations of data repeatability, we feel that our measurements are more accurate than ± 0.5°F.

In Figure A.3 the white valley represents points where the confidence interval is less than 0.5°F. Since this is the maximum accuracy of the thermocouples this means the air split fraction is between 0.84 and 0.88 while the volumetric flow rate is between 60 and 67 cfm. Now understanding that there are a range of values which can satisfy the objective function the values estimated for the spring 94 data set compare well with the values estimated by Admiraal.

A second set of data was taken in the spring of 1995. The same analysis as performed on the Spring 94 was repeated for this data set. Table A.1 indicates that the value for air split fraction and volumetric flow rate are 0.885 and 64 cfm. Figure A.4 shows a contour plot of the confidence interval for the Spring 95 data. This figure indicates the volumetric flow rate is (at worst) between 61 and 72 cfm while the air split fraction is between 0.87 and 0.90. The volumetric flow rate is comparable to the values estimated for the Spring 94 data set, but the air split fraction is considerably different. One major difference between the two data sets is the presence of foam blocks placed in between the return bends of the evaporator. These blocks prevent warm air from bypassing the evaporator and were not present in the Spring 94 data sets, but were replaced before the Spring 95 data set was taken. It is also important to note that the refrigerator has undergone extensive modifications during the year between the Spring 94 and 95 data sets. During this time the mullion and temperature control panel were removed and replaced. It would not be surprising if these changes physically altered the air split fraction.

As can be seen from the above discussion it is hard to nail down the air split fraction and volumetric flow rate given the accuracy of our instrumentation and the limited size of our data sets. Larger data sets spanning a wider range operation conditions would definitely help reduce the uncertainty in the above calculations. It is clear however that in between the Spring 94 and Spring 95 data sets air split fraction changed. It is believed that this change is due to addition of foam blocks in the return bends of the evaporator and modifications made to the refrigerator between data sets.
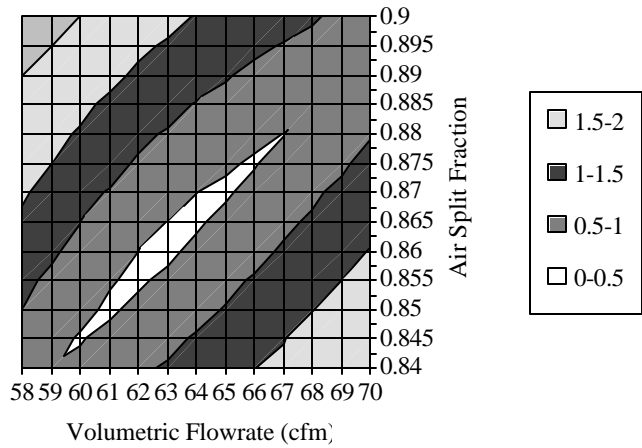
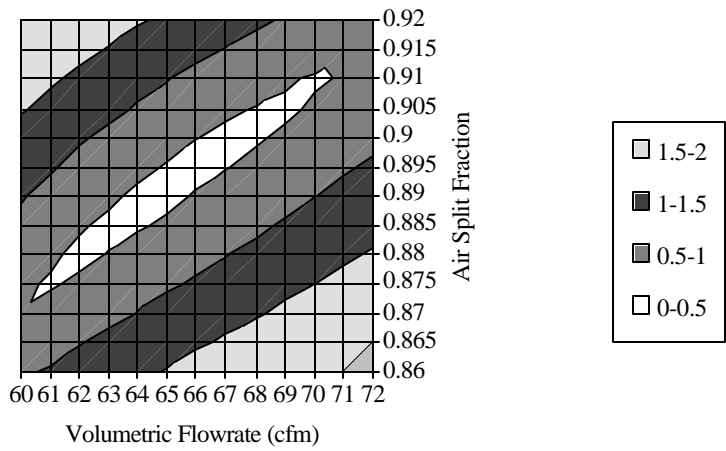Figure A.3 Confidence interval valley for Spring 94 data

Figure A.4 Confidence interval valley for Spring 95 data

Appendix B: Temperature Uncertainty and Error Propagation

In order to quantify the cycling losses of the test refrigerator it is necessary to have an accurate estimation of its evaporator capacity. The analyses presented earlier relied exclusively on an air-side energy balance to make this calculation. Since the temperature difference across the evaporator is small, usually less than 10°F, this method of calculating evaporator capacity is extremely sensitive to the accuracy of the air-side instrumentation. This Appendix will quantify the uncertainty associated with the temperature measurements as well as show how this uncertainty affects the calculation of the evaporator capacity.

B.1 Thermocouple Uncertainty

Temperature, pressure, and power measurements are recorded using a computer based data acquisition system manufactured by Strawberry Tree Incorporated. The current system is capable of recording 48 individual temperature, 5 pressure, and 5 power measurements simultaneously. This section will discuss only the uncertainty associated with the temperature measurements. A complete discussion of the uncertainty associated with the pressure and power measurements are covered in Rubas and Bullard (1993).

The uncertainty a measurement can be divided into two parts, a bias error and a random error. The bias error is a constant off-set by which the measurement differs from the actual value (Marangoni and Beckwith, 1990). Random error represents the ability of the measuring device to duplicate the same measurement more than once. Both sources of error are present while making temperature measurements. The bias error is caused by the thermocouples as well as the data acquisition system. The bias associated with data acquisition system is eliminated by carefully calibrating the terminal panels with a constant temperature water bath (Krause and Bullard (1994) describe this method). This still leaves the bias error associated with the thermocouple itself. According to the manufacturer this error is ±0.5°F. The rest of thermocouple uncertainty is due to the random error. Originally, the thermocouples were estimated to have a random error of approximately ±0.5°F (Rubas and Bullard, 1993). However, more recent tests conducted to demonstrate the repeatability of the measurement system showed the random error was closer to ±0.2°F. Combining both random and bias error, the absolute uncertainty for our temperature measurements is ±0.54°F.

The above analysis gives a description for the error associated with an absolute temperature measurement. Throughout the body of this report the emphasis has been on comparing the temperature of a cycling refrigerator relative the quasi-steady refrigerator. Assuming the bias error is identical during both the cycling and steady state, the only important uncertainty in a comparative analysis such as this one is random error. Therefore, the temperature measurements appear to be accurate within ±0.2°F when comparing the cycling and quasi-steady refrigerators.

The evaporator capacity calculations performed throughout this report are based on air-side temperature measurements. For this reason, it necessary to estimate the uncertainty in the temperature measurements used in these calculations. Initially one would estimate the uncertainty should be ±0.2°F, since we are comparing the cycling and quasi-steady refrigerators. However there is another source of error that is not immediately obvious. This error is caused by our limited ability to experimentally match the evaporator inlet air streams. Ideally the air streams from the freezer and fresh food compartments would be exactly the same in the cycling and quasi-steady refrigerators. However, in practice the ability to match these air streams is limited by the accuracy of the controllers that maintain

the fresh food and freezer compartment temperatures during steady operation. This inability to match the evaporator inlet temperatures introduces an additional ±0.15°F error. Taking into account both the random error and the error produced while matching the inlet air streams, the accuracy of temperatures used to estimate the evaporator capacity is ±0.25°F.

B.2 Error Propagation

In the previous section the uncertainty for the temperature measurements used to calculate the evaporator capacity were found to be ±0.25°F. To understand how this uncertainty affects the accuracy of the evaporator capacity calculations it is necessary to propagate the error. There are many ways to perform this propagation, but the method used was suggested by Kline and McClintock (1953) and is shown in Equation B.1. Using this method and assuming the properties of air remain constant the accuracy of the evaporator capacity calculation is ±25 Btu/hr given an ±0.25°F uncertainty in the temperature measurements.

$$u_f = \sqrt{\left(u_{x1}\frac{\partial f}{\partial x1}\right)^2 + \left(u_{x2}\frac{\partial f}{\partial x2}\right)^2 + ... + \left(u_{xn}\frac{\partial f}{\partial xn}\right)^2}$$

(B.1)

Appendix C: Off-cycle Refrigerant Migration

When the refrigerator shuts off after the on-cycle, refrigerant migrates through the capillary tube from the condenser to the evaporator until the pressures equalize. The migrating refrigerant not only raises the pressure in the evaporator but also increases its temperature. Since the evaporator is located inside the refrigerator cabinet, it is possible that the evaporator could become warmer than the air and reject heat into the compartment which then must removed from the cabinet during the on-cycle. This Appendix provides an in-depth look into the factors contributing to the amount of energy transported by off-cycle migration and whether any of this energy is transferred into the refrigerator cabinet.

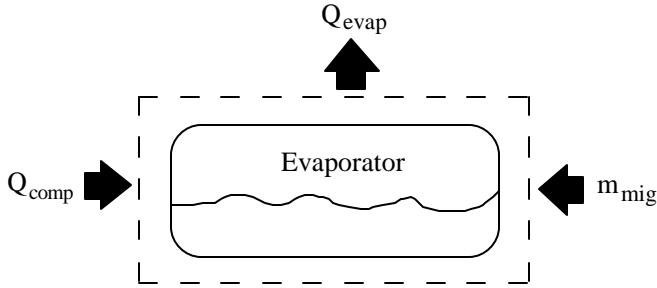## C.1 Change in Energy of the Evaporator

Figure C.1 Control volume around evaporator

To calculate the change in energy of the evaporator it is first necessary to select an appropriate control volume. Figure C.1 shows the control volume drawn around the evaporator. The energy of this control volume is changed by interactions with the surroundings. Theses interactions include free convection from the evaporator (Q_{evap}), conduction from the compressor (Q_{comp}), and finally the addition of mass to evaporator from the condenser (m_{mig}). Actually, some refrigerant migrates from the evaporator to the compressor oil sump during the off-cycle, but this is small (approximately 0.3 oz) compared to the mass of refrigerant migrating from the condenser (approximately 3.5 oz) and can be neglected. The change in energy of the evaporator can be calculated in two ways. First method is to estimate the amount of energy entering and leaving the evaporator during the off-cycle. The second method is to calculate difference in the total energy of the evaporator at the beginning (1) and end (2) of the off-cycle, see Equation C.1.

$$dE_{evap} = E_{mig} - Q_{evap} = E_2 - E_1$$

(C.1)

To estimate the change in energy of the evaporator using the first method, it is necessary to estimate the magnitude of the energy transfer through heat transfer and refrigerant migration. The heat transfer with the surroundings is initially assumed negligible, but will be estimated later to confirm this assumption. This leaves only the energy associated with the migrating refrigerant. Since mass is crossing the control surface the energy added to the evaporator includes both the internal energy of the refrigerant as well as the flow work done by the migrating refrigerant. Since the migration process is very unsteady, the flow work term is hard to estimate, therefore it is necessary to estimate the energy change in the evaporator based on the total energy of the system at states 1 and 2.

The total energy of the evaporator consists of the energy associated with the refrigerant and the aluminum, Equation C.3. Therefore the change in energy of the evaporator during the off-cycle, state 1 to state 2, is shown in Equation C.4. To calculate this change, estimates are needed for the temperature and mass of refrigerant in the evaporator at the beginning and end of the off-cycle. The temperatures of the refrigerant and aluminum were found to be equal by monitoring surface and immersion thermocouples. For these calculations, they are obtained from the thermocouple located near the middle of the evaporator. The mass of refrigerant in evaporator at the beginning of the off-cycle is estimated using RFSIM (Goodson and Bullard, 1994). The mass of refrigerant in evaporator at the end of the off-cycle is be calculated using Equation C.5, equal to the total charge less charge located in the condenser, liquid line, and compressor, assuming the other components such as the suction line and capillary tube contain very little refrigerant. The refrigerant in the evaporator is assumed two-phase, therefore the internal energy of the refrigerant is estimated as shown in Equation C.6. With these assumptions and measured data it is possible to estimate the energy transferred to evaporator during the off-cycle.

$$E_{evap} = E_{alum} + E_{ref}$$

(C.3)

$$\Delta E_{evap} = (m \cdot C)_{alum} \cdot (T_2 - T_1) + (m_1 + m_{mig})u_2 - m_1 u_1$$

(C.4)

$$m_2 = m_{tot} - \frac{V_{cond}}{\upsilon(T,P)_{cond}} - \frac{V_{liq\,line}}{\upsilon(T,P)_{liq\,line}} - \frac{V_{comp}}{\upsilon(T,P)_{comp}} - m_{oil}(T,P)$$

(C.5)

$$u = f\left(T, \upsilon = \frac{Vol_{evap}}{m_{ref}}\right)$$

(C.6)

Table C.1 Evaporator energy change during the off-cycle

Tamb [°F]	?Eevap [Btu/cyc]	?Ealum [Btu/cyc]	?Eref [Btu/cyc]
100	13.5	11.4	2.1
90	14.6	12.4	2.2
75	16.6	14.2	2.4
60	16.5	14.0	2.5

Table C.1 quantifies the energy associated with refrigerant migration at four different ambient temperatures. Generally it was found that more energy is transferred as the ambient temperature is lowered, because more mass is transferred from the condenser in these cases. Another important observation is that 85% of the energy change is associated with heating the aluminum evaporator mass. This is an important observation since the weak link in the above analysis is the predicted initial evaporator charge. As noted above this value is estimated using RFSIM. According Woodall (1995) the model tends to underpredict the subcooling and therefore amount of refrigerant in the condenser. Since charge is conserved underpredicting the condenser charge overpredicts the evaporator charge at the beginning of the off-cycle. To get an order of magnitude estimate indicating how this uncertainty could affect the prediction of energy associated with refrigerant migration, it was assumed that no charge was initially located in the evaporator. Since is the worst possible situation it possible to put an upper bound on the energy transferred through refrigerant migration. In general this assumption increased the energy transferred to the evaporator 2 Btu. This is a

gross exaggeration of the effect, but it demonstrates that small uncertainties in the initial evaporator charge inventory do not significantly effect the prediction of energy transferred through refrigerant migration.

So far in this section we have considered the evaporator to be adiabatic, so none of the energy transported to the evaporator is transferred into the cabinet. This means there is no direct loss associated with off-cycle migration, however Table C.1 reveals an important indirect loss. Between 11.4 and 14.0 Btu of heat are added to the aluminum evaporator. During the on-cycle this heat must be removed from the evaporator by the refrigerant reducing the amount of useful work done cooling the air.

C.2 Heat Transfer between the Evaporator and the Air

The above discussion assumed the evaporator was adiabatic, that is no heat transfer with the surroundings. This section will examine whether or not this is a good assumption. Figure C.2 shows a plot comparing the temperature of the air, fins, and tubes of the evaporator during the off-cycle. As can be seen there is little temperature difference between the air and the surface of the evaporator. This suggests very little heat transfer occurs during the off-cycle and the assumption of an adiabatic evaporator appears reasonable.
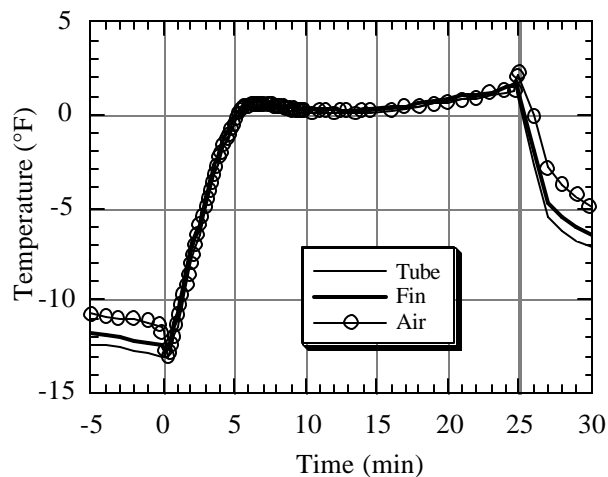

Figure C.2 Evaporator air, fin, and tube temperatures (T_{amb}=90°F)

Since Figure C.2 only compares the temperature of the air and surface for only one location of the evaporator, it is possible other parts of the evaporator are warmer than the air during the off-cycle, allowing the evaporator to reject heat to the freezer compartment. To determine whether these areas could transfer a significant amount of heat it is assumed the evaporator is on average about 1°F warmer than the surrounding air. Equation C.7 shows the relationship between heat transfer and the driving temperature difference (?T). Everything in Equation C.7 is known except for the heat transfer coefficient (h). Since evaporator fan is not running during the off-cycle, heat transfer must occur through free convection. Modeling the evaporator as a series of flat plates the heat transfer coefficient is be estimated using Equations C.8-10, where Equation C.9 is valid for laminar convection over a vertical plate (White, 1988) and x is the height of the vertical plate. With these assumptions approximately 3 Btu of heat would be rejected from the evaporator during a 30 minute off-cycle. This suggests that heat transfer to the freezer compartment could be significant if parts of the evaporator are warmer than the air. For this reason it is suggested that future experimental refrigerators included several air and surface thermocouples in different locations throughout

the evaporator to gain a better understanding of how the evaporator surface temperature compares to the surrounding air.

$$Q_{evap} = hA(T_{surf} - T_{air})\Delta t \tag{C.7}$$

$$h = \frac{k \cdot \overline{Nu}}{L} \tag{C.8}$$

$$\overline{Nu} = 0.535 \cdot Ra^{1/4} \tag{C.9}$$

$$Ra = Gr\,Pr = \frac{\rho^2 C_p g \beta (T_{surf} - T_{air}) x^3}{k\mu} \tag{C.10}$$

C.3 Conduction from the Compressor to the Evaporator

When a temperature difference exists between two connected bodies heat conducts from the warmer body to the cooler one until the temperature difference disappears. Since the compressor is connected to the evaporator by the suction line and there is often more than a 150°F temperature difference between these two components, it is possible that a significant amount of conduction could occur. This section examines whether this heat transfer plays a significant role in transferring energy to the evaporator during the off-cycle.

$$Q = k \cdot \frac{\Delta T}{L} \cdot A \cdot \Delta t \tag{C.11}$$

$$A = \pi \left(\frac{D_o^2}{4} - \frac{D_i^2}{4} \right) \tag{C.12}$$

Assuming one-dimensional steady heat conduction, the heat transfer through the suction line can be approximated as shown in Equation C.11. The physical dimensions of the suction line, length (L) and cross sectional area (A), are determined from the engineering specifications and the thermal conductivity of copper is known to be 225 Btu/hr ft °F. The temperature difference across the suction line is conservatively chosen to be 160°F. In reality this temperature difference decreases as the compressor cools and the evaporator warms up. Therefore the assumption of a constant 160°F temperature difference represents the upper bound on the amount of heat which can be transferred to the evaporator. With these assumptions less than 0.5 Btu of heat can be transferred during a 30 minutes off-cycle. This demonstrates conduction through the suction line is small and can be ignored.

C.4 Vapor or Liquid Migration

Previous work by Rubas and Bullard (1995) and Krause and Bullard (1994) have suggested that state of the refrigerant migrating to the evaporator had a significant impact on the energy transferred to the evaporator during the off-cycle. They argued that if all the refrigerant migrated as vapor, then more energy would be transferred to the evaporator since the enthalpy of vapor is higher than the enthalpy of liquid and therefore vapor migration should be avoided. Implicit in this argument is the assumption that there is sufficient heat transfer from the surroundings to the condenser to vaporize the refrigerant contained in the condenser prior to migration. This section will examine how much heat transfer there is between the condenser and the surroundings and whether vapor migration is possible.

$$Q_{cond} = hA(T_{surf} - T_{air})\Delta t \tag{C.13}$$

Equation C.13 indicates that amount of heat transferred to the condenser is a function of the temperature difference between the condenser and the surroundings, the heat transfer coefficient, and the length of time over which the heat transfer occurs. To understand how the temperature of the condenser and the surrounding air compare during the off-cycle several thermocouples were added to the surface of condenser as well as the surrounding air. Figure C.3 is a schematic of the condenser showing the location of the all relevant temperatures measurements. Figures C.4-7 compare the condenser air, surface, and refrigerant temperatures upstream and downstream of the fan during the off-cycle. Note time equals zero represents the beginning of the off-cycle
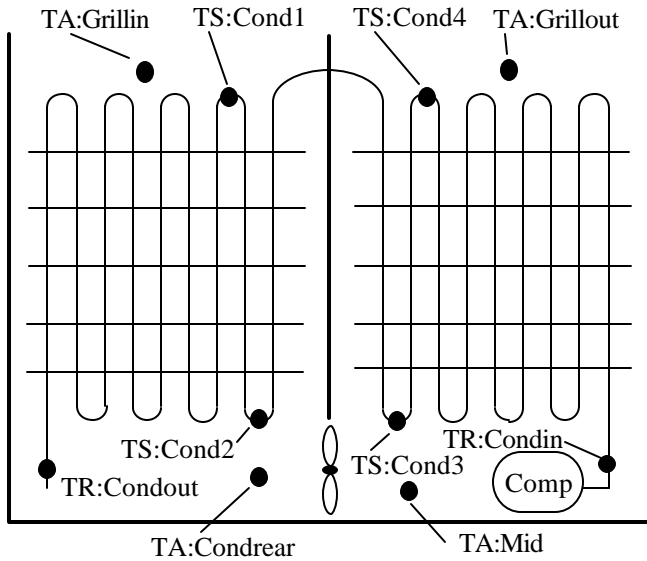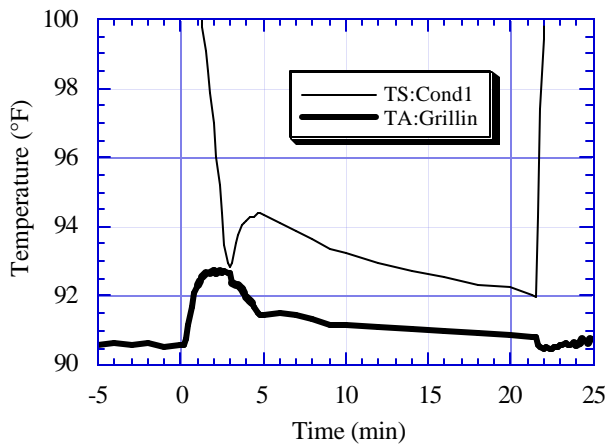

Figure C.3 Schematic of the condenser

Figure C.4 Upstream/front condenser surface and air temperatures (T_{amb}=90°F)

36

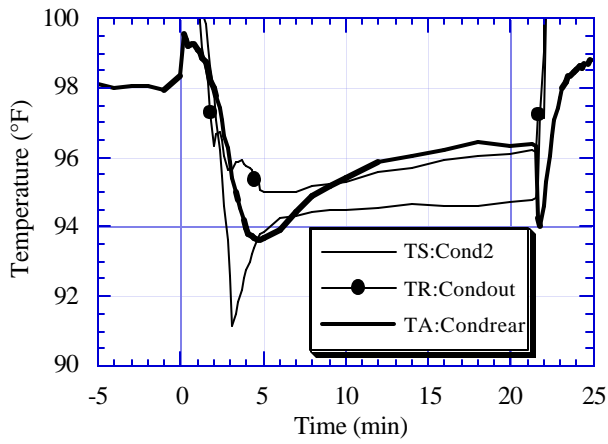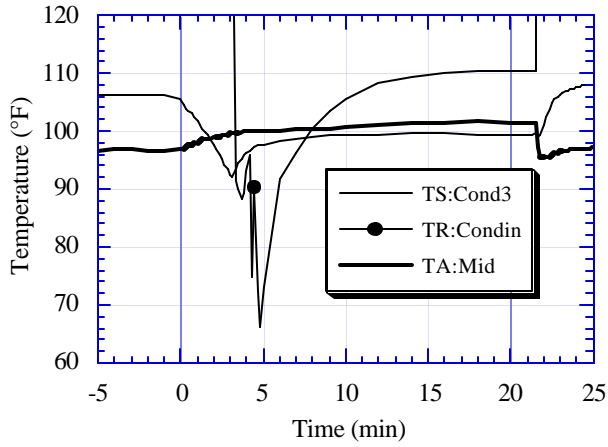Figure C.5 Upstream/rear condenser surface, air and refrigerant temperatures (T_{amb}=90°F)

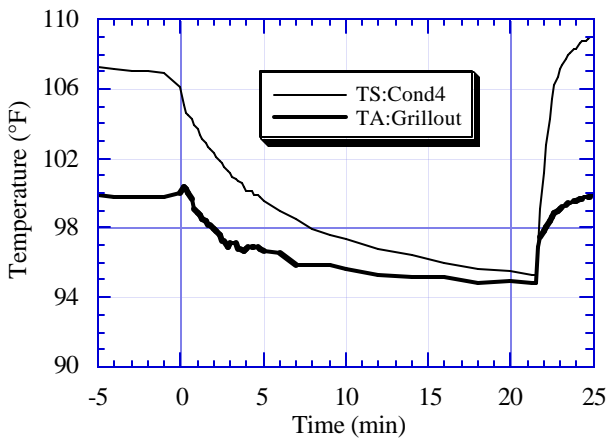Figure C.6 Downstream/rear condenser surface, air, and refrigerant temperatures (T_{amb}=90°F)

Figure C.7 Downstream/front surface and air temperatures (T_{amb}=90°F)

Figures C.4 and 7 shows the temperature of the condenser surface and surrounding air near the grille. In these figures the condenser is warmer than the air during the entire off-cycle, suggesting heat is rejected from the condenser. Figures C.5 and 6 show compare the same condenser and air near the rear of the condenser. In these figures the surrounding air is warmer than the condenser, note TR:Condin is very influenced by the compressor shell and is therefore warmer than the air. These trends at first glance seem inconsistent, but a closer look at the location of the thermocouples suggests a reason for the observed behavior. As pointed out the air in the rear of the condenser is warmer than the condenser, one major reason for this is the condenser. During the off-cycle the warm compressor shell rejects lots of heat warming the surrounding air. Not surprisingly the TA:Mid which is closest to the compressor is warmer than any of the other temperature readings. This effect is magnified since the condenser cabinet has been modified into a calorimeter. In this configuration all holes in the rear panel and floor have been sealed so no ambient air can leak in or condenser air leak out. Near the front of the condenser interaction with the ambient air is no problem. The grille allows plenty of ambient air to mix with the condenser air cooling it below the condenser temperature. These figures suggest that heat is both absorbed and rejected by the condenser therefore further calculations are required to determine which dominates. But first, we will attempt to bound the magnitude of these terms.

Since the condenser fan is not running during the off-cycle any heat transfer to or from the condenser will be due to free convection. To calculate the free convection heat transfer coefficient for the condenser, it is necessary to estimate the heat transfer coefficient for both the wires and tubes. Modeling the wires and tubes as cylinders in cross flow (Cavallaro, 1992) the heat transfer coefficients are found to be the functions of the Rayleigh number shown in Equations C.14 and 15. These individual heat transfer coefficients are combined to estimate the total heat transfer coefficient for the condenser as shown in Equation C.16. Knowing this relationship and the temperature difference between the condenser surface and the surrounding the air it is possible to calculate the rate of heat transfer. However, to estimate the magnitude of this heat transfer it is necessary to know the length of time over which it takes place.

$$h_{wire} = \frac{k \cdot \overline{Nu}_{wire}}{D_{wire}} = \frac{k \cdot (1.02 \cdot Ra^{0.148})}{D_{wire}}$$

(C.14)

$$h_{tube} = \frac{k \cdot \overline{Nu}_{tube}}{D_{tube}} = \frac{k \cdot (0.85 \cdot Ra^{0.188})}{D_{tube}}$$

(C.15)

$$h_{cond} = \frac{A_{wire} \cdot h_{wire} + A_{tube} \cdot h_{tube}}{A_{cond}}$$

(C.16)

Heat transfer to or from the condenser is only important while there is refrigerant in the condenser. Once all the refrigerant has migrated to the evaporator there is no significant amount of energy to be transported from the condenser to the evaporator. Figure C.8 shows how the pressures in the evaporator and condenser vary during the off-cycle. Within eight minutes both heat exchangers are at the same pressure, signaling the end of refrigerant migration from the condenser to the evaporator. In fact, Figure C.9 reveals that most of the mass transfer is completed during the first three minutes of the off-cycle. This figure compares the measured condenser exit

temperature with the condenser saturation temperature. After three minutes only superheated vapor is leaving the evaporator and since vapor has a low density more it is estimated that more than 85% of the charge left as a two-phase mixture during the first three minutes of the off-cycle. Therefore heat transfer between the refrigerant the surroundings can only occur during the first three minutes of the off-cycle.
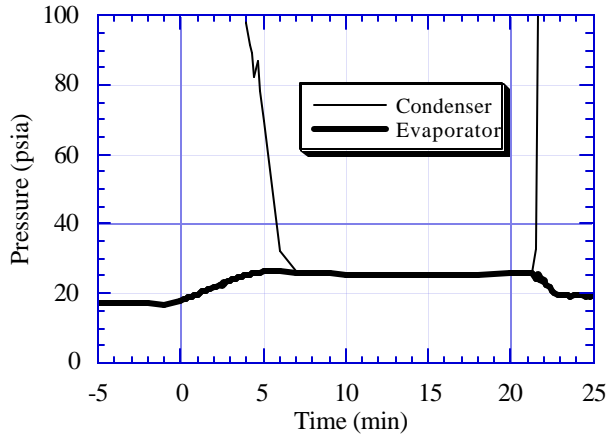

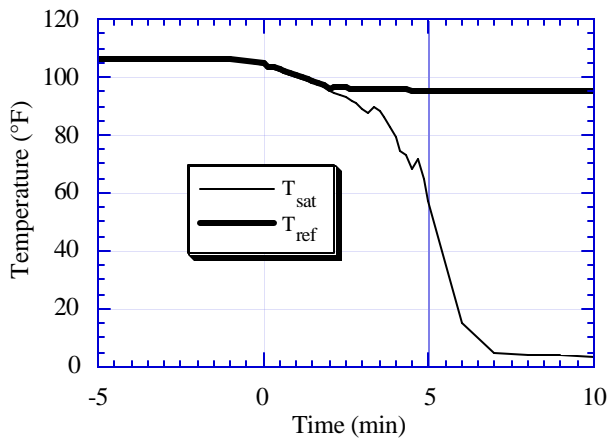Figure C.8 Evaporator and condenser pressures (T_{amb}=90°F)

Figure C.9 State of refrigerant leaving the condenser (T_{amb}=90°F)

Assuming the temperature profiles shown in Figures C.4-7 are representative the condenser in each quarter of the calorimeter it is possible to estimate integrate Equation C.13 to determine the heat transfer during the first three minutes of the off-cycle. Since three quarters of the condenser is upstream of the fan the heat transfer area was weighted appropriately to reflect this fact. With these assumptions it is estimated that approximately 5 Btu of heat are rejected from the condenser prior to refrigerant migration. In fact 90% of this heat transfer happened during the first two minutes while the all sections of the condenser are still warmer than the air. Since the condenser seems to rejects heat during the refrigerant migration process it seems unlikely any significant portion of the refrigerant migrates as vapor. Ideally, if the condenser remains warmer than the air prior to refrigerant migration it would be advantageous to delay refrigerant migration so more heat could be rejected from the condenser and the refrigerant.

However, there is no practical way of delaying this refrigerant migration significantly short of placing a valve after the condenser and metering the flow.

C.5 Heat Transfer from the Compressor to the Condenser

The previous section examined whether heat transfer with the surrounding air significantly affected the amount of energy carried to the evaporator by off-cycle refrigerant migration. This is not the only way energy can be added to the refrigerant in the condenser. Another possible heat source is the compressor shell, since it is often as much as 50°F warmer than the condenser it is possible some heat could conduct from the shell to condenser. This section will look into whether or not heat transfer from the compressor to the condenser plays a significant role in increasing the amount of energy transferred to the evaporator during the off-cycle.

$$Q = k \cdot \frac{\Delta T}{L} \cdot A \cdot \Delta t$$
(C.17)

$$A = \pi \left(\frac{D_o^2}{4} - \frac{D_i^2}{4} \right)$$
(C.18)

Assuming one-dimensional steady heat conduction, the heat transfer to the condenser can be approximated as shown in Equation C.17. This equation really defines the amount of heat transferred to the condenser metal, however for this analysis it is assumed (in the worst case) any heat transferred to the metal is added to the refrigerant inside the condenser. The inner and outer diameters of the condenser tubing are taken from the engineering specifications and the thermal conductivity of steel is known to be 25 Btu/hr ft °F. The temperature difference between the condenser and compressor is 50°F, while the length (L) over which heat transfer occurs is arbitrarily chosen to be 1 foot. The assumptions of a constant 50°F temperature difference and a length of 1 foot represent an upper bound on the amount of heat which can be transferred to the condenser since in reality the temperature difference should decrease with time and the actually more than 1 foot of tubing between the compressor shell and a point in the condenser where the surface temperature no longer changes. With these assumptions less than 0.01 Btu of heat can be transferred during the 10 minutes in which refrigerant is present in the condenser. This demonstrates that conduction to the condenser from the compressor is small and can be ignored.

C.6 Power Penalty due to Migration

One indirect loss associated with off-cycle migration is the refrigerant redistribution which must take place during the next on-cycle. During the redistribution process the compressor performs extra work it would not have to do if no migration occurred during the off-cycle. One (admittedly crude) method for estimating this extra work is shown in Equation C.19. Assuming an average condensing and evaporating pressure and using the compressor maps it is possible to estimate how much power is required to remove the excess refrigerant from the evaporator. Using this method the extra work done by the compressor ranges from 2.0 W-hr of extra work at 100°F to approximately 2.5 W-hr at 60°F. Where m_{mig} is the amount of "excess" charge in the evaporator at the beginning of the on-cycle, which is multiplied by the average work per unit mass pumped by the compressor, determined using the maps for evaporating and condensing pressures measured during the first minute of the on-cycle.

$$W = \frac{\dot{W}_{comp}}{\dot{m}_{comp}} \cdot m_{mig}$$

(C.19)

A second, and probably more accurate, method of estimating the extra work associated with redistribution involves comparing the cycling and quasi-steady refrigerators. While redistributing the refrigerant the evaporating and condensing pressures of a cycling refrigerator differ from the quasi-steady machine. Since the power requirements of the compressor are a strong function of evaporating and condensing pressure these differences will effect the compressor power consumption. To estimate the impact of refrigerant redistribution the power penalty due to pressure differences is calculated using the measured pressures, the compressor map and Equation C.20. Using this method the extra work done by the compressor ranges from 0.5 W-hr at 100°F to 2.0 W-hr at 60°F.

$$W = \int_0^t \dot{W}_{map}(P_{evap}, P_{cond})_{cyc} \partial t - \int_0^t \dot{W}_{map}(P_{evap}, P_{cond})_{ss} \partial t$$

(C.20)

Ideally, both methods would yield similar results. However, the first method consistently predicts a larger penalty. In addition the magnitude of the discrepancy is greater at higher ambient temperatures then it is at lower ones. One explanation for this is that during the higher ambient cases the cycling refrigerator actually operates during the first few minutes with a combination of evaporating and condensing pressures which require less compressor work to maintain than the corresponding quasi-steady points. This potential energy saving is neglected in first calculation making the power penalty due to redistribution appear larger. As the ambient temperature decreases so does this potential savings and therefore the two methods produce similar results at lower ambients. For this reason the second method, which involves a direct comparison between the cycling and quasi-steady data, is believed to be the more realistic approach and was used in the body of the report to estimate the power penalty.

C.7 Conclusion

During the off-cycle the system pressure equalizes through migration of refrigerant from the condenser to the evaporator. This refrigerant raises the total energy of the evaporator by 13.5 to 16.5 Btu, 85% this energy is absorbed by the aluminum evaporator. This is significant since the evaporator must be cooled during the off-cycle reducing its useful work. Initial studies indicate there is little heat transfer from the evaporator during the off-cycle justifying the assumption of adiabatic migration, while the condenser rejects heat during the initial portions of the off-cycle making vapor migration unlikely. In addition, conduction from the compressor shell to the condenser and the evaporator is negligible and can be ignored. Finally, it was shown the off-cycle migration cause the compressor to perform as much as 2.0 W-hr worth of extra work in order to redistribute the refrigerant during the on-cycle.

Appendix D: Thermal Mass

To maintain the food in the fresh food and freezer compartments at a desired temperature, the refrigerator cycles on and off allowing the food to cool below then warm above the desired temperature. This way the average temperature of the food is acceptable and the refrigerator does not run all the time. One consequence of this cyclic behavior is that like the food, components such as the compressor and heat exchangers change temperature over time. This change in temperature requires one to ask the question of how the thermal mass of the components affects the performance of the refrigerator. This appendix will look into how the compressor, evaporator, evaporator ductwork and condenser thermal masses affect system performance.

D.1 Compressor

When the refrigerator cycles off the compressor shell temperature begins to cool down, therefore when compressor turns back on its shell initially much cooler than it would be if the refrigerator operated continuously (see figure D.1).
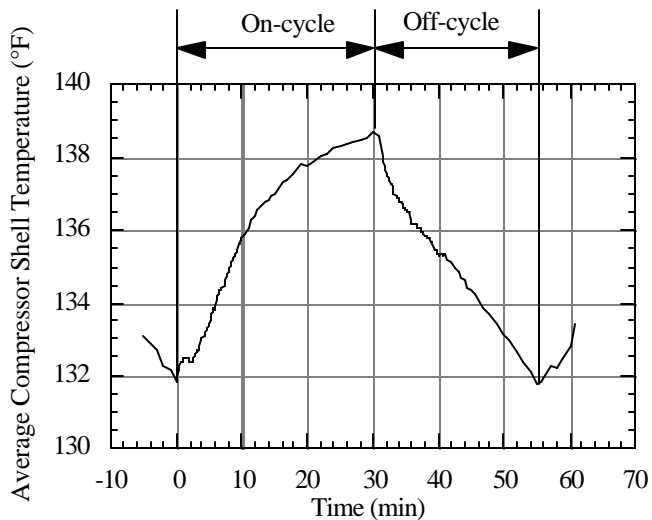
Figure D.1 Compressor shell temperature during a typical cycle (T_{amb}=90°F)

The fact the compressor shell is cooler during cycling than in continuous operation could have some serious implications on system performance. First, a cooler compressor shell means the refrigerant leaving the compressor is cooler. This cooler refrigerant requires a smaller de-superheating region meaning there may be larger sub cooled region. Since sub cooled liquid is more dense than vapor, this should shift charge from the evaporator to the condenser. A second effect of a cool compressor shell is to cool the compressor sump oil. This cold compressor has the potential of trapping refrigerant in the oil.

As mentioned earlier one effect of a cool compressor is to lower the temperature of the discharge gas. Figure D.2 illustrates graphically how a smaller de-superheating region could cause an increase in the amount of sub cooling and thereby increasing amount of charge in the condenser.

42
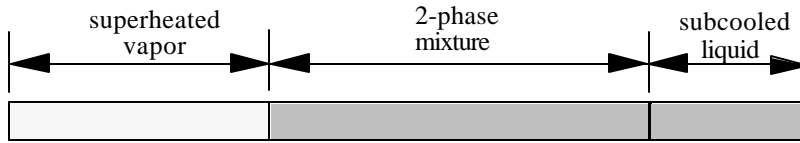
a) High Discharge Temperature
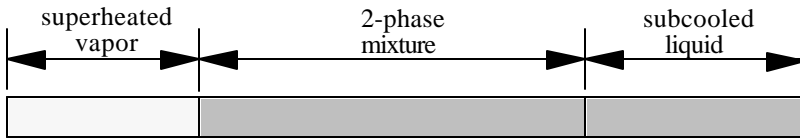
b) Low Discharge Temperature

Figure D.2 Effect of lowering compressor discharge temperature

To understand the magnitude of this effect the computer program RFSIM developed by Goodson and Bullard (1994) was utilized.

The model was run twice. The first time no changes were made; this point represents a refrigerator operating under normal steady state conditions. The model was then modified to simulate a compressor with a cool compressor shell. To simulate this condition the compressor heat transfer coefficient was increased until the discharge temperature dropped 20°F. Table D.1 summarizes the results.

Table D.1 Effect of compressor shell temperature on condenser charge level

	High T_{shell}	Low T_{shell}
$A_{supcond}$ [ft^2]	0.871	0.759
$A_{2phcond}$ [ft^2]	5.383	5.487
$A_{subcond}$ [ft^2]	0.396	0.404
$T_{discharge}$ [°F]	160.5	140.0
$P_{discharge}$ [psia]	105.0	104.5
M_{cond} [lbm]	0.342	0.346

The results shown in Table D.1 are as expected. The cooler compressor shell reduces the discharge temperature and the amount of superheated area ($A_{supcond}$) in the condenser. This decrease in the de-superheating area causes an increase in the subcooled area ($A_{subcond}$). This increase is not as great as it could have been since the amount of the condenser filled with two-phase refrigerant ($A_{2phcond}$) also increases as the condensing temperature decreases slightly. The final row of Table D.1 shows net effect on the condenser. As the compressor shell temperature is lowered the proportion of charge in the condenser increases. However, the magnitude of this change is small (0.004 lbm or 0.06 oz), so it is unlikely this could significantly effect refrigerator performance.

In addition to changing the proportion of charge in condenser, a cooler compressor shell will effect the amount of refrigerant dissolved in the oil sump. Previous work at the ACRC by Grebner and Crawford (1992) showed that the amount of refrigerant dissolved in oil is proportional to pressure and inversely proportional to temperature.

Assuming the compressor shell temperature is a good indicator of the oil sump temperature, and everything else being equal, a cooler compressor will hold more refrigerant in its oil sump than a warmer compressor.

$$T^* = (1 - w)(A + B \cdot P) \tag{D.1}$$

$$T^* = \frac{T - T_{sat}(P)}{T_{sat}(P)} \tag{D.2}$$

$$A = x_1 + \frac{x_2}{w^{\frac{1}{2}}} \tag{D.3}$$

$$B = x_3 + \frac{x_4}{w^{\frac{1}{2}}} + \frac{x_5}{w} + \frac{x_6}{w^{\frac{3}{2}}} + \frac{x_7}{w^2} \tag{D.4}$$

Table D.2 R-12/Naphthene constants for Grebner-Crawford model

x_1	$-5.9927652e^{-3}$
x_2	$4.1661510e^{-2}$
x_3	$2.0046597e^{-3}$
x_4	$-3.2682848e^{-3}$
x_5	$1.7368443e^{-3}$
x_6	$-2.8552230e^{-4}$
x_7	$1.6092949e^{-5}$

Using the Grebner-Crawford model (equations D.1-4) and data collected from the Amana test stand the effect of compressor shell temperature on amount of refrigerant dissolved in the oil sump can be quantified. Before any calculations can be made reasonable values for the temperature of oil, pressure of surrounding vapor, and amount of oil need to be determined. Since our compressor in a reciprocating compressor with a low side sump the choice of vapor pressure was the suction pressure, the oil sump temperature was taken to be the average compressor shell temperature, and there are 13 ounces of grade 32 Naphthenic mineral oil in the compressor sump. Figures D.3 and D.4 show how the amount of oil dissolved in the sump during cycling compares with steady state points at two different ambient temperatures.
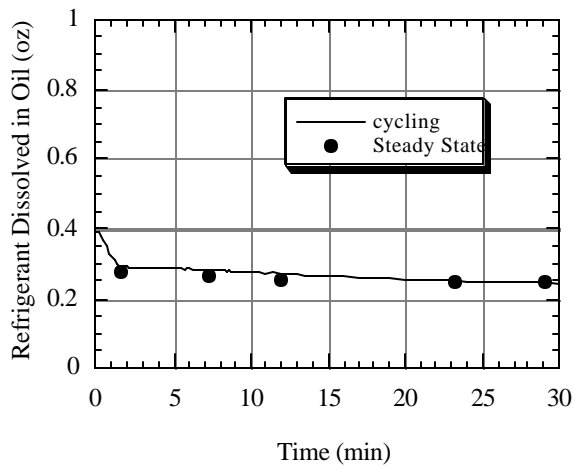
Figure D.3 Amount of oil dissolved in compressor oil sump ($T_{amb} = 90°F$)
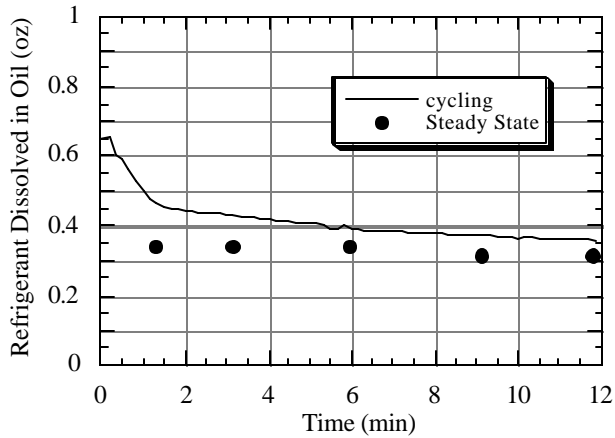
Figure D.4 Amount of oil dissolved in compressor oil sump ($T_{amb} = 60°F$)

As can be seen from the figures D.3 and D.4 more oil is dissolved in the compressor oil sump during cycling than during any corresponding steady state point. This discrepancy becomes more pronounced in the 60°F ambient case where the cycle length is short and the compressor shell does not have time to warm up. While this effect is present the amount of the extra refrigerant dissolved in the compressor sump is small (< 0.05 oz most of the time) compared with the total system charge (8.0 oz) and therefore does not change system performance. These results are for a compressor with a low side oil sump and should not be applied to systems equipped with a compressor having a high side sump. Work by Krause and Bullard (1994) showed that as much as 2.0 ounces of refrigerant could be trapped in a high side oil sump causing significant changes in system performance.

D.2 Evaporator

The compressor is not the only component in the refrigerator to experience temperature changes as a result of cycling. The evaporator also experiences changes and therefore its thermal mass could play an important role in system performance. When the compressor shuts off the evaporator warms up, this warm evaporator must then be cooled before the system performance can its reach steady state level.

The amount of heat removed from the air passing over the evaporator is related to the difference in temperature between the air and the surface of the heat exchanger. The larger this temperature difference the greater the amount of heat which can be removed from the air. If the heat exchanger takes a long time cool down then the refrigerator's efficiency will be reduced. To determine whether this is a potential problem the evaporator is treated as a "lumped" body (Rubas and Bullard, 1993).

A body can be considered lumped if its internal temperature is nearly constant. To put it another way, the external convective resistance is much larger than the internal conductive resistance. To treat the evaporator as a lumped body the Biot number (equation D.5) must be less than 0.1.

$$Bi = \frac{h_{\infty}L}{k}$$

(D.5)

The length scale (L) for the evaporator is wall thickness, h_8 is chosen to be the (on-cycle) convection heat transfer coefficient on the refrigerant side (h_r in Table D.3), and k is the thermal conductivity of the metal. Using the

parameters shown in Table D.3 the Biot number is calculated to be 0.0014. Since this is much less than 0.1 the evaporator can be treated as a lumped body.

Table D.3 Evaporator parameters

Parameter	Value
m [lbm]	3.46
L [ft]	0.00233
A_r [ft^2]	3.26
A_a [ft^2]	16.30
k [Btu/h ft °F]	120
c [Btu/lbm °R]	0.22
h_r [Btu/hr ft^2 °R]	75
h_a [Btu/hr ft^2 °R]	5

One characteristic of a lumped body is its thermal time constant. In one time constant a body undergoing a sudden temperature difference would undergo 66% of this change. After five time constants the body will be in equilibrium with its surrounding. Therefore, an evaporator with a small time constant will quickly respond to changes in temperature. To calculate the thermal time constant an energy balance is performed on a section of the heat exchanger. Equation D.6 represents this energy balance, where the right side of the equation is the net heat flow into the evaporator while the left side represents the storage of heat by the evaporator.

$$h_r A_r (T_r - T_s) - h_a A_a (T_s - T_a) = mc \frac{dT_s}{dt}$$

(D.6)

Where the subscript r represents the refrigerant side, a represents the air side, and s represents the surface of the heat exchanger. After solving the above differential equation the thermal time constant can be represented as shown in equation D.7. Using the manufacturer's drawings both the internal and external surface area can be calculated. The air and refrigerant side heat transfer coefficients are from Cavallaro and Bullard (1994) and Admiraal and Bullard (1993). Using the above information the time constant is calculated to be 8.4 seconds. This is considerably shorter the length of a typical cycle. Since this value is so small it is unlikely that the thermal mass of the heat exchanger will degrade the refrigerator's efficiency.

$$\tau = \frac{m \cdot c}{h_r \cdot A_r + h_a \cdot A_a}$$

(D.7)

While the evaporator cools down quickly, it still must be cooled. This is important because the evaporator capacity calculations shown in this report are based upon air side energy balances which account only for work done cooling the air. For steady state points this difference is insignificant since the temperature of the evaporator does not change. However, as pointed out earlier the temperature of the evaporator can change significantly during a typical cycle. Therefore, to fairly compare the cycling data with the steady state data the heat removed from the evaporator itself must be account for. Equation D.8 is the equation which represents the heat removed from the evaporator during an on-cycle.

$$Q = mc(T_{on} - T_{off})$$

(D.8)

Using the parameters found in Table D.3 the amount of heat removed from the evaporator can be found if the temperature of the evaporator is known at both the beginning and end of the on cycle. Table D.4 summarizes the results. As can be seen between 12 and 14 Btu of heat are removed from the evaporator each cycle. This heat transfer should be added to the heat removed from the air in order to correctly calculate the amount of heat removed from the refrigerator during the on cycle.

Table D.4 Heat removed from the evaporator metal

T_{amb} [°F]	T_{on} [°F]	T_{off} [°F]	Q [Btu]
100	1.0	-14.0	11.4
90	1.5	-14.9	12.4
75	1.1	-17.6	14.2
60	1.3	-17.1	14.0

D.3 Evaporator Ducts

The test refrigerator is equipped with several square feet of plastic and foam ductwork used to transport air to and from the fresh food and freezer compartments. Like other parts of the refrigerator, the temperature of the ductwork changes as the refrigerator cycles on and off. A change in duct temperature requires heat transfer with the air passing through the ductwork. This heat transfer can affect the evaporator inlet and exit air temperatures and influence an air side energy balance. This section will examine whether this heat transfer is significant.

Air side energy balances are used exclusively in this report. In the past, the fresh food and freezer return air temperatures have been used to calculate the evaporator inlet temperature, while the exit of the control volume is defined as the freezer discharge (see Rubas and Bullard, 1992). The appropriate choice of evaporator inlet and exit temperature becomes very important when comparing cycling and steady state data points. To make an accurate comparison of cycling and steady state evaporator capacities it is important to match both the condenser and evaporator air inlet temperatures. If the ductwork influences the air before (or after) the evaporator then a comparison based on the freezer and fresh food return air temperatures is incorrect.

Equation D.9 illustrates the importance of understanding any influence the evaporator ductwork has on air side temperature measurements.

$$\dot{Q}_{evap} = \dot{m}_{air}\left(h(T_{evapin}) - h(T_{evapout})\right)$$

(D.9)

The heat removed from the air by the evaporator is proportional to the temperature difference across the evaporator. For this reason any changes in air temperature will affect the calculation of evaporator capacity. Compounding this problem is the small change in air temperature across the evaporator. This temperature change is usually close to 7°F. Therefore, a 1°F error in the air temperature would cause a 14% change in the calculated evaporator load.

Figure D.5 shows a schematic drawing of the evaporator ductwork in the Amana test stand. In addition to showing the layout of the evaporator ductwork, Figure D.5 also shows the relevant temperature measurements taken within the ducts. Thermocouples record the freezer and fresh food return air temperatures. Next, an array of thermocouples located under the evaporator measures the evaporator inlet air temperature. Following the evaporator four thermocouples are averaged to give a representative evaporator exit temperature, while thermocouples at the freezer and fresh food discharge monitor the air entering the cabinet.
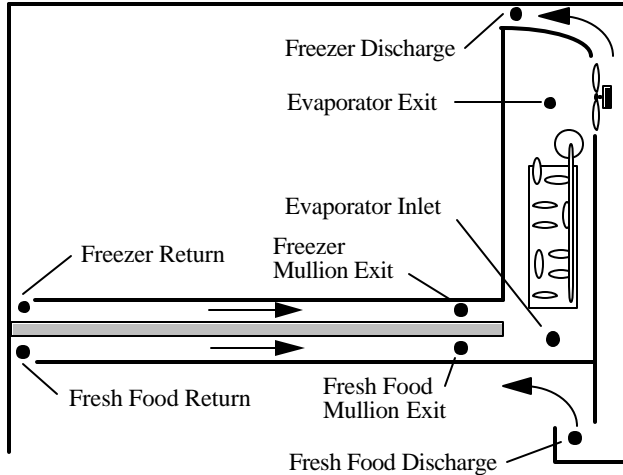
Figure D.5 Schematic of Amana ductwork

Air passes through the entrance duct, returning air from the fresh food and freezer compartments, and then enters the evaporator. Prior to entering the evaporator the fresh food and freezer return air streams mix forming one stream at a single temperature. The temperature of this mixed air stream is calculated using Equation D.10, where T_{evapin} is the evaporator inlet temperature, T_f and T_z are the fresh food and freezer return air temperatures, and f is air split fraction estimated to be 0.89 in Appendix A.

$$\frac{h(T_{evapin})}{\rho(T_{evapin})} = (1-f) \cdot \frac{h(T_f)}{\rho(T_f)} + f \cdot \frac{h(T_z)}{\rho(T_z)}$$

(D.10)

Using Equation D.10 and the measured return air temperatures it is possible to calculate what the evaporator inlet temperature would if ductwork does not exchange heat with the air (i.e. massless ductwork). The actual evaporator inlet temperature is calculated using Equation D.10 and the measured mullion exit temperatures, see Figure D.5. Both methods of calculating the evaporator inlet temperature are compared in Figure D.6. As can be seen both methods of calculating the evaporator inlet temperature give similar results, therefore it appears the actual inlet ductwork behaves as if it were massless. Therefore any heat transfer between the inlet ductwork and the fresh food and freezer return air is insignificant and can be neglected. Finally, only the results for the 100°F ambient test condition are presented here, but the same trends were at other ambient temperatures.
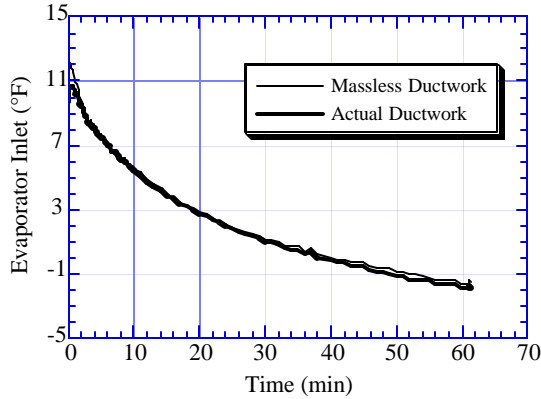
Figure D.6 Effect of evaporator entrance ductwork (T_{amb}=100°F)

After the air flows across the evaporator, it must pass through more ducts before it is discharged to the fresh food and freezer compartments. Again it is important to understand the effect of the duct's thermal capacitance has on the measured air temperatures. It is possible to related the evaporator exit temperature to fresh food and freezer discharge temperatures using Equation D.11. Where $T_{discharge}$ is the either the fresh food or freezer discharge temperature, $T_{evapout}$ is the average temperature of four thermocouples located at evaporator exit, and $?T_{mix/fan}$ represents the temperature difference between the measured evaporator exit and fan discharge temperatures caused by the addition of fan heat and incomplete mixing at the evaporator exit. Using the steady state data these differences were calculated to be 2.1°F and 2.7°F for the freezer and fresh food discharge temperatures respectively.

$$T_{discharge} = T_{evapout} + \Delta T_{mix/fan}$$

(D.11)

$$Q_{cabinet} = UA_{wall}(T_{amb} - T_{cabinet})$$

(D.12)

Only 0.7°F is attributable to the fan power, the remainder probably reflects poor mixing at the evaporator outlet or heat gain in the ducts. The difference seen between the fresh food and freezer offsets is likely due to heat transfer through the back of the refrigerator (see Figure D.6). A simplified calculation showed the air could be heated as much as 1°F by heat transfer through this wall. This more than accounts for the 0.6°F difference between the calculated offsets. Before continuing, it should be noted that these values were calculated using data collected at a 100°F ambient temperature. The freezer offset was found to be constant at 2.1°F for all ambient temperatures, while the fresh food discharge offset was smaller for lower ambient temperatures. The fresh food discharge air travels along the back wall of the refrigerator as it returns to the fresh food compartment. This allows the air to be warmed by heat transfer through the wall. Since this heat transfer is larger at higher ambient temperatures (see Equation D.12) it is not surprising the offsets are larger as well. Using Equation D.11 and the measured (average) evaporator exit air temperature it is possible to calculate what the discharge temperatures would be if the ductwork behaved the same during cycling as it does in steady state. Comparing these calculated temperatures with the measured temperatures collected during cycling, it is possible to determine to what extent the ductwork affects the measured discharge temperatures during cycling. Figures D.7 and D.8 show that the cycling discharge temperatures are essentially equal to those at steady state. Therefore the temperatures are not significantly affected by the thermal capacitance of the

ductwork leading to the freezer and fresh food compartments. Finally, only the 100°F results are presented here but the same trends were observed at other ambient temperatures.
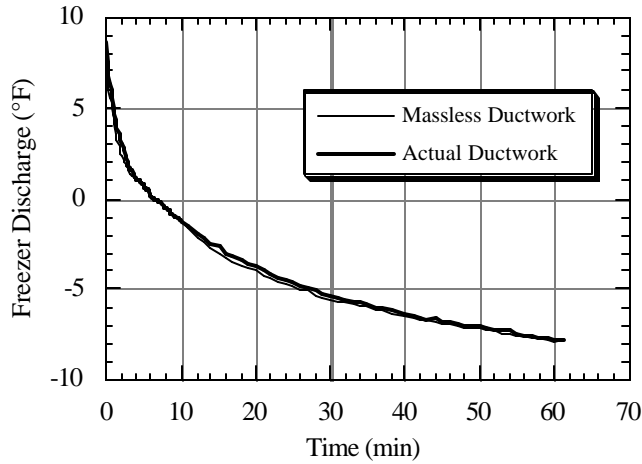
Figure D.7 Effect of freezer discharge ductwork (T_{amb}=100°F)
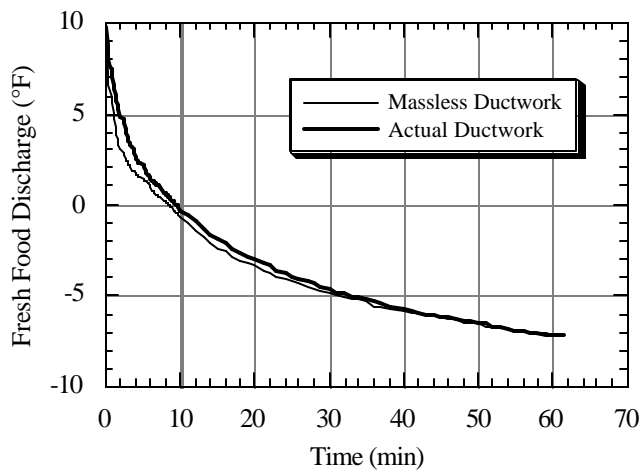
Figure D.8 Effect of fresh food discharge ductwork (T_{amb}=100°F)

D.4 Condenser

During the off-cycle the condenser cools. If the condenser is very massive then it may act to reduce the condensing temperature during the initial portions of the on-cycle. Lowering the condensing temperature would reduce the temperature difference between the high and low temperature reservoirs and should in theory improve the system efficiency (Van Wylen, 1986). To understand whether this effect is could be significant the condenser is treated as a "lumped" body in the same manner as the evaporator.

Table D.5 Condenser parameters

Parameter	Value
m [lbm]	3.95
L [ft]	0.00208
A_r [ft^2]	2.02
A_a [ft^2]	6.40
k [Btu/h ft °F]	25
c [Btu/lbm °R]	0.11
h_r [Btu/hr ft^2 °R]	60
h_a [Btu/hr ft^2 °R]	5

To treat the condenser as a lumped body the Biot number (Equation D.5) must be less the 0.1. The appropriate length scale (L) for the condenser is the wall thickness, h_8 is convection heat transfer coefficient on the refrigerant side (h_r in Table D.5), and k is the thermal conductivity of steel. Using the information provided in Table D.5 the Biot number is calculated to be .005. Since this is much less than 0.1 the condenser can be treated as a lumped body.

As pointed out in section D.2, one characteristic of a lumped body is its thermal time constant. The thermal time constant is a measure how quickly a body responds to a sudden change in surrounding temperature. A condenser with a small time constant will respond quickly to temperature changes and not impact refrigerator performance. This time constant is calculated with Equation D.7. The manufacturer's drawings provide enough information so both the internal and external surface area can be calculated. The air and refrigerant heat transfer coefficients are from Cavallaro and Bullard (1994) and Admiraal and Bullard (1993) respectively. Using this information the thermal time constant is calculated to be 10.2 seconds. Since this is considerably shorter than length of a typical cycle it appears the condenser warms quickly indicating that there is little time to take advantage of a lowered condensing pressure.

Even though the condenser appears to respond quickly to temperature changes it still must be warmed by the refrigerant. The amount of heat required to warm the condenser during the on-cycle can be calculated with Equation D.13. Using the parameters in Table D.5 and the measured condenser surface temperature, it appears between 4.3 and 4.8 Btu of heat go into warming the condenser metal. Like the evaporator this energy should be added to an air-side energy balance in order to accurately account for all the heat rejected by refrigerant in the condenser. However, unlike the evaporator where the heat removed from the evaporator metal represents as much as 10% of the total heat removed by the refrigerant during the on-cycle, the 4 to 5 Btu of heat rejected to the condenser metal represents less than 4% of the total heat rejected during the on-cycle.

$$Q = mc(T_{off} - T_{on}) \qquad\qquad \text{D.13}$$

Table D.6 Heat added to the condenser metal

T_{amb} [°F]	T_{on} [°F]	T_{off} [°F]	Q [Btu]
100	104	114	4.3
90	95	105	4.3
75	80	91	4.8
60	66	77	4.8

D.5 Conclusion

Since the refrigerator cycles on and off, all of its components undergo changes in temperature. For this reason the thermal mass effects of four components the compressor, evaporator, evaporator ducts, and the condenser were examined. This investigation revealed that the thermal mass of the compressor does affect the distribution of refrigerant in the system. The magnitude of this effect was very small and it can be neglected. Likewise it was shown that the evaporator and condenser quickly reach a temperature close to that of the refrigerant and are not a major factors contributing to cycling losses. However, since air side energy balances are used throughout this report it is necessary to account for the 12-14 Btu of heat removed from the evaporator during each cycle, but not detected by an air-side energy balance. Finally, it appears the thermal mass of the evaporator ductwork does not affect the air as it passes through it.

Appendix E: Role of Accumulator during Cycling

Sometimes refrigerators are equipped with accumulators to protect the compressor from slugs of liquid refrigerant, especially during startup after the off cycle. During the off-cycle most of the charge flows to the evaporator; therefore the compressor must redistribute the excess refrigerant from the evaporator to the condenser and other components before the refrigerator can reach quasi-steady performance. A large portion of this redistribution takes place when the compressor turns on. During this initial portion of the on-cycle some of the refrigerant leaves as slugs of liquid (Rubas and Bullard, 1993). The accumulator collects these liquid slugs, to protect the compressor. One consequence is this trapped refrigerant must be evaporated before the refrigerator can reach its steady state efficiency. This Appendix examines how long the accumulator holds charge and how much charge is trapped in the accumulator.

E.1 Experimental Evidence

If the accumulator holds charge during the initial portions of the on-cycle then it should be noticeable by a change in the superheat levels before and after the accumulator. Figure E.1 illustrates this phenomena. If a superheated vapor flows over a pool of liquid refrigerant, the hot vapor will evaporate some of the liquid cooling the vapor before it leaves the accumulator. This is similar to the process used in a "swamp" cooler, where a superheated refrigerant represents the air and liquid refrigerant represents the water.

Accumulator

$$T_{in} > T_{out}$$
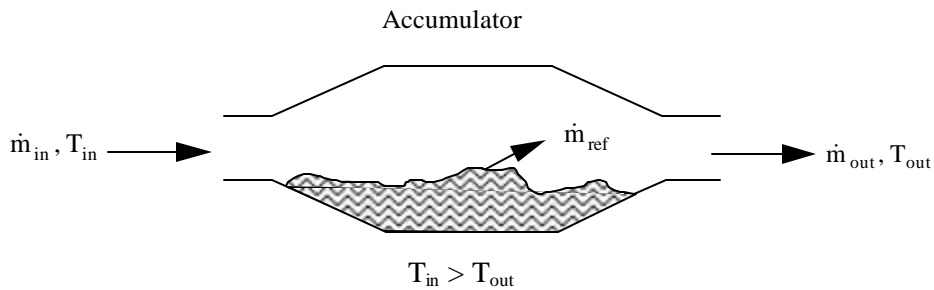
Figure E.1 Schematic of accumulator as a "swamp" cooler

If this analogy between the accumulator and a "swamp" cooler is true then the temperature of the refrigerant entering and leaving the evaporator would indicate whether refrigerant is trapped after start up. To test this hypothesis, the Amana test stand was equipped with surface thermocouples before and after the accumulator. Both of these thermocouples were insulated to insure the temperature readings were representative of the refrigerant and not the surrounding air. Using these readings along with the evaporator saturation pressure (temperature) Figure E.2 was developed.
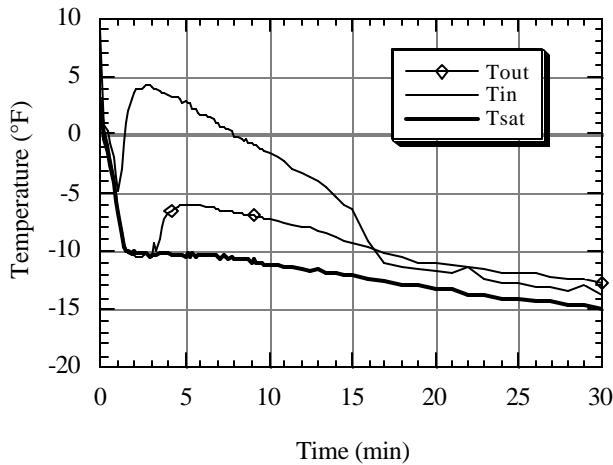
Figure E.2 Refrigerant temperature before and after accumulator (T_{amb}=90°F)

As can be seen from Figure E.2 the temperature leaving the accumulator is clearly cooler than the refrigerant entering the accumulator. This indicates the accumulator is initially filled with liquid refrigerant. It is also clear that this temperature discrepancy disappears after 15 minutes. This suggests liquid refrigerant remains in the accumulator for up to 15 minutes after start up.

E.2 Estimation of How Much Charge Is Trapped By Accumulator

Since it seems clear the accumulator holds liquid refrigerant, the next logical question is how much? As pointed out earlier a superheated vapor entering the accumulator is cooled as it evaporates the liquid it flows over. Figure E.3 represents a control volume drawn around the superheated refrigerant flowing through the accumulator.
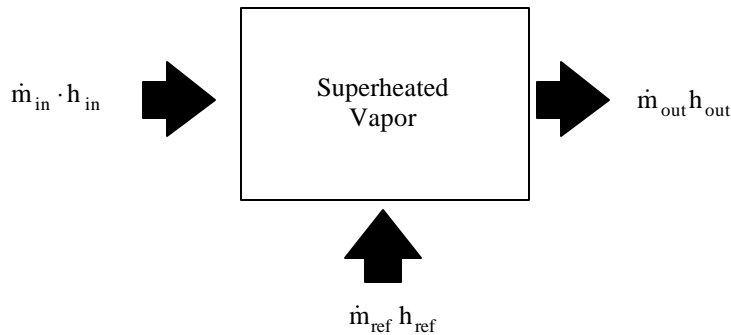
Figure E.3 Control volume around vapor within the accumulator

Assuming an accumulator in adiabatic, Equation E.1 represents an energy balance for the above control volume.

$$\dot{m}_{in} \cdot h_{in} + \dot{m}_{ref} \cdot h_{ref} = \dot{m}_{out} \cdot h_{out}$$

(E.1)

Rearranging equation E.2 yields the following expression for the rate of evaporation of liquid refrigerant.

$$\dot{m}_{ref} = \frac{\partial m_{ref}}{\partial t} = \dot{m}_{in} \frac{(h_{in} - h_{out})}{(h_{out} - h_{ref})}$$

(E.2)

The accumulator inlet and exit enthalpies are calculated with pressures and temperatures recorded on the test stand. The enthalpy of the liquid in the accumulator is assumed to be the enthalpy of saturated liquid at the evaporator pressure and the inlet mass flow rate is calculated using the compressor map.

Equation E.2 gives information about the rate of liquid evaporation, at a single instant. To calculated how much charge is removed from the accumulator, or how much refrigerant is trapped after start up, Equation E.2 must be integrated over the period of time showing reduced superheat. Since the data is collected every ten seconds the integration can be approximated numerically as shown in Equation E.3.

$$\Delta m_{ref} = \sum_{i=1}^{n}\left(\dot{m}_{in} \frac{(h_{in} - h_{out})}{(h_{out} - h_{ref})} \right)_i \cdot \Delta t \quad \text{where} \quad n = \frac{t_{total}}{\Delta t}$$

(E.3)

Where ?t is ten seconds and t_{total} is the total length of time a difference exist between the inlet and exit temperatures of the accumulator. The above numerical integration was performed on data collected at several different ambient temperatures. The results are shown in Table E.1.

Table E.1 Mass of refrigerant collected in the accumulator

Tamb	Mass (oz)
100°F	0.65
90°F	0.75
75°F	0.78
60°F	0.60

E.3 Conclusion

One of the main factors contributing to evaporator capacity degradation is refrigerant maldistribution, for this reason anything that slows this redistribution process contributes to cycling losses. The above analysis demonstrated that the accumulator traps between 0.5 to 0.75 ounces of refrigerant. This refrigerant remains within for approximately 15 minutes as it is evaporated. These results tend to suggest that a refrigerator equipped with an accumulator would take longer to reach steady state performance than a system without an accumulator.

Appendix F: Graphs for Ambients 60°F through 100°F

The analyses presented in this report mainly refers to trends in refrigerator performance at 90°F ambient temperature. However, data were also taken at 60°F, 75°F, and 100°F. This Appendix presents the results for all four ambient temperatures to provide a more complete picture of system behavior.
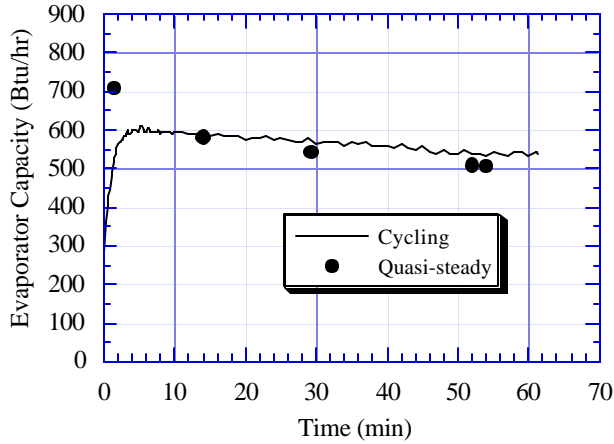
Figure F.1a Evaporator capacity (T_{amb}=100°F)
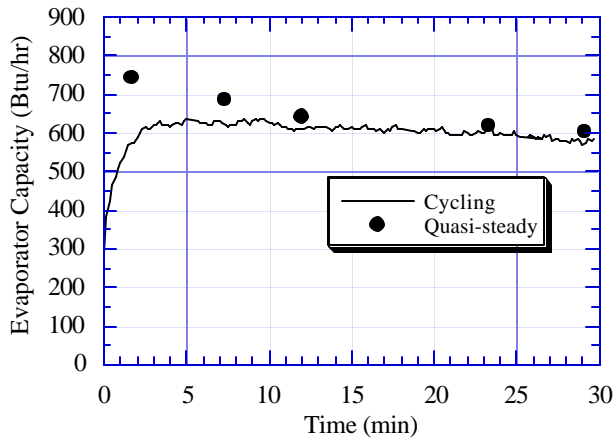
Figure F.1b Evaporator capacity (T_{amb}=90°F)
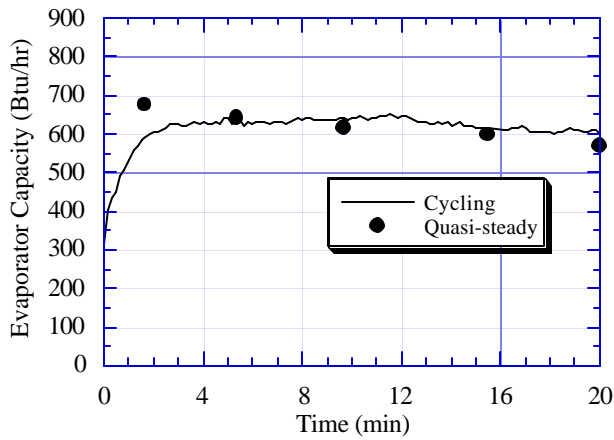
Figure F.1c Evaporator capacity (T_{amb}=75°F)
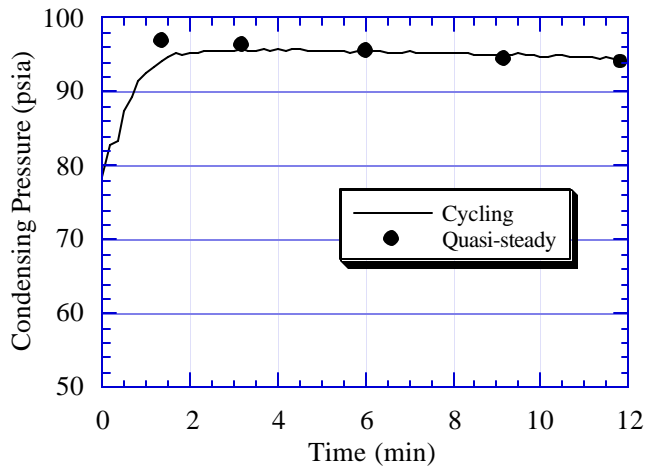
Figure F.1d Evaporator capacity (T_{amb}=60°F)
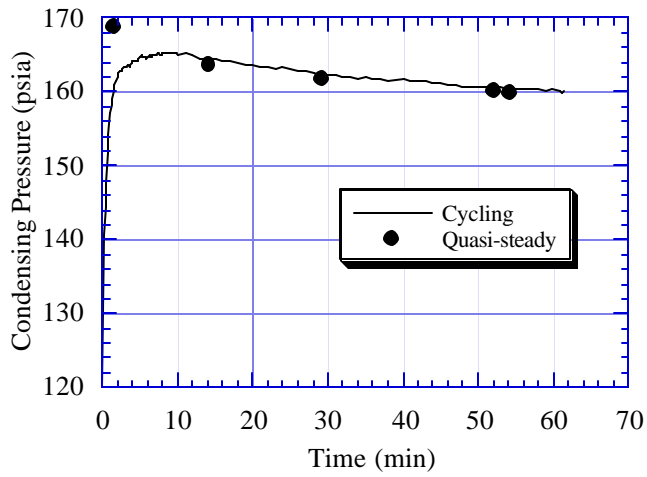
Figure F.2a Condensing pressure (T_{amb}=100°F)
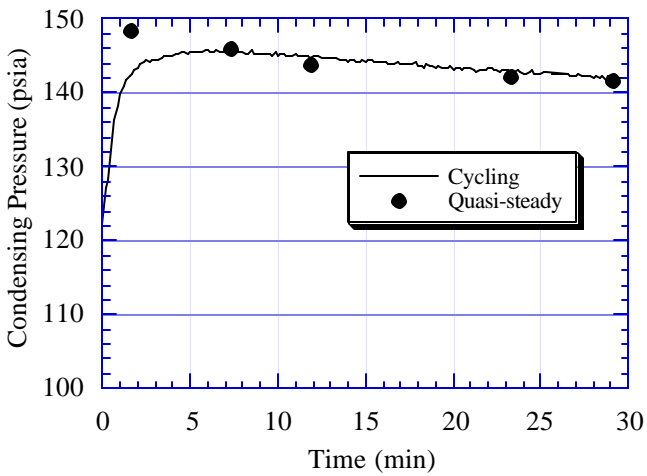
Figure F.2a Condensing pressure (T_{amb}=90°F)
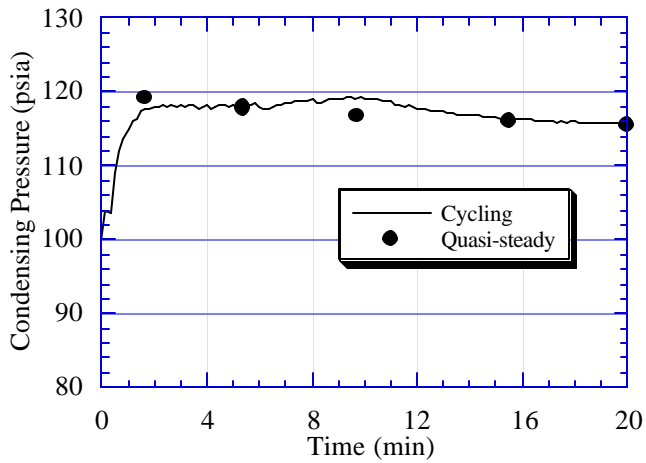
Figure F.2c Condensing pressure (T_{amb}=75°F)
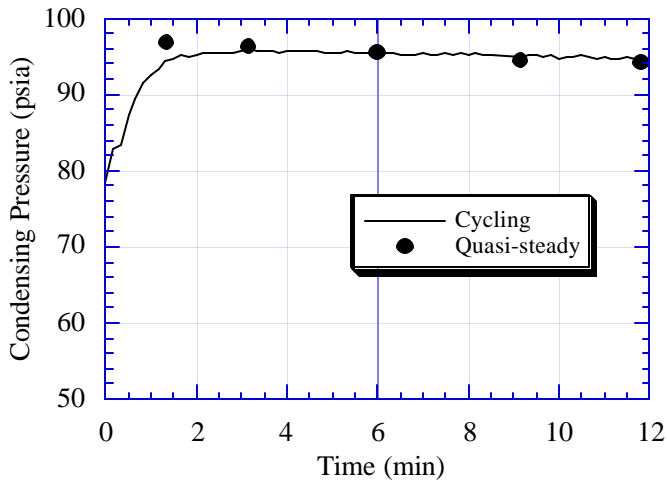
Figure F.2d Condensing pressure (T_{amb}=60°F)
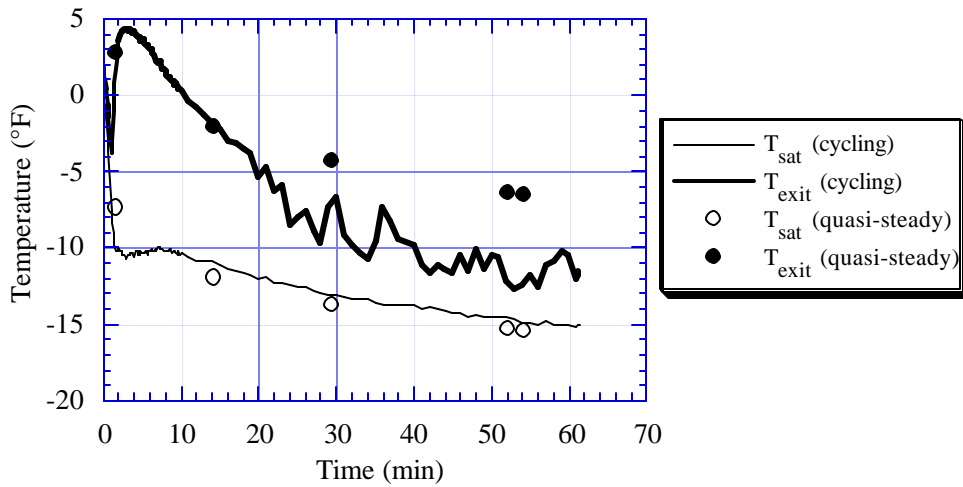
Figure F.3a Evaporator exit and saturation temperatures (T_{amb}=100°F)

58
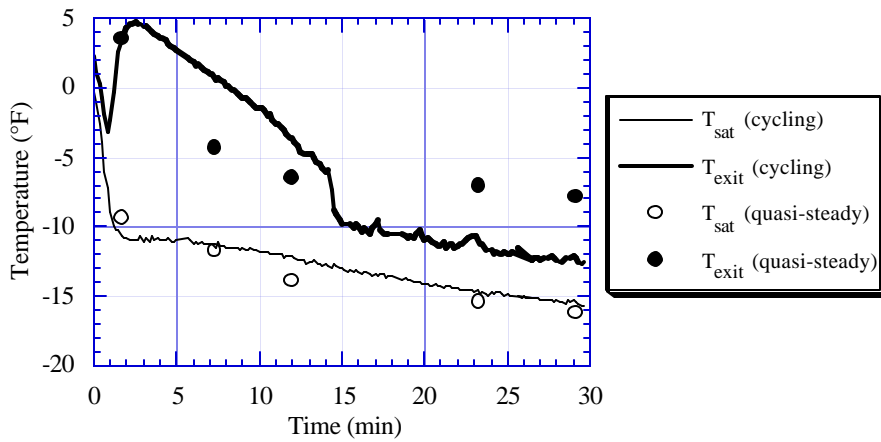
Figure F.3b Evaporator exit and saturation temperatures (T_{amb}=90°F)
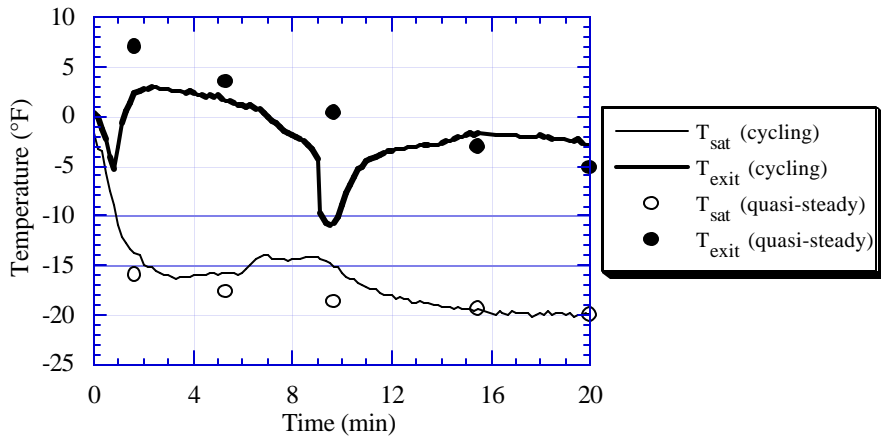
Figure F.3c Evaporator exit and saturation temperatures (T_{amb}=75°F)
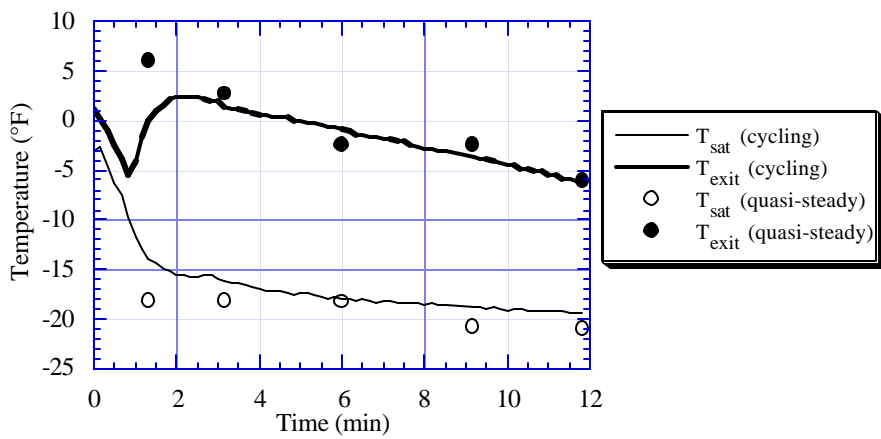
Figure F.3d Evaporator exit and saturation temperatures (T_{amb}=60°F)
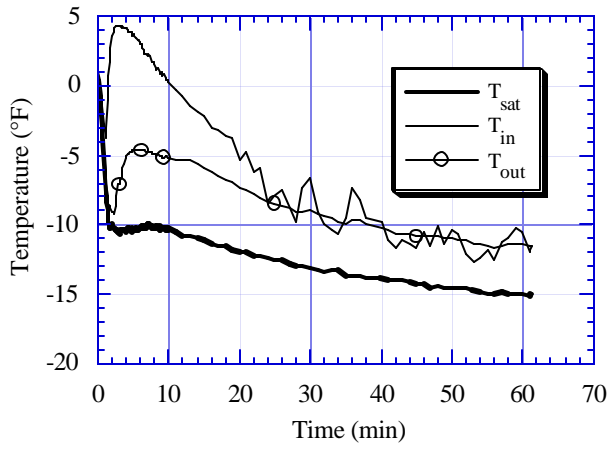
Figure F.4a Refrgerant trapped in the accumulator after start-up (T_{amb}=100°F)
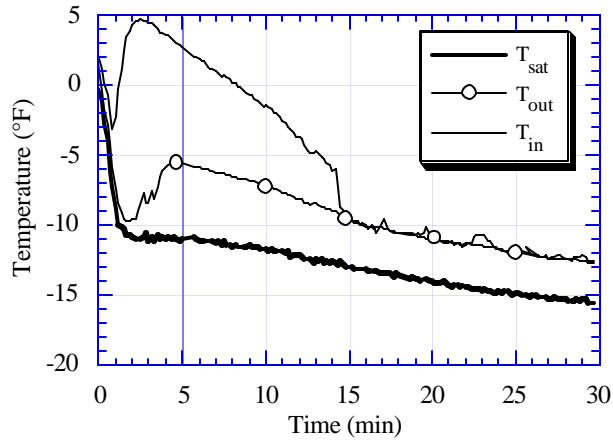
Figure F.4b Refrigerant trapped in accumulator after start-up (T_{amb}=90°F)
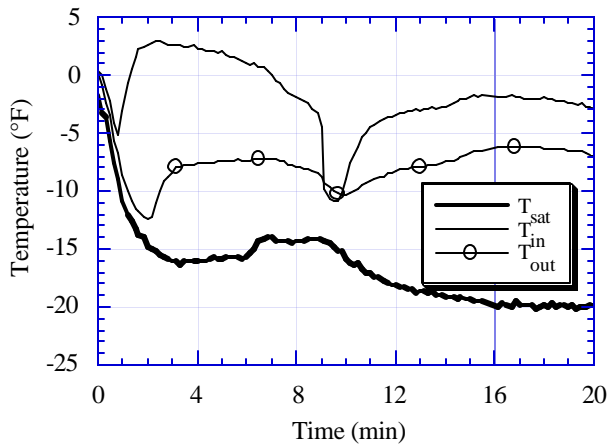
Figure F.4c Refrigerant trapped in the accumulator after start-up (T_{amb}=75°F)
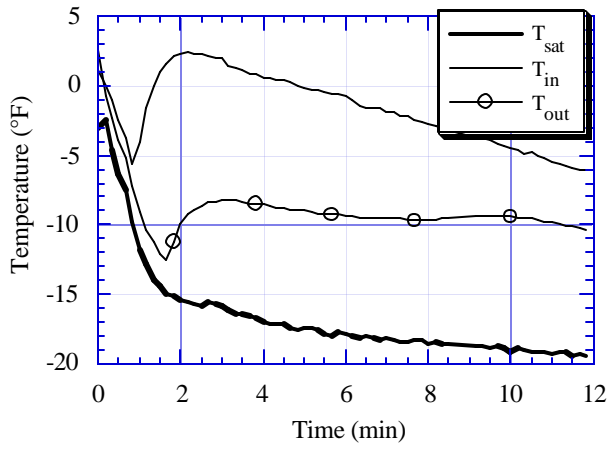
Figure F.4d Refrigerant trapped in the accumulator after start-up (T_{amb}=60°F)
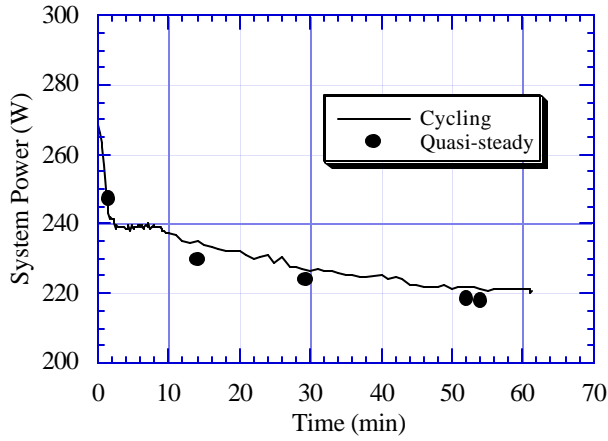
Figure F.5a System power (T_{amb}=100°F)
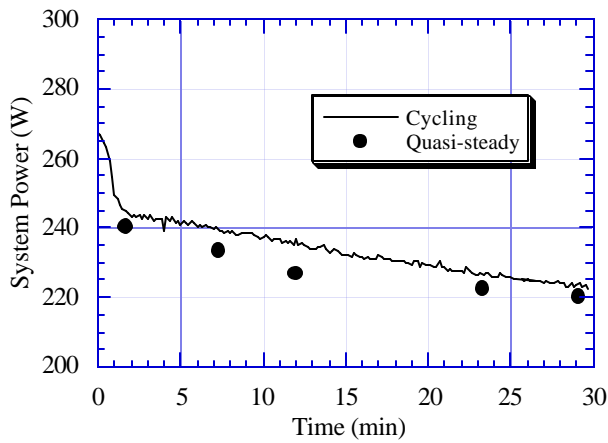
Figure F.5b System power (T_{amb}=90°F)
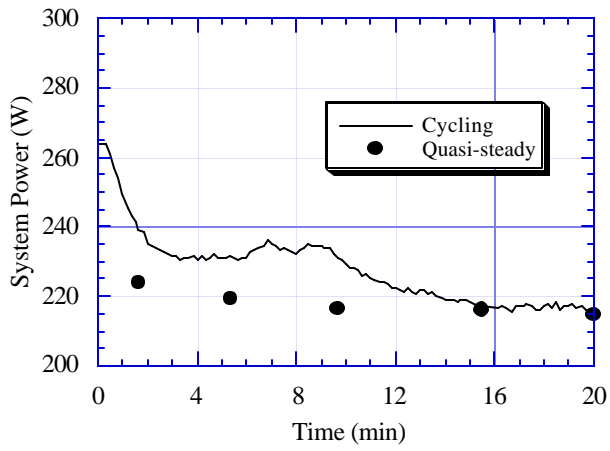
Figure F.5c System power (T_{amb}=75°F)
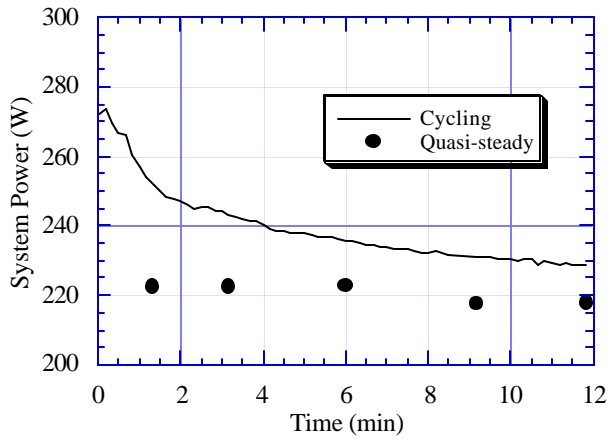
Figure F.5d System power (T_{amb}=60°F)
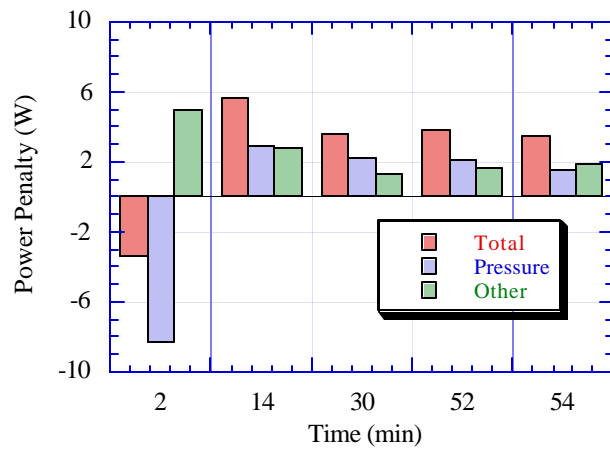
Figure F.6a Breakdown of power penalty (T_{amb}=100°F)
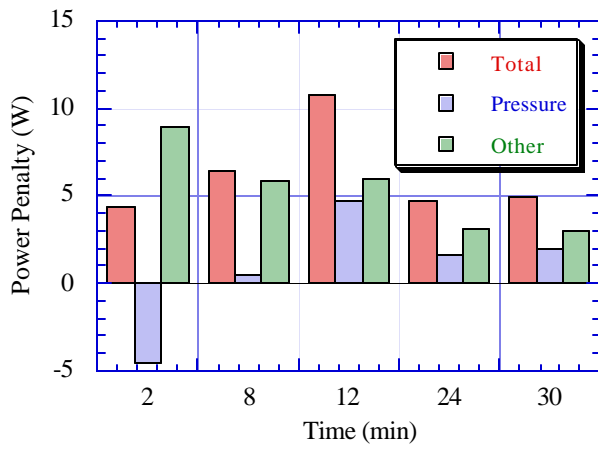
Figure F.6b Breakdown of power penalty (T_{amb}=90°F)
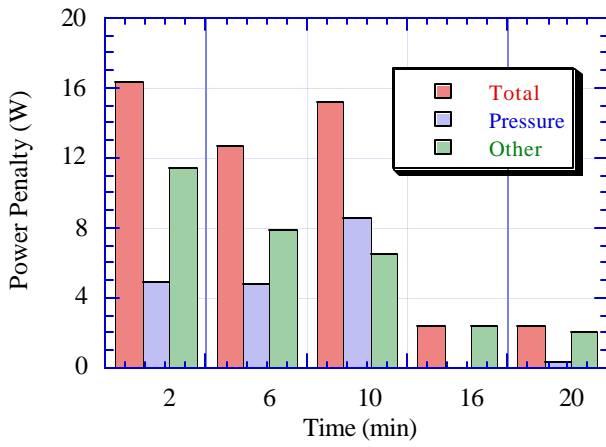
Figure F.6c Breakdown of power penalty (T_{amb}=75°F)
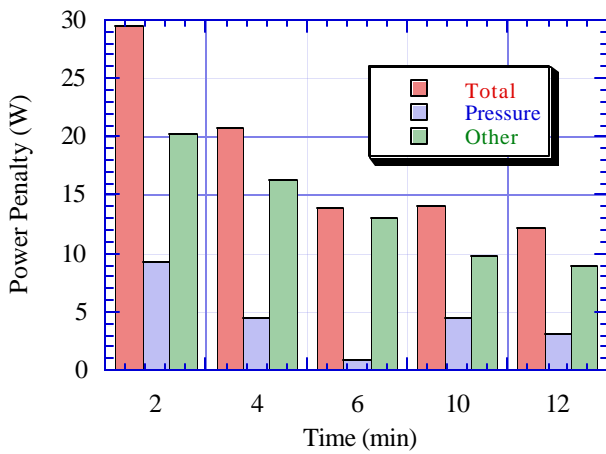
Figure F.6d Breakdown of power penalty (T_{amb}=60°F)
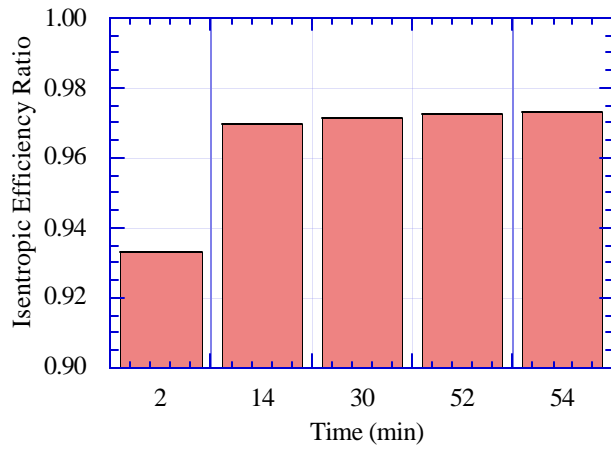
Figure F.7a Isentropic efficiency ratio (T_{amb}=100°F)
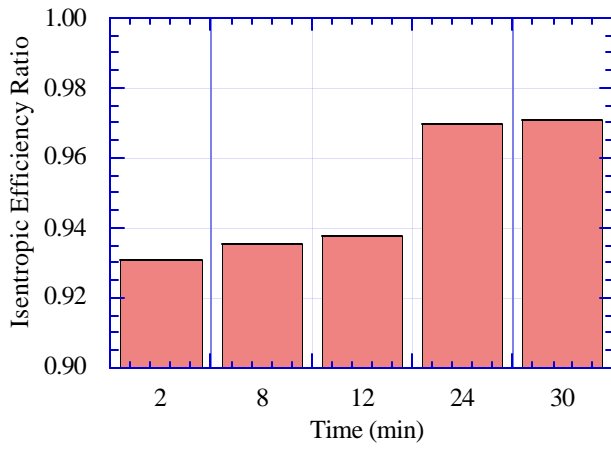
Figure F.7b Isentropic efficiency ratio (T_{amb}=90°F)
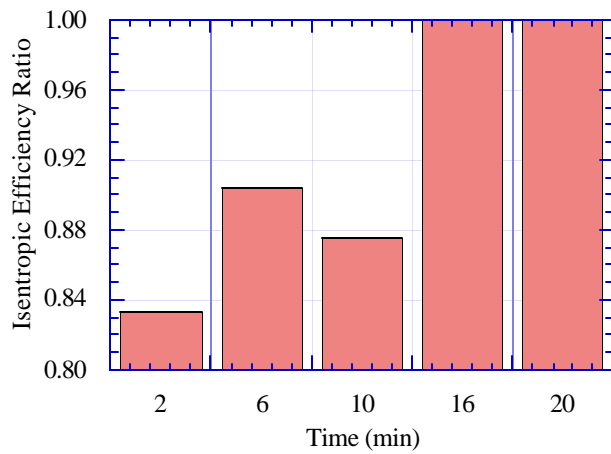
Figure F.7c Isentropic efficiency ratio (T_{amb}=75°F)
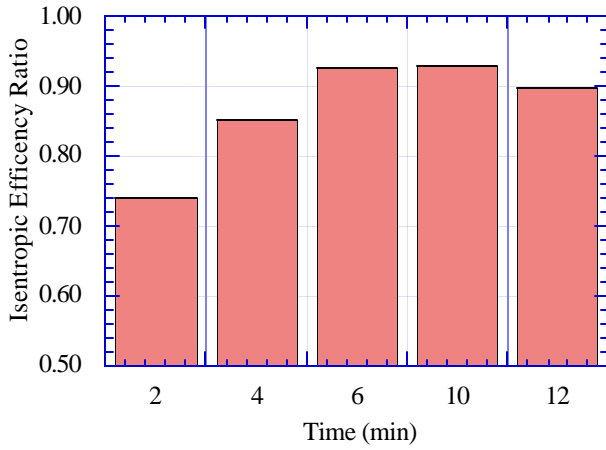
Figure F.7.d Isentropic efficiency ratio (T_{amb}=60°F)
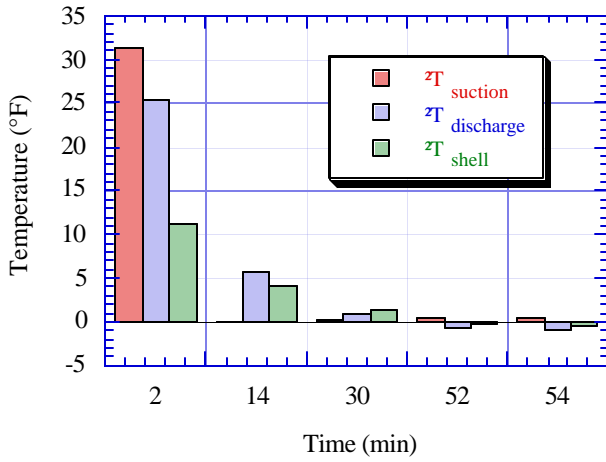
Figure F.8a Differences in suction, discharge, and shell temperatures (T_{amb}=100°F)
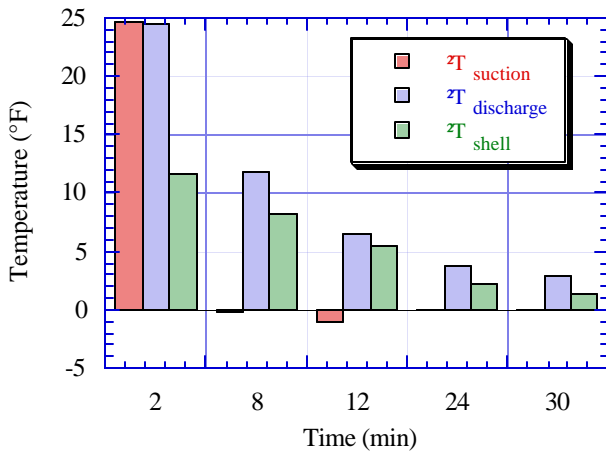
Figure F.8b Differences in suction, discharge, and shell temperatures (T_{amb}=90°F)

65
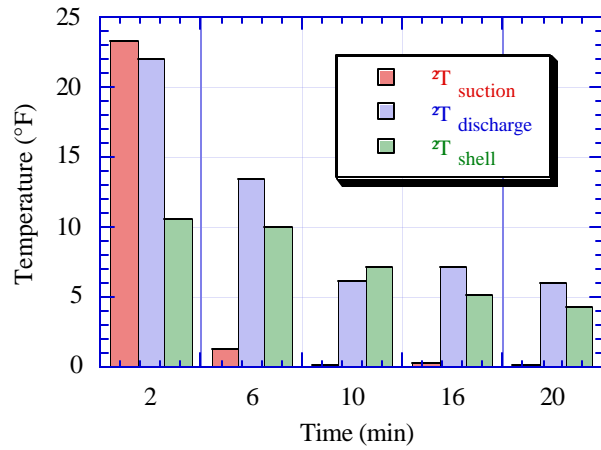
Figure F.8c Differences in suction, discharge, and shell temperatures (T_{amb}=75°F)
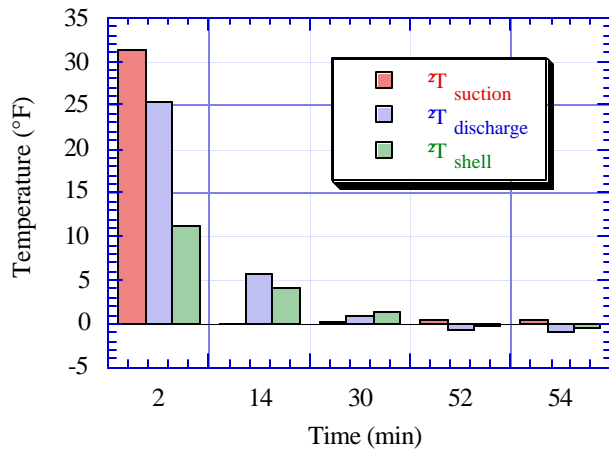
Figure F.8d Differences in suction, discharge, and shell temperatures (T_{amb}=60°F)

Appendix G: Repeatability of Experiments

To test whether the trends of the data presented in the body of this report were repeatable, a new set of cycling and steady state data were collected at 90°F and 75°F ambient temperatures. Between data sets, the refrigerator was accidentally connected to 240 VAC by electricians who were modifying the lab wiring and a leak in the evaporator appeared and was repaired. Therefore this analysis concentrates mainly on whether the overall system trends were repeatable and not whether the exact values of the individual measurements could be repeated.

G.1 Repeatability of Data for 90°F Ambient

To demonstrate the trends seen in the earlier data sets were repeatable Figures G.1-8 compare 90°F data collected in January 1995 with data collected in May 1995. These figures demonstrate the general trends of both data sets are identical. However, there were several subtle differences which need to be addressed. First, the length of the on-cycle increased for the May data set. Past experience has shown the compressor run time can vary ±3 minutes from cycle to cycle. Therefore, the differences seen in the cycle length is within the normal variation of cycle length. It was observed the refrigerator operated with a slightly elevated condensing pressure and the evaporator was superheated for a shorter period of time than during the May data set. These observations suggest the refrigerator was charged with more refrigerant. Prior to collecting the May data set the refrigerator was charged with 8.0 ounces of refrigerant R-12. Since the January tests were conducted with 7.0 ounces of R-12, approximately one ounce of refrigerant was removed. Since removing charge from refrigerator is an inexact science it likely the refrigerator remained slightly overcharged.
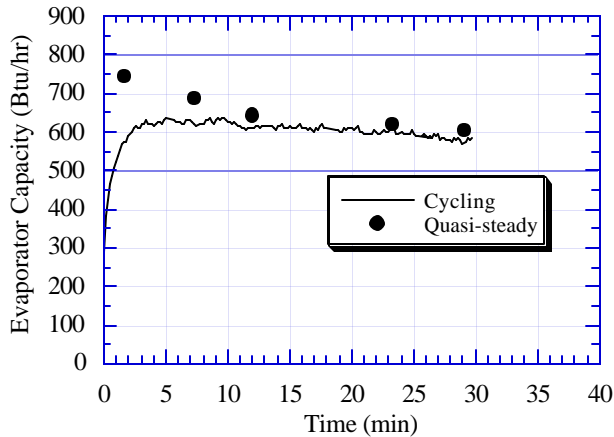

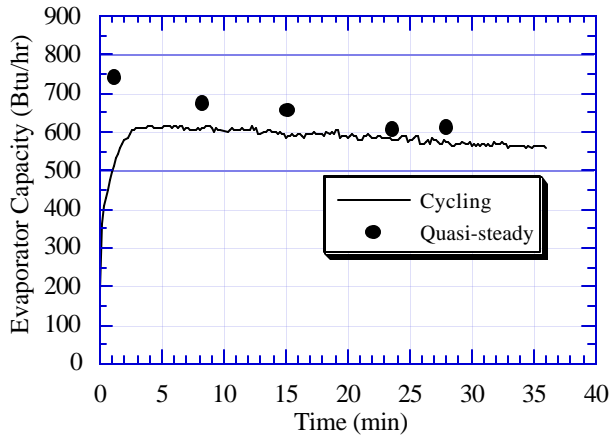Figure G.1a Evaporator capacity (January, 1995)

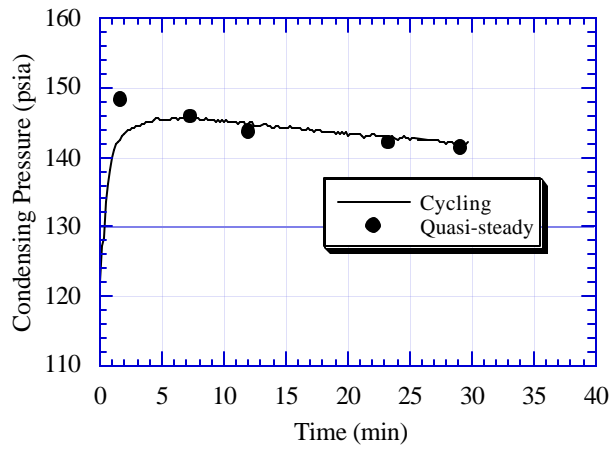Figure G.1b Evaporator capacity (May, 1995)

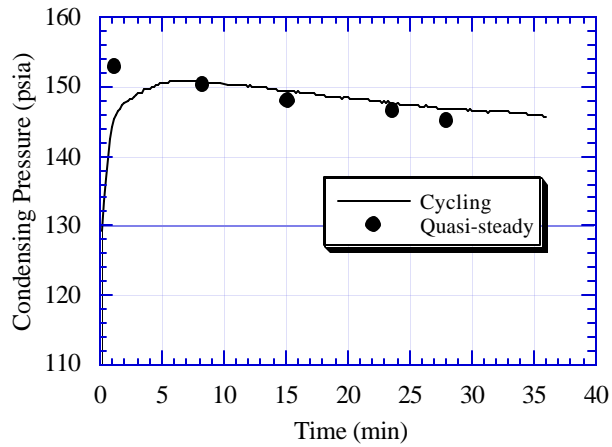

Figure G.2a Condensing pressure (January, 1995)

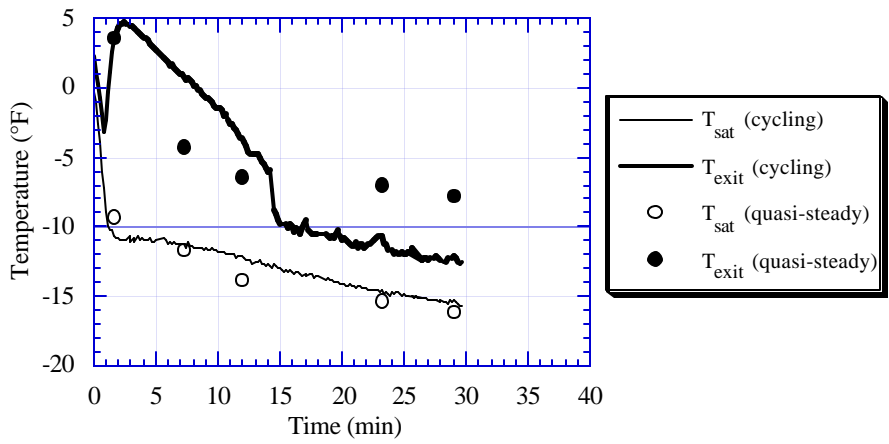Figure G.2b Condensing pressure (May, 1995)

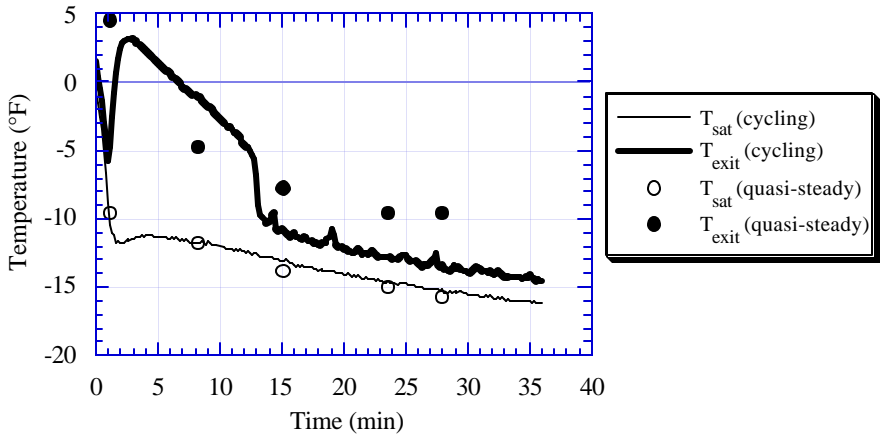Figure G.3a Evaporator exit and saturation temperatures (January, 1995)

Figure G.3b Evaporator exit and saturation temperatures (May, 1995)
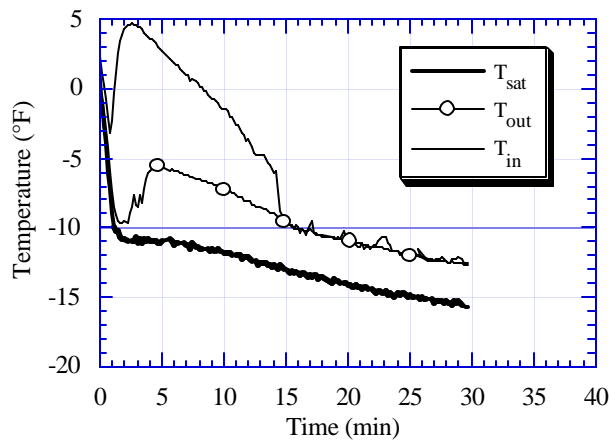

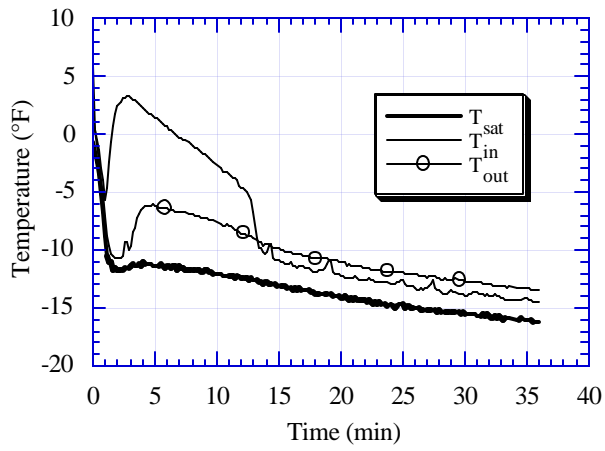Figure G.4a Refrigerant trapped in accumulator after start-up (January, 1995)

69

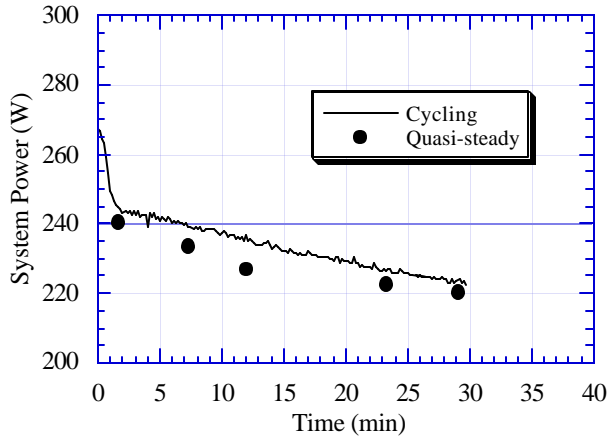Figure G.4b Refrigerant trapped in accumulator after start-up (May, 1995)

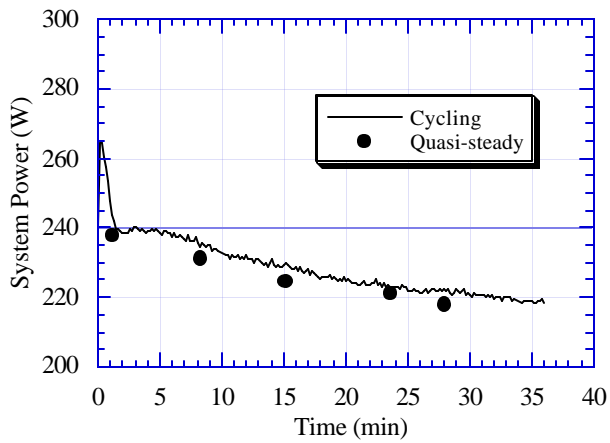Figure G.5a System power (January, 1995)

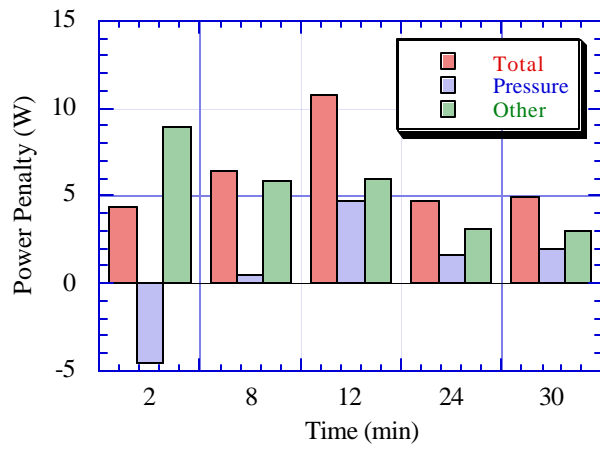
Figure G.5b System power (May, 1995)

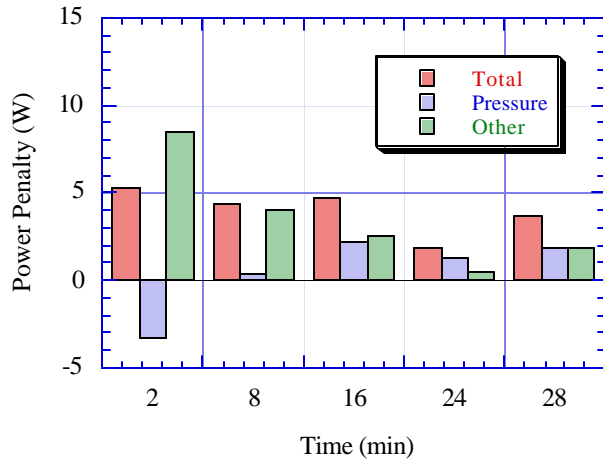Figure G.6a Power penalty breakdown (January, 1995)
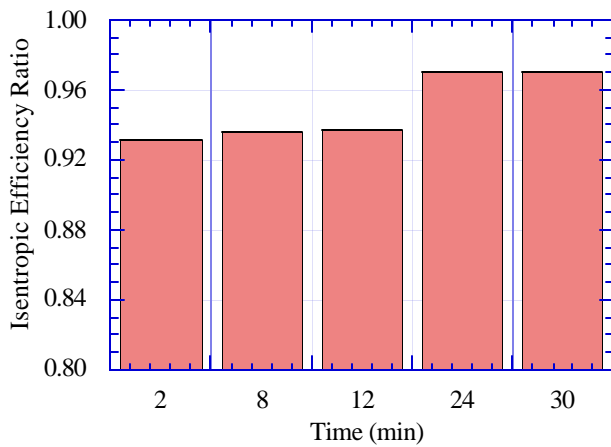

Figure G.6b Power penalty breakdown (May, 1995)

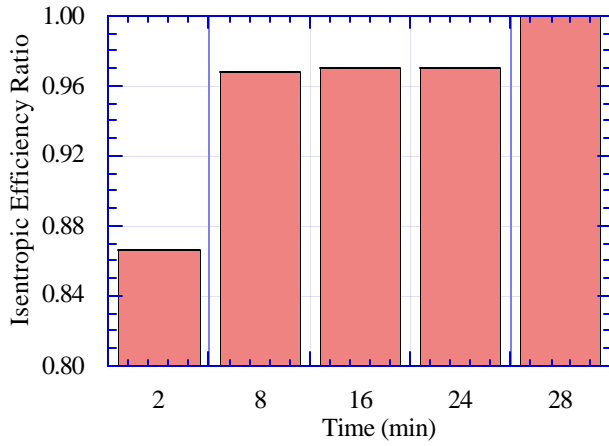Figure G.7a Isentropic efficiency ratio (January, 1995)

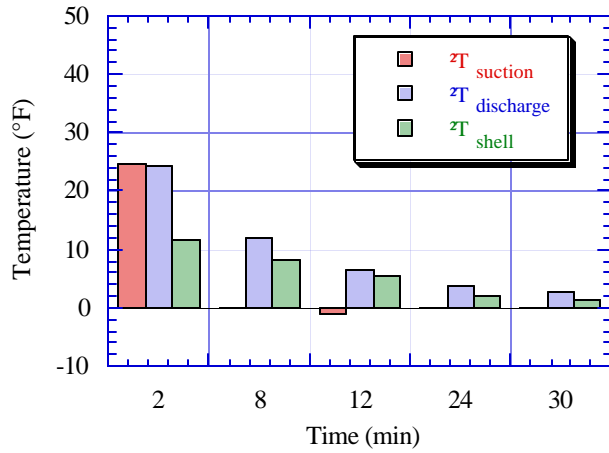Figure G.7b Isentropic efficiency ratio (May, 1995)

Figure G.8a Differences in suction, discharge, and shell temperatures (January, 1995)
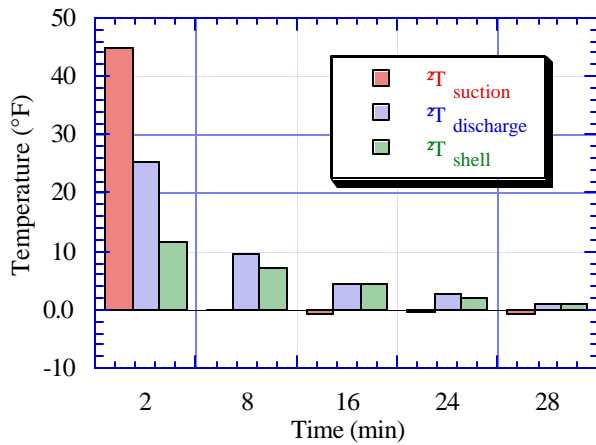

Figure G.8b Differences in suction, discharge, and shell temperatures (May, 1995)

G.2 Repeatability of Data for 75°F Ambient

Figures G.9-16 demonstrate that the trends seen in the January data were repeatable. In general the observation made earlier concerning the 90°F ambient data apply to the 75°F data as well. An additional trend reproduced in the May 1995 data set was the unusual surge in the system power requirements. This phenomenon was not present at other ambient conditions but has consistently appeared for the 75°F ambient conditions. Figure G.13a/b shows the phenomenon. Approximately six minutes into the on-cycle, the system power requirements increase by almost 10 Watts (about 5%). Since the measured evaporator and condenser fan powers do not show this increase the increased power requirements must be caused by the compressor. This increased compressor power requirement is accompanied by increases in evaporating and condensing pressure, as well as a sudden decrease in evaporator superheat. These symptoms suggest a sudden increase in refrigerant mass flow rate. This observation is supported by the fact the voltage output from the mass flow meter also increased six minutes into the cycle indicating an increase in refrigerant mass flow rate.

While an increase in mass flow rate may be the reason for the sudden increase in compressor power, this does not explain why it happened. The refrigerant mass flow rate is controlled by two pieces of equipment: the capillary tube and the compressor. It is likely this change is caused by the capillary tube. It appears the conditions entering the capillary cause a sudden increase in mass flow rate, possibly due to re-condensation in the suction line heat exchanger. The rest of the system responds to this increase in mass flow rate with the elevated system pressures and increased compressor power demand. Unfortunately this explanation cannot be verified, when the refrigerator is charged with seven ounces of refrigerant the capillary tube inlet is two-phase during the entire on-cycle and therefore only the pressure and temperature are known and not the quality.

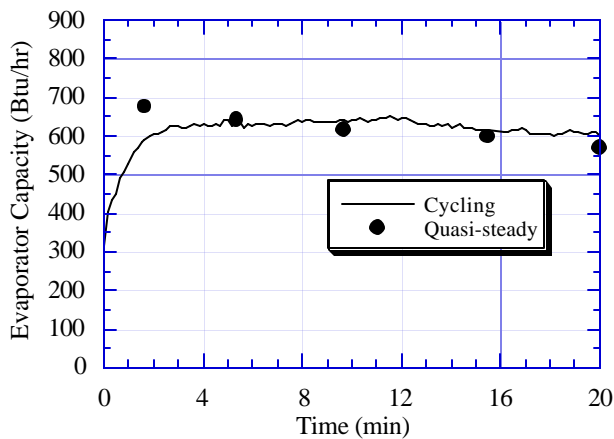Figure G.9a Evaporator capacity (January, 1995)
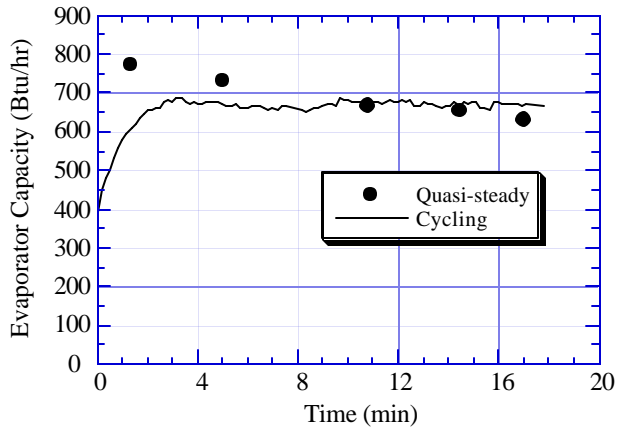
Figure G.9b Evaporator capacity (May, 1995)
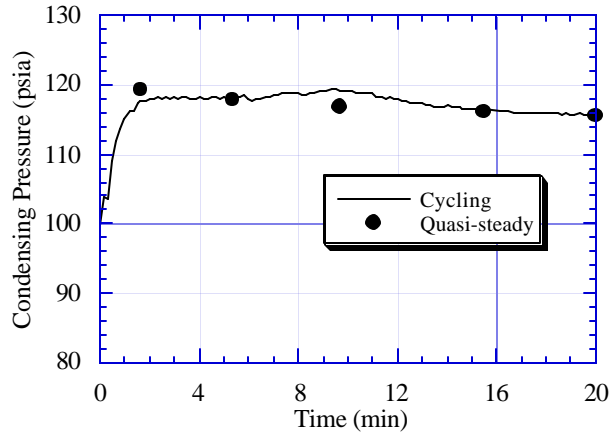
Figure G.10a Condensing pressure (January, 1995)
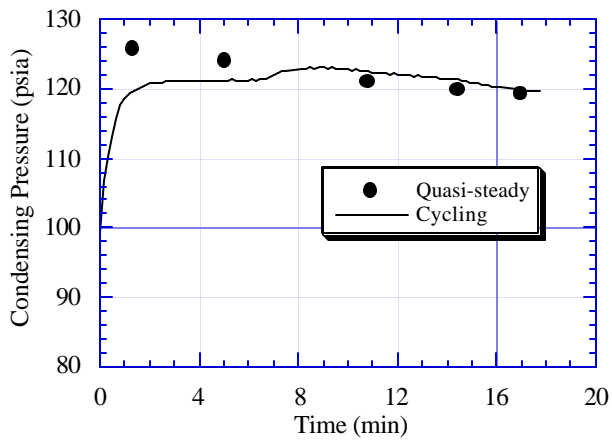
Figure G.10b Condensing pressure (May, 1995)
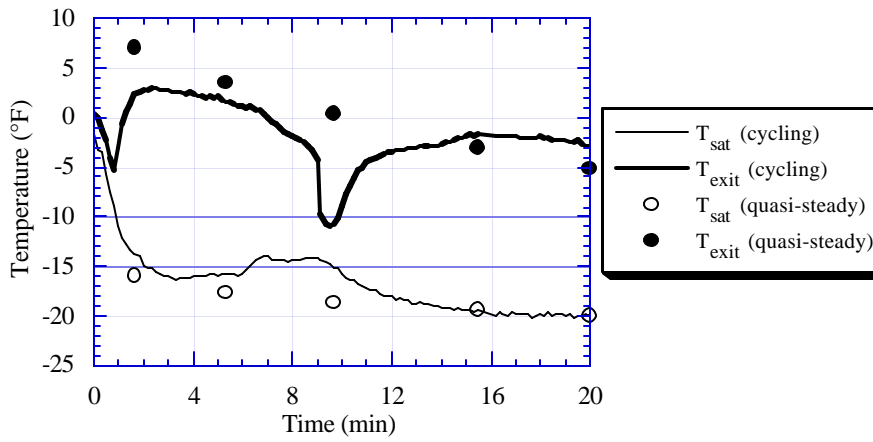
Figure G.11a Evaporator exit and saturation temperature (January, 1995)
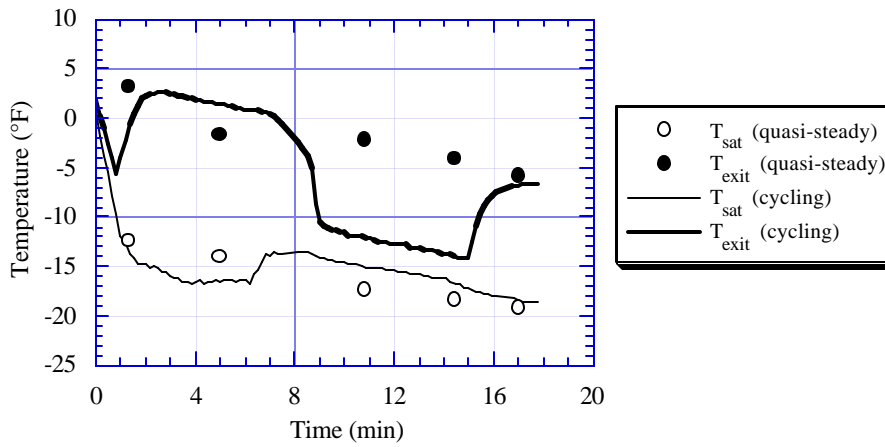
Figure G.11b Evaporator exit and saturation temperatures (May, 1995)
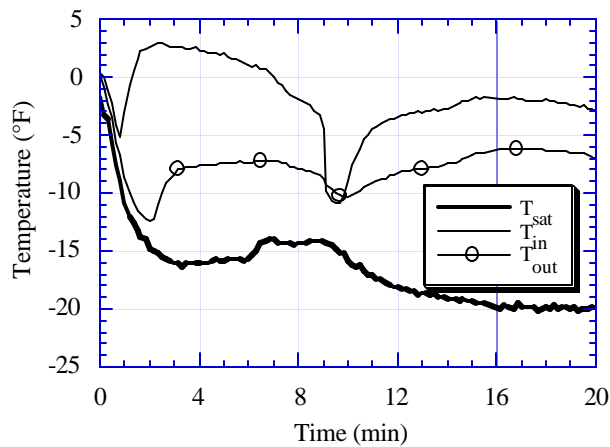
Figure G.12a Refrigerant trapped in accumulator after start-up (January, 1995)
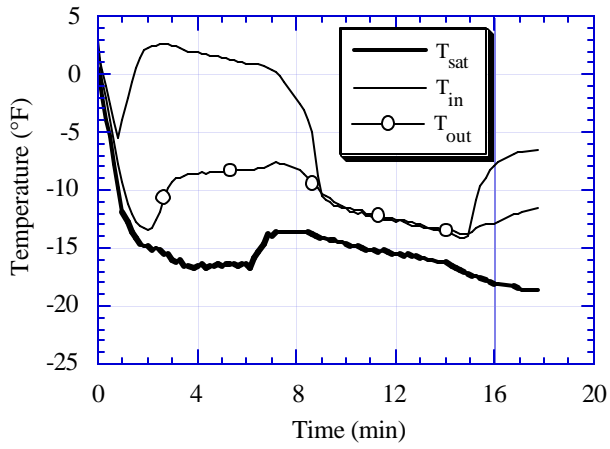
Figure G.12b Refrigerant trapped in accumulator after start-up (May, 1995)
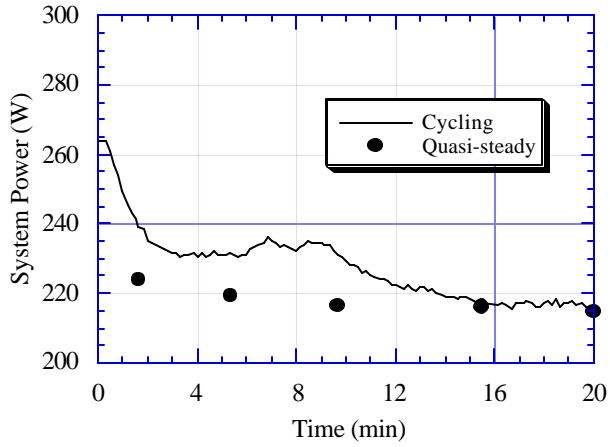
Figure G.13a System power (January, 1995)
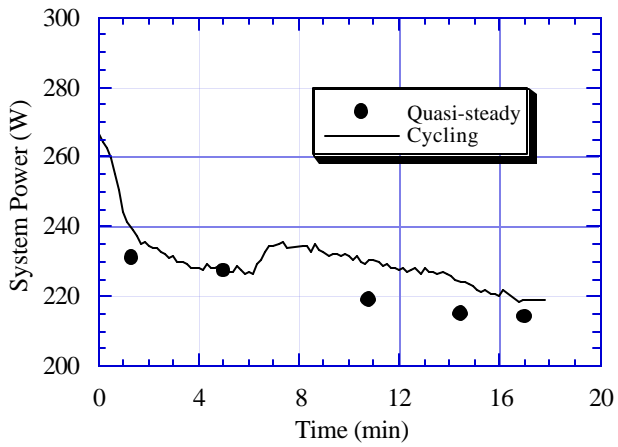
Figure G.13b System power (May, 1995)
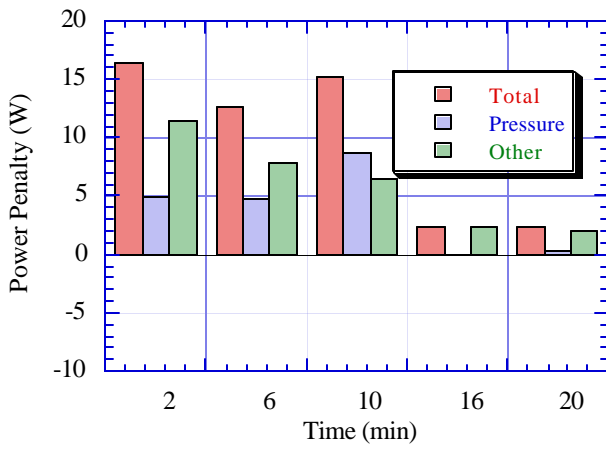
Figure G.14a Breakdown of power penalty (January, 1995)
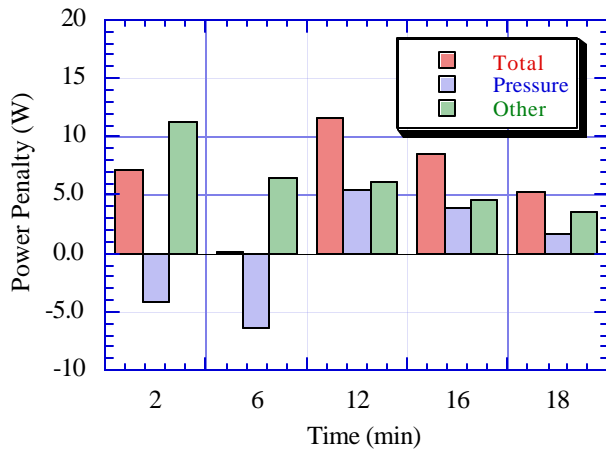
Figure G.14b Breakdown of power penalty (May, 1995)
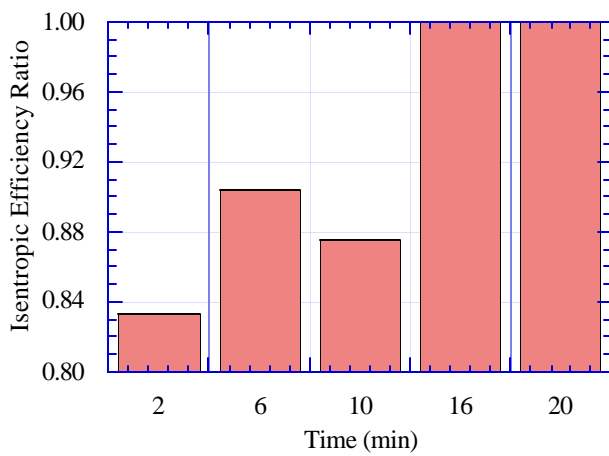
Figure G.15a Isentropic efficiency ratio (January, 1995)
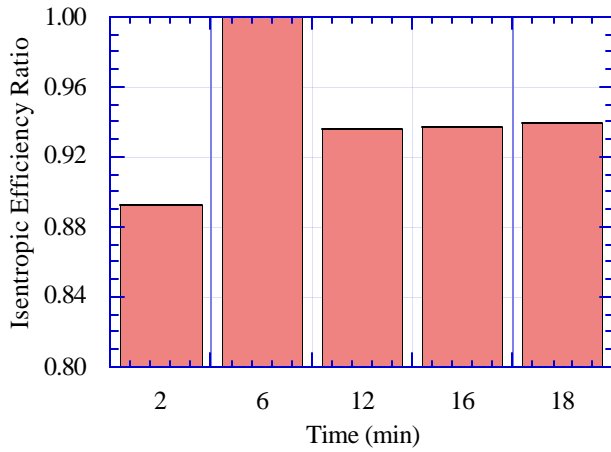
Figure G.15b Isentropic efficiency ratio (May, 1995)
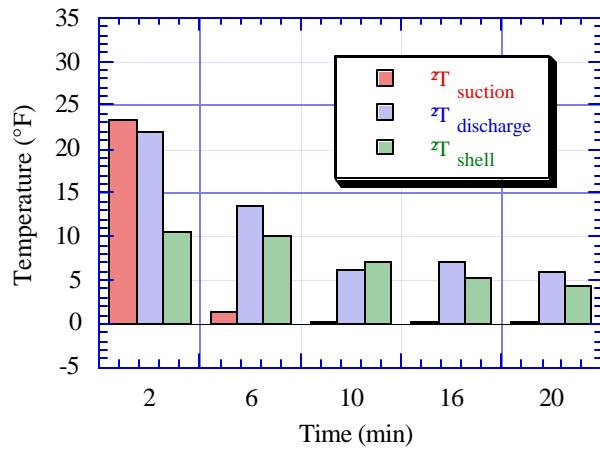
Figure G.16a Differences in suction, discharge, and shell temperatures (January, 1995)
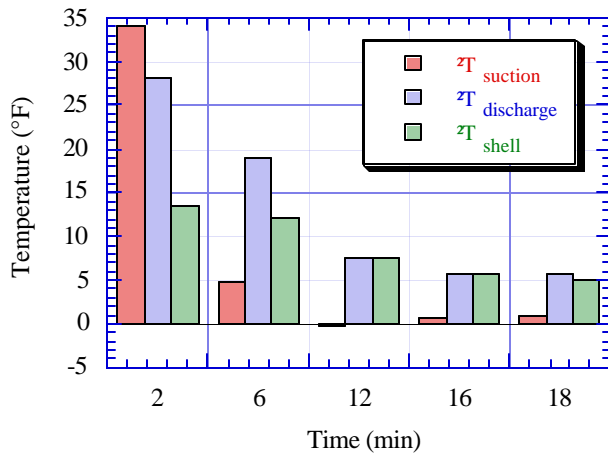
Figure G.16b Difference is suction, discharge, and shell temperatures (May, 1995)

Appendix H: Internal Volume and Oil in the Compressor Sump

The ability to accurately predict the refrigerant charge inventory is an important step in the development of a refrigerator simulation model since the refrigerator performance in off-design condition is determined by the amount of total charge in the system. In addition this ability also provides a design tool for determining ways to minimizing total refrigerant charge which has many beneficial implications. This Appendix will outline work done to improve estimates of the Amana refrigerator's internal volume and amount of oil in its compressor sump. In addition a computer program has been developed to aid in determining refrigerant leaks in future experiments.

H.1 Oil in the Compressor Sump

Originally the compressor used in the Amana was lubricated with 13 ounces of grade 32 Naphthanic mineral oil (Heckstedde, 1995). Over the years that the Amana has served as a test stand, it has undergone numerous chargings and dischargings, resulting in undetermined amounts of oil being removed from the compressor sump, leaving it with less than the original 13 ounces. To understand exactly how much oil remains in the sump several tests were conducted. In these experiments the Amana was charged with a known quantity of refrigerant R-12 and let "soak" at four different ambient temperatures with the compressor off and the doors open. After soaking for at least 2 days both the system pressure and temperature were recorded.

When the refrigerator is left to soak the refrigerant either dissolves in the compressor sump oil or becomes a superheated vapor filling the remaining internal volume (Equation H.1). Estimating the amount of refrigerant present in vapor form is accomplished using Equation H.2, where the specific volume of the refrigerant is calculated using measured pressure and temperature readings. The internal volume of the refrigerator is calculated by adding the volumes of the individual components shown in Table H.1 and subtracting the volume of the oil in the compressor sump. With this information the amount of refrigerant present as a superheated vapor and dissolved in the oil is known. Grebner and Crawford related the liquid refrigerant concentration in the oil as a function of temperature, pressure, and mass of oil as shown symbolically in Equation H.3. This provides all the information necessary to calculate the mass oil present in the sump Using data shown in Table H.1 the mass of oil in the sump is estimated to be 11.1 ± 0.2 ounces. This means approximately 2 ounces of oil have been removed from the compressor sump.

$$m_{total} = m_{refoil} + m_{refvap} \tag{H.1}$$

$$m_{rvap} = \frac{Vol_{sys}}{\upsilon_r(T,P)} \tag{H.2}$$

$$m_{refoil} = f(T,P,m_{oil}) \tag{H.3}$$

Table H.1 Mass of oil in compressor sump

Tamb [°F]	Tsys [°F]	Psys [psia]	mref [oz]	moil [oz]
100	99.0	77.2	8.0	11.2
90	89.9	70.4	8.0	11.0
75	74.9	58.1	8.0	11.4
60	60.2	48.0	8.0	10.9

H.2 Refrigerator Internal Volume

The ability to accurately predict the refrigerator charge inventory is contingent upon accurate volume estimates of the individual components. Table H.2 contains the latest estimates for the various refrigerator components. A detailed description was provided by Goodson and Bullard (1994) showing how all but the compressor volume were calculated. The compressor volume has been updated after Tecumseh Products Company provided a more detailed description of the compressor.

As an independent check to verify that summing the volumes in Table H.2 would accurately predict the total system volume, the refrigerator was charged with 0.194 lbm (3.1 oz) of R-134a. This refrigerant was chosen because it is less soluble in mineral oil than R-12, thus reducing the uncertainty associated with liquid refrigerant dissolving into the oil. Assuming initially that R-134a was insoluble in mineral oil, the volume of the refrigerator was calculated using Equation H.4 and data collected at three different ambient temperatures.

$$\mathrm{Vol}_{sys} = m_r \cdot \upsilon_r(T, P)$$

(H.4)

Table H.2 Amana component volumes

Component	Volume (ft^3)
Accumulator	3.40e-3
Bell Caps	9.60e-5
Capillary Tube	6.20e-5
Compressor (less oil)	8.91e-2
Condenser	1.12e-2
Discharge Line	4.80e-4
Evaporator	2.17e-2
Filter Dryer	4.80e-4
Liquid Line	5.40e-4
Suction Line	2.00e-3
Total	0.126 (217 in^3)

Table H.3 Calculated internal volume using R-134a

Tsys [°F]	Psys [psia]	Calculated Volume [in^3]	wWitco1GS [%]	wbreak-even [%]
59.9	62.3	261	4.8	4.5
75.2	68.9	243	4.9	3.0
90.6	75.2	230	4.9	1.6

As can be seen from Table H.3 the calculated volume, assuming the refrigerant and oil to be immiscible, exceeds the volume based on sum the individual components. The approximation becomes more accurate, however, with increasing ambient temperature. One explanation for these results is that R-134a is slightly soluble in mineral oil and the solubility can not be neglected at temperatures this low.

Fortunately Witco Corporation (J. Reyes-Gavilan et al, 1993) provided information detailing the interaction between R-134a and three different viscosity mineral oils (1GS, 2GS, and 3GS). Solubility data are presented in terms of "percent concentration" defined by Equation H.5, which is a function of both temperature and pressure.

Unfortunately, data for the 3GS mineral oil , the same viscosity as the oil in Amana compressor, was available only for 212°F test conditions Since the solubility of liquid refrigerant in oil is a function of both temperature and pressure this data are insufficient to determine the solubility of R-134a for the above test conditions. However, data were available for a 1GS mineral oil at 32°F and 140°F which may provide some insight. Assuming that 1GS and 3GS mineral oils have similar solubility characteristics, its possible to linearly interpolate between the two temperatures at a given pressure and estimate the solubility of R-134a in a 1GS mineral oil. Using this assumption the percent concentration of liquid refrigerant dissolved in the oil sump would be expected to be around 5%, see Table H.3.

$$w = \frac{m_{ref}}{m_{oil} + m_{ref}}$$

(H.5)

To determine whether this level of solubility is sufficient to produce the errors seen in Table H.3, the calculated volume is set equal the total volume shown in Table H.2. The resulting "break-even" concentration shown in Table H.3 range from 1.6 to 4.5%. These break-even solubilities are less than solubility predicted using the Witco data for a 1GS mineral oil. Since the solubility calculations made with the Witco data are rough approximations they cannot be used to correct the calculated volume, but they do indicate that the amount of error seen in calculated volume shown in Table H.3 could easily be caused by refrigerant dissolving into the oil sump. Unfortunately, the R-134a/Witco oil data are not detailed enough to accurately correct for this phenomena.

The above analysis suggests the volume based on the sum of the components is reasonable, assuming that the sump oil contains between 1-4% R-134a. To gain a more accurate estimate of total volume it would be necessary to use a gas which is totally insoluble in oil, or to find more detailed solubility data for R-134a and mineral oil, especially in the 60 to 100°F range. This would provide only a check on the total volume, so if the volume is different no information is available to suggest which component estimate is incorrect. Since refrigerator simulation model requires accurate component volumes future efforts should be conducted with this in mind.

H.3 Refrigerant Charge Determination

Over the past two years the Amana test unit has experienced numerous leaks. Since the refrigerator is charged with only a small amount of refrigerant (8.0 oz.) even small leaks can change system performance. Therefore it was necessary to develop an accurate method of determining the amount of charge in the refrigerator. This way the charge level can be verified while data is being taken so if leaks occur they can be repaired immediately. This section outlines the current method used.

Currently "soak" tests are used to test for refrigerant leaks. To perform a "soak" test the test chamber is set to a temperature between 60°F and 100°F. Next the refrigerator is unplugged and the doors are opened. Then it is allowed "soak" for at least a day and a half allowing the system has reach thermal equilibrium. When the soak is completed the system pressure and temperature are recorded. With this information and an computer program (see Appendix I) developed it is possible to calculate the amount of charge in the system. This value can be compared to amount of refrigerant the refrigerator was originally charged to check for a leak. Since running a computer program can be some what time consuming, therefore Figure H.1 was developed to provide a graphical way of calculating charge level from pressure and temperature data.
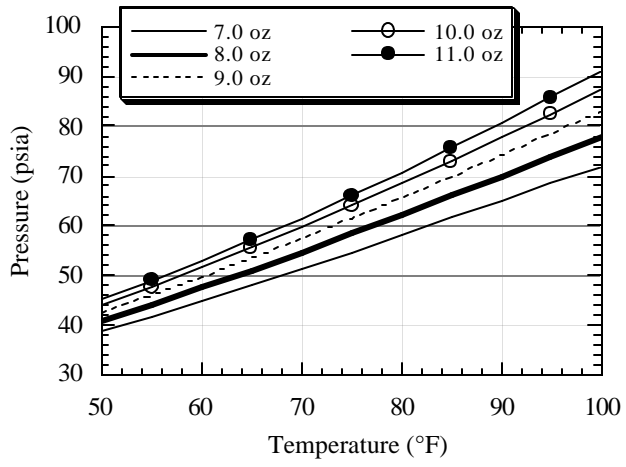
Figure H.1 Temperature/pressure curves for different charge levels

Appendix I: Amana Charge Estimation Code

Attached is an EES (Engineering Equation Solver) program written to calculate the charge level in the Amana test stand given the system temperature and pressure recorded after a "soak" test. The program solves Equations I.1-I.3, where equation I.3 represents the Grebner-Crawford model for R-12 solubility in mineral oil. To extend this program to other refrigeration systems with the same refrigerant oil combination it is only necessary to modify the system internal volume calculations. To model other refrigerant oil combinations requires replacing the Grebner-Crawford model with the proper relations.

$$m_{tot} = m_{roil} + m_{rvap} \tag{I.1}$$

$$m_{rvap} = \frac{Vol_{sys}}{\upsilon_r(T,P)} \tag{I.2}$$

$$m_{roil} = f(T,P,m_{oil}) \tag{I.3}$$

I.1 Source Code

```
{Sample inputs}
Tf = 75  {Soak Temperature [°F]}
P = 59.00 {Soak pressure [psia]
T = Tf+459.67 {°F to °R}

{Grebner-Crawford oil solubility equations}

Tstar = (1-w)*(a+b*P)
Tstar = (T-Tsat)/(Tsat)
a = x1+x2/w^(.5)
b = x3+x4/w^(.5)+x5/w+x6/w^(1.5)+x7/w^2

{Grebner-Crawford constants for R-12}
x1 = -5.9927652*10^(-3)
x2 = 4.1661510*10^(-2)
x3 = 2.004697*10^(-3)
x4 = -3.2682848*10^(-3)
x5 = 1.7368443*10^(-3)
x6 = -2.8552230*10^(-4)
x7 = 1.6092949*10^(-5)

Tsat = Temperature(R12,P=P,x=0.5) {Saturation temperature of R-12}
v = Volume(R12,P=P,T=T) {Specific volume of R-12}

w = m_roil/(m_roil+m_oil) {% concentration of refrigerant in the oil}
m_rvap = 16*(Vol_tot/v)  {refrigerant present as vapor [oz]}
m_tot = m_roil+m_rvap  {total refrigerant charge [oz]}


{Total internal volume of the Amana refrigerator [ft^3]}

{Volume of individual components}
Vol_disline = 0.48e-3  {discharge line}
Vol_bcap = 0.96e-4  {bell cap of mass flowmeter}
Vol_fltr = 0.48e-3  {filter dryer}
```

Vol_liqline = 0.54e-3 {liquid line}
Vol_cap = 0.62e-4 {capillary tube}
Vol_accum = 0.34e-2 {accumulator}
Vol_suctline = 0.20e-2 {suction line}

{Volume of the condenser}
D_cond = 0.017 {diameter of condenser [ft]}
L_cond = 49.2 {length of condenser [ft]}
Vol_cond = (pi*(D_cond/2)^2)*L_cond

{Volume of the evaporator}
D_evap = 0.0266 {diameter of evaporator [ft]}
L_evap = 39.0 {length of evaporator [ft]}
Vol_evap = (pi*(D_evap/2)^2)*L_evap

{Volume of the compressor}
Vol_free = 170/(12^3) {internal free volume of compressor}
rho_oil = 56.211-0.020808*(T-459.67) {density of oil [lb/ft^3]}
m_oil = 11.2 {mass oil in compressor sump [oz]}
Vol_oil = (m_oil/16)/rho_oil {volume of oil}
Vol_comp = Vol_free-Vol_oil {volume compressor less volume of oil}

{Total internal volume}
Vol_tot =   Vol_disline+Vol_bcap+Vol_fltr+Vol_liqline+Vol_cap+Vol_accum+Vol_suctline+
               Vol_cond+Vol_evap+Vol_comp

Appendix J: Refrigerant Charge Optimization

One of the parameters which affects refrigerator cycling performance is the amount of charge in the system. When the refrigerator is undercharged there is a degradation in COP and likewise a similar effect can be seen if the system is overcharged. This appendix will outline the procedure used to calculate the optimum charge for a modified Amana refrigerator for two different refrigerants, R-12 and propane.

J.1 Factory Charge Optimization

The charge optimization procedure used in the refrigerator industry can be summarized as follows. First, the refrigerator is charged with an amount of refrigerant known to be in excess of the optimal amount and placed in a 90°F test chamber. The thermostat and fresh food damper are set to in the middle positions. The amount of energy used for a typical cycle and freezer temperature are recorded and the energy usage extrapolated to the amount used in a year. The thermostat and fresh food damper are then set in the warmest positions. Again the energy usage and freezer temperature recorded. Using these values of energy consumption and freezer temperature, the energy needed to maintain the freezer at 5°F is calculated using linear interpolation. Next, a quarter ounce of refrigerant is released and the energy usage for a 5°F freezer compartment is calculated. This procedure is followed until a minimum energy usage is reached.

J.2 Charge Optimization Procedure Used

After adding pressure taps, immersion thermocouples, and a mass flow meter it was unclear whether the recommend charge level of 8.0 ounces of R-12 refrigerant would still be the optimum for the modified Amana refrigerator. To perform the charge optimization we charged the refrigerator with a 6.5 ounces of R-12 and placed it inside a 90°F test chamber. Then a modified version of the industry procedure of optimizing charge was performed.

The Amana refrigerator has been modified so that the damper used to control fresh food temperature is fixed in the open position. Therefore, data was taken at cold-warm and cold-mid temperature settings. With the data collected an average energy usage for a freezer temperature of 5°F was calculated. Finally, 0.5 ounces of refrigerant was added to the system an the above process repeated. This procedure was followed for charge levels ranging from 6.5-8.5 ounces. The reason for adding refrigerant rather than removing refrigerant was a matter of accuracy. Using this charging method refrigerant was added into the refrigerator with an accuracy of $\pm$ 1g (due to inaccuracies of the scale; unaccounted refrigerant in the hose is considered insignificant).
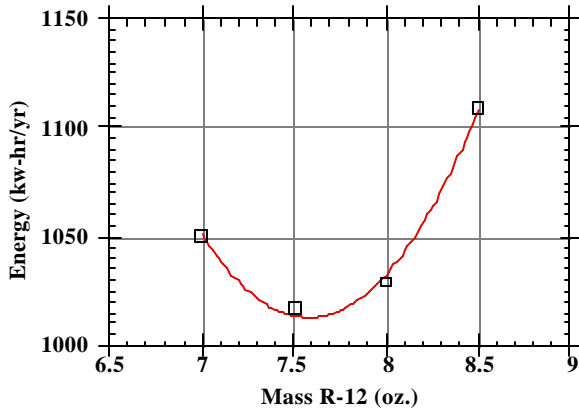
Figure J. 1 Effect of charge level on energy use (R-12)

Figure J.1 shows the experimental results. The minimum energy usage lies between 7.5 and 8.0 ounces of refrigerant. Ideally, several charge levels between 7.5 and 8.0 would be tried to determine a more accurate minimum. However, there is no reliable method to remove charge it would be necessary to completely discharge the refrigerator, charge it with 7.5 ounces of refrigerant and then slowly add increments refrigerant to try to obtain a better idea of where the minimum lies. With this in mind, the refrigerator was charged with 8.0 ounces of refrigerant as recommended by the manufacturer.

A second charge optimization was done using propane. To start these charge optimization experiments the refrigerator was initially charged with 2.5 oz of propane. Propane was added in increments of 0.25 oz. and the energy usage measured. Figure J.2 shows the results of these tests.
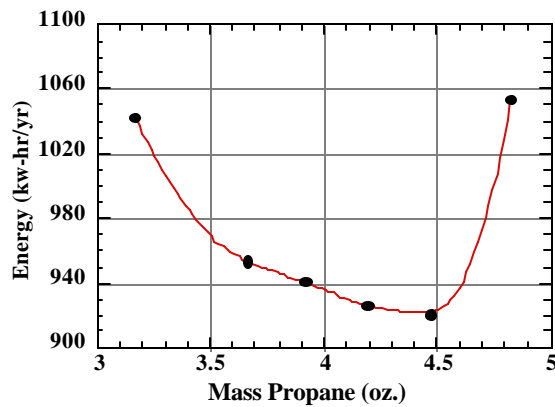

Figure J.2 Effect of charge level on energy use (Propane)

From figure J.2 it appears the optimal charge level lies between 4.25 and 4.5 ounces of propane. To further narrow down the optimal charge level several points between 4.25 and 4.5 ounces would need to be tested. Since this refrigerator was used to collect data to validate the ACRC refrigerator model, the refrigerator was charged with 4.5 ounces of propane. By charging the refrigerator with 4.5 ounces the condenser exit was sub-cooled for the majority of operating conditions allowing the refrigerant mass flow rate to be calculated using an energy balance across evaporator.